UNLV Theses, Dissertations, Professional Papers, and Capstones

5-1-2015

The Design, Build, And Validation Of A Hybrid Tower Used To Conduct Helmet Impact Tests

Darren Benn
University of Nevada, Las Vegas, dibenn11@gmail.com

Follow this and additional works at: https://digitalscholarship.unlv.edu/thesesdissertations

Part of the Mechanical Engineering Commons, and the Sports Sciences Commons

THE DESIGN, BUILD, AND VALIDATION OF A

HYBRID TOWER USED TO CONDUCT

HELMET IMPACT TESTS

By

Darren Benn

Bachelors of Science in Mechanical Engineering

University of Nevada, Las Vegas

2012

A thesis submitted in partial fulfillment

of the requirements for the

Masters of Science – Mechanical Engineering

Department of Mechanical Engineering

Howard R. Hughes College of Engineering

The Graduate College

University of Nevada, Las Vegas

May 2015

We recommend the thesis prepared under our supervision by

Darren Benn

entitled

The Design, Build, and Validation of a Hybrid Tower Used to Conduct Helmet Impact Tests

is approved in partial fulfillment of the requirements for the degree of

Master of Science in Engineering - Mechanical Engineering
Department of Mechanical Engineering

Douglas D. Reynolds, Ph.D., Committee Chair

Brendan O'Toole, Ph.D., Committee Member

William G. Culbreth, Ph.D., Committee Member

Samaan Ladkany, Ph.D., Graduate College Representative

Kathryn Hausbeck Korgan, Ph.D., Interim Dean of the Graduate College

May 2015

ABSTRACT

The National Operating Committee on Standards for Athletic Equipment (NOCSAE) was established to enlist research directed towards the reduction of head injuries in organized sports. The function of the test methods developed by NOCSAE is to provide the blueprint for reliable and repeatable procedures to measure the evaluation of various types of protective sports headgear and projectiles. In addition, the methods also govern hardware such as testing apparatus and data acquisition instrumentation. In helmet testing, the method dictates whether the impact is induced by a projectile system or by a drop tower system with an anvil at the base. Altogether, the methods and procedures are used to determine a pass/fail for a Severity Index (SI) within specified tolerances. The SI is a measure of the severity of impact with respect to the instantaneous acceleration experienced by the headform (fitted with helmet) as it is impacted, and is defined as:

$$SI = \int_0^T a(t)^{2.5} dt$$

where '$a(t)$' is the instantaneous acceleration expressed in g's. Also, NOCSAE standards for (drop) impact testing require the impact velocities to be measured during the last 1.5 in. (40mm) of free fall.

Although the NOCSAE standard uses the SI as a performance characteristic, the standard does not provide a means to measure the force of the impact to the headform (fitted with helmet) either by the helmet impacting an object or by the helmet being impacted by an object. Therefore, this analysis seeks to incorporate the measurement of the force of the impact as a viable test parameter without deviating from the protocols established by NOCSAE.

The objective of this research was to design, build, and validate a test structure for testing and measuring the effectiveness of baseball helmets in reducing shock to the head. Further, the design incorporated two test methods into one structure. The three primary components of the test

structure were the Pendulum, the Pedestal, and the Linear Bearing Table (LBT). The design of the test structure and the test methods were guided by the following NOCSAE standards:

ND-001: 'Standard Test Method and Equipment Used in Evaluating the Performance Characteristics of Protective Headgear/Equipment'.

ND-021: 'Standard Projectile Impact Testing Method and Equipment Used in Evaluating the Performance Characteristics of Protective Headgear, Faceguards or Projectiles'.

ND-022: 'Standard Performance Specification for Newly Manufactured Baseball/Softball Batter's Helmets'.

ND-023: 'Laboratory Procedural Guide for Certifying Newly Manufactured Baseball/Softball Batter's Helmets'.

Congruent with ND-001, the NOCSAE medium headform was used for all tests. Of course, two major modifications to the preceding test methods were implemented. First, a single test structure was designed to conduct both the drop tower test and the projectile test. This is in contrast to ND-001 and ND-021, which employ a separate apparatus for each test. Second, a means to measure the force of the impact into the headform was developed.

Further, the applications of theoretical equations, in particular energy equations, were applied to the collected data with the hopes of forming a basis for comparison with established findings.

The results revealed that certain energy equations could be applied with a certain level of confidence to determine impact velocity, especially without the presence of impact attenuation. In addition, an unforeseen development suggested that an object in a stationary setting, such as a batter in baseball, may incur more damage from the rebound of an impact than the impact itself.

The results generated by the supplementary procedures will aid in developing a basis for comparison and creation of a means to reasonably measure the contributing biomechanical factors, such as linear acceleration, to the shock created by head impacts, which is the leading cause of sports related concussions.

ACKNOWLEDGMENTS

TABLE OF CONTENTS

LIST OF TABLES

LIST OF FIGURES

1. CHAPTER 1 – INTRODUCTION

In the 1960's spectator attendance at athletic events had surpassed previous decades. The burgeoning popularity of the events resulted in increased media coverage, which eventually gave rise to greater exposure of organized sports. The increased publicity generated more opportunities for athletic scholarships and also ushered in an era of profitable professional sports contracts. Driven by those opportunities, athletes engaged in more aggressive and forceful performances. Unfortunately, with the increased voracity in play serious injuries occurred more frequently, especially in the sport of football. The decade culminated with 32 fatalities documented in 1968 from head and neck injuries directly due to participation in organized football. In 1969, with the injuries in football as the catalyst, the National Operating Committee on Standards for Athletic Equipment (NOCSAE) was established to enlist research directed towards the reduction of head injuries in organized sports. Based on the research commissioned from several academic institutions, NOCSAE developed methods, rigging, and performance requirements for testing football protective headgear. Subsequently, over the years NOCSAE developed performance standards for the protective headgear and equipment used in a variety of sports. Currently, NOCSAE performance standards are in compliance with the testing codes specified by the American National Standards Institute (ANSI) and the American Society for Testing and Materials (ASTM).

1.1. NOCSAE versus the Other Standards

Since its inception, NOCSAE has evolved into the archetypical governing body for the testing methods of, and for the development of, performance standards for protective sports equipment. However, in the years following NOCSAE's origin several organizations have been created with the directive of developing performance standards for protective sports equipment.

1

Included in these establishments are companies, such as Biokinetics®, Cadex®, and the Safety Equipment Institute (SEI)®. Although most of these enterprises establish certifications in accordance with the specifications of organizations such as ANSI and ASTM, some of the testing equipment is different from those used by NOCSAE, in particular the headform. Some laboratories use metal headforms to simulate the human head during helmet impact testing. However, NOCSAE employs an instrumented model human head possessing a high bio-fidelity which offers a reasonable mechanical analog of the human skull. As a result, the NOCSAE test methods and equipment were used during this experimental analysis.

Despite some procedural and hardware differences implemented in helmet testing, all of these companies are in pursuit of the common goal of mitigating the shock responsible for the occurrence of most sports related head injuries. The motivation behind this experimental analysis was to quantify certain properties that lead to head shock.

1.2. Motivation and Goal for This Experimental Analysis

Head shock is the leading cause of sports related concussions. The focal point of this analysis was to develop a procedure to quantify the properties associated with head impact, such as the impact force. Then use those findings to form a basis for comparison with other research. In recent years research has shown that multiple concussions sustained over time can lead to Traumatic Brain Injury (TBI) and subsequently Chronic Traumatic Encephalopathy (CTE). According to a report published by the Center for Disease Control (CDC), between the years of 2001 and 2005 the average annual number of emergency department visits due to non-fatal sports related TBIs for all age groups was 207,830 (CDC-MMWR: July 27, 2007 / 56(29),733-737). During the same time frame the average annual number of emergency department visits for baseball related non-fatal TBIs was 10,103, which was 6.2% of all sports related TBI emergency visits. The average annual number of hospitalizations was 811, which accounted for 5.6% of all

2

sports related TBIs (CDC-MMWR: July 27, 2007 / 56(29), 733-737). The report also claimed that persons in the age group of 5-18 years comprised 65% of the average annual number of emergency department visits due to non-fatal sports related injuries (SR) TBIs (CDC-MMWR: July 27, 2007 / 56(29),733-737).

A more recent report published by the CDC focused on the average annual number of emergency department visits due to non-fatal SR TBIs for the age group ≤19 between the years of 2001 and 2009. The average annual number of emergency department visits for baseball related non-fatal TBIs during this time frame was 9,634, which surmised 7.9% of all reported sports related TBIs (CDC-MMWR: Oct 7, 2011 / 60(39), 1337-1342). The findings in these reports emphasize that there is a need to reduce the occurrence of sports related TBIs particularly by improving the preventative equipment used in organized sports.

Ultimately, one of the goals of this analysis was to more effectively measure and quantify the biomechanical measures that can lead to sports related head shock, in particular linear acceleration. In addition, it was desired to apply theoretical applications and analytical techniques to the collected data to form a basis for comparison with the current pedagogy dedicated to reducing SR TBIs. Tables 1-1 and 1-2 itemize a portion of the information presented in the CDC's report spanning 2001 to 2005, while Table 1-3 summarizes some of the findings from the report covering the period from 2001 to 2009.

The information used to generate the CDC's reports was gathered from data compiled by the National Electronic Injury Surveillance System (NEISS), which is a data bank maintained by the Consumer Product Safety Commission (CSPC).

Table 1-1: Est. Annual No. & Percentage of ED Visits for Non-Fatal SR TBIs [3] [4]

ALL AGES (2001-2005)			5-18 yrs. (2001-2005)		
Activity	Annual Average # of TBIs	% of all ED visits[3]	Activity	Annual Average # of TBIs	% of all ED visits for TBIs
Football	22689	5.7	Football	20293	89.4
Baseball	10103	6.2	Baseball	7433	73.6
Basketball	14680	2.4	Basketball	11506	78.4
Total[1]	47472	14.3		39232	**64.9[2]**

Table 1-2: Est. Annual No. & Percentage of Hospitalizations for Non-Fatal SR TBIs [3] [4]

ALL AGES (2001-2005)			5-18 yrs. (2001-2005)		
Activity	Annual Average # of TBIs	% of all Hosp.[4]	Activity	Annual Average # of TBIs	% of all Hosp.[3]
Football	891	13.1	Football	775	13.7
Baseball	811	21.6	Baseball	419	21.8
Basketball	465	9.7	Basketball	365	13.6
Total[1]	2167	44.4		1559	**17.9[2]**

Table 1-3: Est. Annual No., Percentage, & Rank of ED Visits for Non-Fatal SR TBIs [3] [4]

AGES ≤19 (2001-2009)								
Activity	Annual Avg. # of TBIs	% of all SR ED visits attributed to TBIs	MALE			FEMALE		
			Annual Rank	Annual Avg. Total	Annual Avg. % Total	Annual Rank	Annual Avg. Total	Annual Avg. % Total
Football	25376	7.2	1	24431	19.9	N/A	N/A	N/A
Baseball	9634	7.9	5	8030	6.5	N/A	N/A	N/A
Basketball	13987	3.7	4	9372	7.6	4	4615	9.2

4

2. CHAPTER 2 – REVIEW OF PREVIOUS WORK

The primary structural design focus of this research was to incorporate NOCSAE's drop impact and projectile impact tests, two separate test methods, into one test structure. ND-021 recommends using an air-cannon to conduct projectile impact tests. However, in order to create a test structure that could accommodate drop tests and projectile tests, a pendulum seemed like a plausible alternative. In general, the intention was to conduct tests that could generate results that could form a basis for comparison with research aimed at head impact and sports related head injury.

The preeminent study in the field of sports related head injury and the quantification of the kinetic biomechanical factors associated with head impact was the groundwork conducted at Virginia Tech (V-tech). Through the use of laboratory research and field tests conducted with football helmets fitted with Head Impact Telemetry (HIT) ® technology, V-tech managed to compile the most referenced compendium of information on sports related head injury due to impact. However, although the body of work created by V-tech is considered the tip of the spear in head injury analysis, the breadth of that study was too encyclopedic. Thus, the aspiration of the literature search was to target prior work with a more intimate scope and with objectives more closely aligned to those of this experimental analysis.

This experimental analysis consisted of two elements which included the physical concept and the theoretical applications. The physical concept was concerned with the tower's structural design and the intricacies of fabricating a single structure that incorporated multiple impact test methods. The theoretical consideration was driven by the desire to apply analytical processes to empirical data. Guided by these factors the literature search uncovered three relevant findings. One project addressed the structural design aspect by proposing to modify the NOCSAE

impact method through the use of a pendulum. The subject of the other two research papers was the application of analytical tools to collected data.

2.1. Method and Apparatus for Testing Football Helmets

United States Patent US 6,871,525 B2 'Method and Apparatus for Testing Football Helmets' summarizes the embodiment of an impact test structure designed by inventors Withnall and Bayne. The design consists of a weighted pendulum arm which is utilized to impart an impact force on a football helmet mounted to the base stand of the structure. The linear and rotational acceleration caused by the impact is measured and used to calculate a Head Impact Power Index (HIP). The HIP is then used as a standard to quantify the effectiveness of the helmet in preventing injury to a player. The inventors claimed that the advantage that their invention had over the NOCSAE standard was attributed to the modification of how the impact was delivered and the collection of additional data.

The NOCSAE standard ND-002 'Standard Performance Specification for Newly Manufactured Football Helmets', which governs the evaluation of the performance characteristics of football helmets, dictates that helmet impact tests can be conducted by performing a drop test. A headform fitted with the helmet being tested is dropped from a prescribed height and allowed to strike an anvil at the base of the drop assembly. Also, the standard designates that an accelerometer mounted on the inside of the headform measure only the linear acceleration of the impact. The inventors state that their method incorporates two essential differences from the NOCSAE test method. First, Withnall and Bayne claim that because the impact face of their pendulum has the same radius of curvature as a football helmet and is covered with the same polycarbonate plastic material, it delivers a glancing impact, which is a more realistic simulation of the head to head impacts that occur in football. Second, their system measures both the linear and rotational acceleration of the headform caused by the impact. Withnall and Bayne stated that

their test method and subsequent test standard was developed to supplement but not replace ND-002.

Although Withnall and Bayne's structure was designed to test football helmets, their concept of modifying the test method by utilizing a pendulum was identical to the central structural design concept of this analytical experiment. Figure 2-1 is an illustration of Withnall and Bayne's helmet impact apparatus.
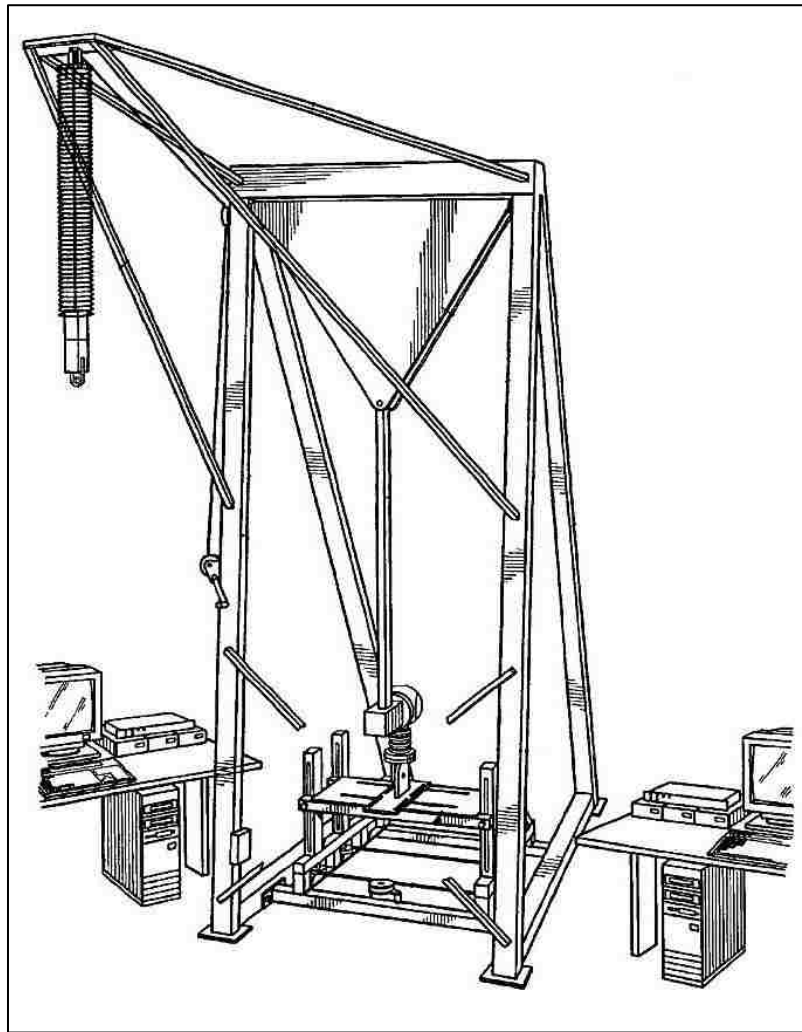
Figure 2-1: Withnall & Bayne's Impact Pendulum [12]

7

2.2. Research Papers Addressing Analytical Techniques

This experimental analysis was composed of two facets. In the previous section, research relating to the design aspect of the structure was covered. The focus now shifts to the analytical processes that can be used to quantify the collected data.

NOCSAE as one of the governing entities for developing performance standards for protective sports equipment developed its own analytical tool to quantify test data.

The Severity Index (SI) value is a measure of the severity of impact with respect to the instantaneous acceleration experienced by the headform as it is impacted and is defined as:

$$SI = \int_0^T a(t)^{2.5} dt \qquad (2\text{-}1)$$

where '$\mathbf{a(t)}$' is the instantaneous acceleration expressed in g's. It is essentially a weighted integration under the acceleration curve for specific time durations. The SI value only dictates the pass/fail criterion for a particular piece of sport equipment, but it offers no measure for the correlation between impact severity and probability of a concussion. Dissatisfied with the short comings of the SI, researchers later developed the Head Injury Criterion (HIC). The HIC is a measure of the likelihood of head injury arising from an impact. The equation for HIC is as follows:

$$HIC = \left\{ (t_2 - t_1) \left[\frac{1}{t_2 - t_1} \int_{t_1}^{t_2} a(t) dt \right]^{2.5} \right\}_{\mathbf{max}} \qquad (2\text{-}2)$$

where $\mathbf{t_1}$ and $\mathbf{t_2}$ were the initial and final times in seconds respectively and similar to the SI '$\mathbf{a}$' is the acceleration value expressed in g's.

In the paper '*Concussion in professional football: reconstruction of game impacts and injuries*', 2003 researchers Pellman, Viano and Tucker et al. sought to find a way to correlate the SI and HIC values to the occurrence of a concussion. They created a knowledge bank of impact

8

and concussion data by observing videotapes of head impacts and concussions filmed by the National Football League during games between the years of 1996 and 2001. Based on the application of analytical tools, the researchers stated that in most of the athletes concussions occurred at an SI value of 300 and above and a HIC value of 250 and above. Other researchers believe that the HIC is restricted because it places emphasis on the linear acceleration, as well as, the fact it is a measure of severe brain injury rather than Mild Traumatic Brain Injury (MTBI). This perspective is covered in the second of the two research papers.

In the published paper titled '*Head Impact Severity Measures for Evaluating Mild Traumatic Brain Injury Risk Exposure*', 2009 authors Greenwald and Gwin et al. sought to quantify the sensitivity of various biomechanical measures of head impact, such as linear acceleration, rotational acceleration, and impact duration. The researchers suggested that values such as the HIC treat these variables as separate entities. However, Greenwald et al. hypothesized that the elements of head shock and TBIs can better be quantified if they are treated as inter-related. Hence, they applied analytic methods, such as Principal Component Analysis (PCA) that account for the relationships among the variables (Greenwald). Their goal was to quantify the sensitivity of various biomechanical measures of head impact and then use those values to identify the percentage of all concussions that were incorrectly identified by the conventional measures, an occurrence they termed as a 'false response'.

After applying their analytical tools to data collected from instrumented helmets used at 13 institutions, their results revealed that linear acceleration measures exhibited the lowest false response rate among the biomechanical measures. For correct prediction levels, linear acceleration had a false response rate of 1.6% (Greenwald). In addition, they stated that the HIC false response rate was greater at 1.9%. In general, they discovered that, for prediction levels

above 70%, linear acceleration had the lowest false responses, and rotational acceleration yielded the lowest false response for prediction levels below 70%.

The results of the aforementioned papers suggest that there is no ubiquitous analytical method that can be applied to the data to form a quantifiable basis for comparison. In contrast, a combination of techniques should be used to develop more congruent findings. The SI and HIC values as they were applied in this experimental analysis are addressed in greater detail in Chapter 6.

3. CHAPTER 3 – NOCSAE'S GENERAL AND BASEBALL STANDARDS

There are four NOCSAE documents that encompass the breadth of this study. Two of the documents govern the general test methods for protective sports headgear, the third dictates the performance standards for baseball/softball batter's helmet, and the fourth governs the laboratory procedural guide for baseball/softball batter's helmet. In general, this analysis did adhere to the instructions outlined in these documents. However, modifications to the guidelines were introduced. Indeed, those modifications form the essence of this study, as will be discussed in chapter four. The information in the documents cover a wide range of topics ranging from laboratory test equipment for the general testing of sports protective headgear to the specific practices for baseball/softball batter's helmet certification. Therefore the subsequent coverage of these documents will focus only on the material pertinent to this analysis.

3.1. NOCSAE DOC ND-001

The NOCSAE Document (ND) titled 'Standard Test Method and Equipment Used in Evaluating the Performance Characteristics of Protective Headgear/Equipment', or more commonly referred to as ND-001 regulates the test method for drop testing protective headgear/equipment. The scope of this method incorporates the impact test instruments and equipment, the testing environment, and the drop test procedure.

3.1.1. Impact Test Instruments and Equipment

Sections 15.1~15.5 in ND-001 describe the hardware that is required to conduct a helmet drop impact test. The primary apparatus is the drop tower which is a metal structure anchored to a wall with its base mounted and securely attached to a formidable stone slab. The tower is comprised of two vertical guide rods used for the linear movement of a carriage assembly. The guide rods are tautly attached to the top mount plate and an anvil base plate. In addition,

NOCSAE recommends the use of a hoist motor with a reversible speed controller and a pulley system to retract the carriage assembly. As the name suggests, the anvil base plate is used to mount the impact anvil. The impact surface of the anvil is covered with a Modular Elastomer Programmer (MEP) Pad. Figure 3-1 is a numbered schematic of the NOCSAE drop impact structure, and Table 3-1 provides a brief description of the numbered items. The two other major pieces of equipment are the NOCSAE headform and the data acquisition system.
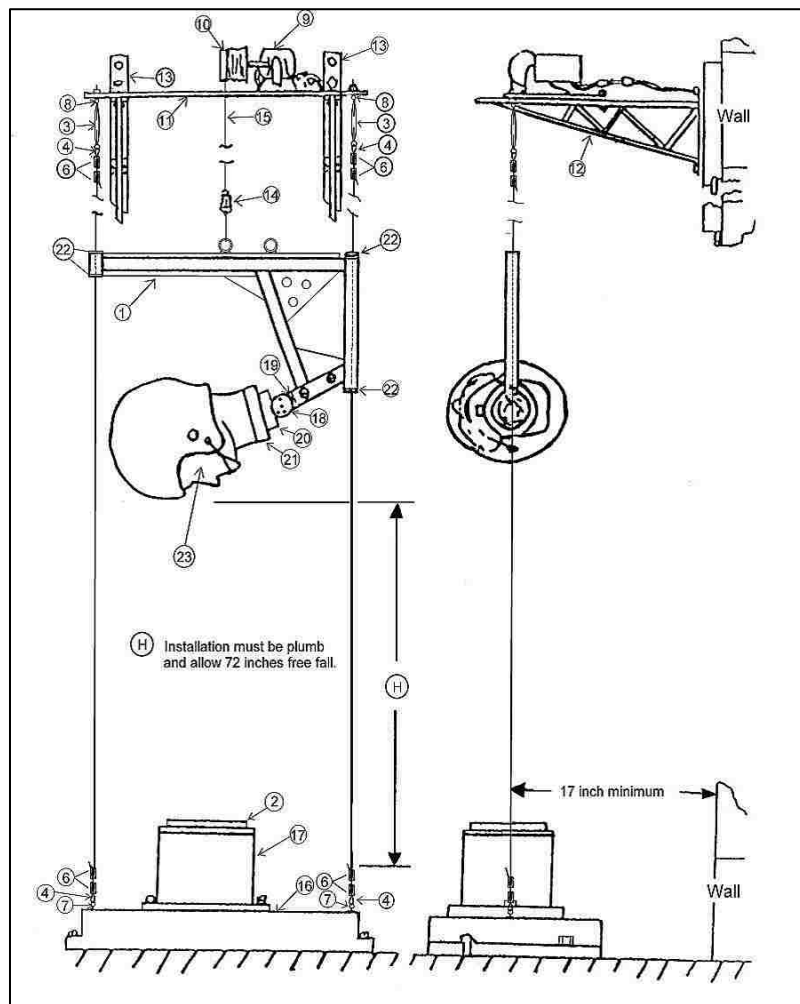
Figure 3-1: NOCSAE's Complete Drop Impact Structure [8]

Table 3-1: NOCSAE's Drop Impact Structure Components

Item Number	Description
1	Drop carriage
2[1b]	½" MEP Testing Pad
3	Hook-eye Turnbuckle, Forged Steel 3/8" w/ 6" take-up
4	1/8" Wire Rope Thimble
5	1/8" Spring Music Wire
6	1/8" Wire Rope, Tiller Rope Clamp, Bronze
7	3/8" 16 x 3 Eye Bolt
8	3/8" Forged Eye Bolt
9	Right Angle DC Hoist
10	Single Groove Sheave (Pulley) 3¾"
11	Top Mount Plate
12	18" Top Channel Bracket
13	Wall Mount Channel Bracket 4" x 1 5/8"
14	Mechanical Release System
15	Lift Cable, Wire Rope, 20' Coil
16	Anvil Base Plate
17	Anvil
18	Headform Adjuster
19	Headform Rotator Stem
20	Headform Threaded Lockring
21	Headform Collar
22	Nylon Bushing
23[2b]	Medium Headform

NOCSAE defines its headforms as an instrumented model human head designed to fit the carriage assembly and possessing a high bio-fidelity. NOCSAE standards require the use of headforms manufactured by Southern Impact Research Center (SIRC). The headforms are available in three color-coded sizes red for large headforms, blue for medium, and green for small headforms. Mounted at the center of gravity of each headform is a small piezoelectric tri-axial accelerometer, which is designed for vibration measurements in the three orthogonal axes. Measurements collected by the accelerometer are analyzed by the data acquisition system. NOCSAE prescribes the KME 200 data analyzer. However, the organization states that any computer equipped with appropriate data acquisition software can be substituted providing its properties are equivalent to those of the KME data analyzer. Table 3-2 itemizes the

anthropometric measurements of the medium headform, Figure 3-2 is a picture of the NOCSAE medium headform, and Figure 3-3 is a picture depicting the drop impact structure as assembled by SIRC.

Table 3-2: Approximate Dimensions of NOCSAE Medium Headform

Point Of Measure	Headform Dimension-inches (mm)
Stetson Size	7¼
Head Breadth	5.98 (152)
Max. Brow width (Frontal Diameter)	5.20 (132)
Ear hole to ear hole (Bitragion Diameter)	5.51 (140)
Max. Jaw Width (Bigonial Diameter)	4.65 (118)
Head Length (Glabella to back of head)	7.87 (200)
Outside eye corner to back of head	6.81 (173)
Ear hole to back of head	3.86 (98)
Ear hole to outside corner of eye	2.95 (75)
Ear hole to top of head	5.24 (133)
Eye pupil to top of head	4.53 (115)
Ear hole to jaw angle	3.03 (77)
Bottom of nose to point of chin	2.80 (71)
Top of nose to point of chin	4.88 (124)
Head circumference	22.68 (576)
Head weight including mounting interface	10.8 lb. (4.90kg)

Figure 3-2: NOCSAE Medium Headform

Figure 3-3: NOCSAE Drop Assembly As Assembled By SIRC [10]

3.1.2. The Testing Environment

Sections 12.1~12.4 of ND-001 chiefly cover the protocol for conditioning and testing environments for protective headgear/equipment. The sections state that for the objective of conditioning, the headgear/equipment should be exposed to the testing environment for a minimum of four hours in ambient temperatures, and up to a maximum of twenty-four hours for high temperature environments. However, the standard recommends that testing be conducted in an environment with a temperature of 75 F° ±5F° (22 C° ±2 C°).

3.1.3. The Drop Test Procedure

Generally, the NOCSAE drop test method requires the headgear being tested to be placed on the appropriate headform and dropped to achieve an accepted free fall velocity. Initially, the headform is attached to the drop carriage and then the helmet is placed on the headform. The drop carriage, carrying the helmet fitted headform, is raised to a determined height and released for free fall. The impact velocities are measured in the last 1.5in. (40mm) of free fall, which is just prior to the helmet impacting the anvil. The impact velocities outlined in NOCSAE standards are based on specific velocities and not impact heights. Therefore, according to ND-001, if height adjustments made to attain the proper velocity account for more than ten percent of the drop height the system should be evaluated for repair. Further, impacts that result in velocities that exceed the performance criteria are declared inconclusive. The other criterion defined in the document is the impact locations on the headform/helmet.

The headform adjuster and rotator stem, items 18 and 19 in Figure 3-1, allows the headform to be rotated through seven and three numbered positions respectively. The position of the headform is adjusted by rotating either the adjuster or the stem (or both) to a desired numbered position. For testing purposes, NOCSAE dictates six compulsory positions, and twenty

16

valid random positions. Figure 3-4 is a graphic of the adjuster and rotator stem as depicted in ND-001, and Table 3-3 itemizes the six compulsory and four valid random headform testing positions.
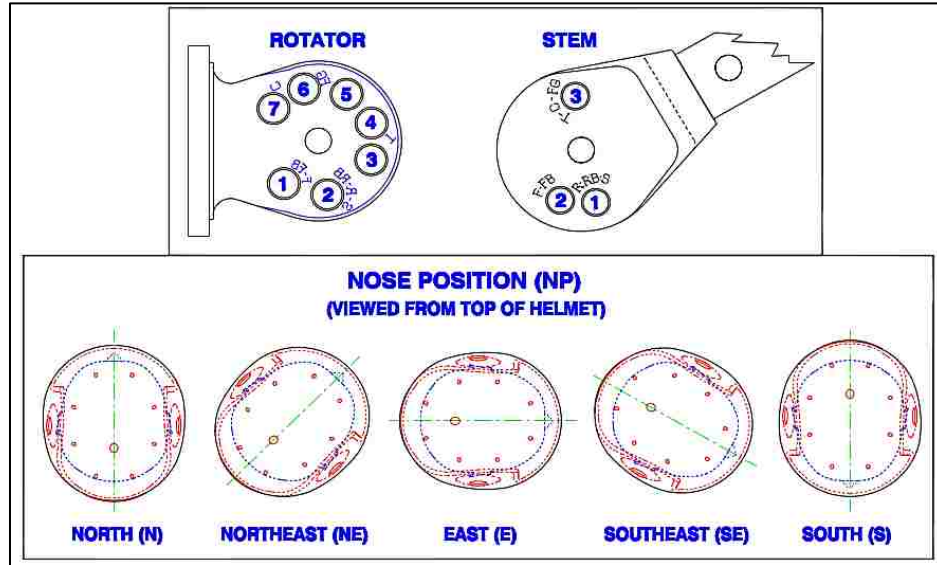
Figure 3-4: Headform Adjuster and Rotator Stem [8]

Table 3-3: Compulsory and Valid Random Headform Testing Positions

Position	Rotator	Stem	Headform Nose Position	NOCSAE Definition
1	1	2	South	Normal Front Position
2	1	2	Southeast	Normal Right Front Boss Position
3	2	1	East	Normal Side Position
4	2	1	Northeast	Normal Right Ear Boss Position
5	2	1	North	Normal Rear Position
6	4	3	North	Normal Top Position
7	4	3	South	Valid Random Position
8	4	3	Southeast	Valid Random Position
9	4	3	East	Valid Random Position
10	4	3	Northeast	Valid Random Position

The objective of the drop test method is to acquire the resultant acceleration and use it to calculate the Severity Index (SI). The SI is a measure of the severity of impact with respect to the instantaneous acceleration experienced by the headform (fitted with helmet) as it impacts the

17

anvil. The value for SI is obtained from equation (2-1). The integration for this calculation must begin after the data acquisition system triggers just before the value of the signal reaches 4 g's on the up side of the pulse and must end when the signal drops below the 4 g point on the down side of the pulse. ND-001 does not specify a pass-fail SI. However, the document does state that appropriate SI levels range from 300 SI ±3% to a maximum of 2000 SI ±2%. The next general standard to be addressed delineates the projectile method for testing headgear/equipment.

3.2. NOCSAE DOC ND-021

ND-021 is the 'Standard Projectile Impact Test Method and Equipment Used in Evaluating the Performance Characteristics of Protective Headgear, Faceguards or Projectiles'. The basis of this test method is to outline the laboratory equipment and procedures relevant to projectile testing of protective headgear/equipment and certain projectiles, such as baseballs and softballs. The content of ND-021 is identical to that of ND-001 in regards to the conditioning and testing environments. However, there are some differences in the required testing instruments and equipment, test method, and data acquisition procedure. Considering ND-021 describes projectile testing as well, only the information pertinent to helmet testing will be covered in this outline.

3.2.1. Projectile Test Instruments and Equipment

Sections 12.1~12.10 of ND-021 summarize the instruments and equipment necessary to conduct projectile impact tests on headgear and the projectile itself.

The primary instruments of concern are the air cannon assembly, the linear bearing table, and a major league baseball. ND-021 recommends the use of an air cannon capable of launching a baseball at speeds of 60 mph ±2 mph. The document also suggests that two velocity sensors should be positioned between the nozzle of the air cannon and the headform as it is mounted on the linear bearing table. The linear bearing table is the structure on which the headform is

mounted during a test, and according to the standard it should have a maximum mass of 5.7kg ± 0.5kg (12.57lb ± 1.102lb). The baseball should be constructed as specified by Major League Baseball and should have a mass of between 140~145 grams (5~5.25oz), a circumference of 9.00~9.25 inches, and a compression-deflection value between 200~300 pounds. Figure 3-5 and 3-6 are drawings of the air cannon as part of the projectile impact test assembly and linear bearing table respectively as represented in ND-021.
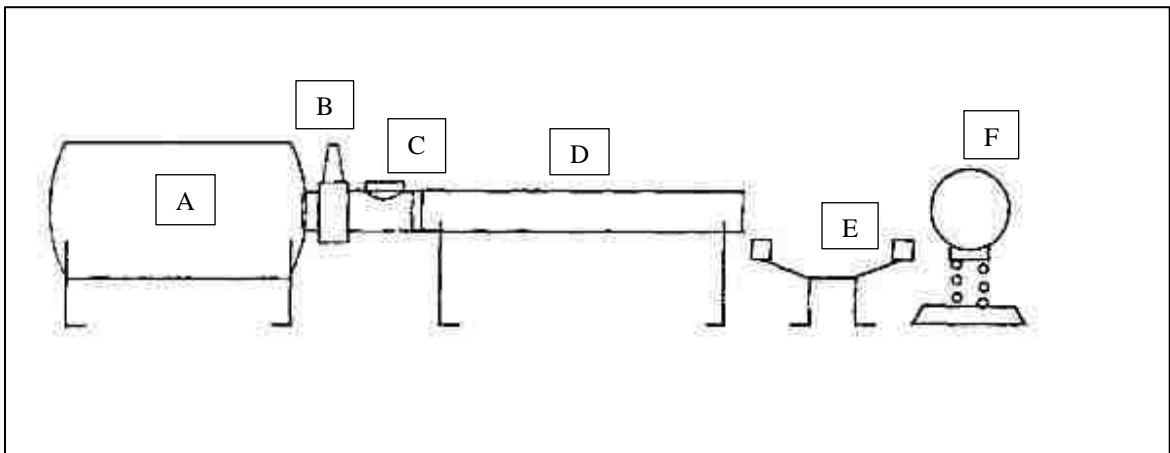
Figure 3-5: Projectile Impact Test Assembly (Air Cannon) [8]

A: Air Reservoir

B: Air Solenoid

C: Loading Breech

D: Interchangeable Barrel

E: Velocity Measurement Sensors

F: NOCSAE Headform Mounted on Linear Bearing Table
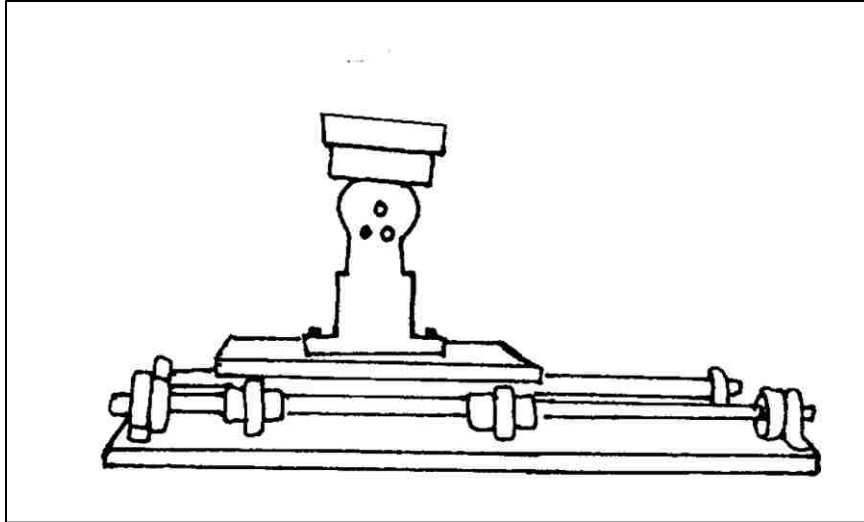
Figure 3-6: Linear Bearing Table (LBT) for Projectile Impact Test [8]

3.2.2. Projectile Impact Test Procedure

The test method for projectile impact testing is relatively straight forward. The headform fitted with a helmet is positioned on the linear bearing table, and then the projectile is propelled at the headform. NOCSAE headforms are manufactured with the left ear, therefore, the method specifies that the projectile impacts the right side of the headform. The projectile must be propelled in such a manner that the impact velocity is within 3% of the velocity specified by the standard. The specified velocities are based on the SI response of the headform. Consequently, a value of 1200 SI between 36~44 mph is an appropriate response for a medium headform.

As with the drop impact method, the goal of the projectile method is to use the resultant acceleration to derive the SI value. However, because this method can also be used to evaluate baseballs and softballs, different data can be collected. The velocity measurement sensors along with additional instruments and equipment can be used to determine the Coefficient of Restitution (COR) of the projectile. The COR is a unit less number between 0 and 1 derived from the ratio of

the velocity of the baseball after impact with the velocity of the baseball before impact. Figure 3-7 is a picture of the projectile impact test as assembled by SIRC.

Figure 3-7: NOCSAE Projectile Impact Test as Assembled by SIRC [10]

3.3. NOCSAE DOC ND-022

ND-022 focuses on helmet test preparation and is titled 'Standard Performance Specification for Newly Manufactured Baseball/Softball Batter's Helmet'. Most of the directives in this document are referenced from ND-001 and ND-021. However, Section 5.1~5.8 lists the procedure for baseball/softball batter's helmet impact attenuation tests. The relevant information

in section five relates to the position of the helmet in reference to the muzzle of the air cannon and the impact locations on the helmet.

ND-022 specifies that the headform fitted with a helmet must be positioned within twenty-four inches from the end of the muzzle of the air cannon or from the point of release of the baseball. The standard restates the properties of the baseball as cited in ND-021, but additionally it requires the baseball to have a COR range of 0.5~0.55. The test method stipulates that a minimum of three helmets should be tested at ambient temperatures. The first two helmets should be impacted with a softball at a velocity of 55mi./hr. (24.6m/s) at the mandatory locations tabulated in Table 3-3. The third helmet should be impacted with a baseball, with the same velocity, at the location that resulted in the highest SI reading of the two previously impacted helmets. ND-022 does not cover data acquisition. The fourth NOCSAE manual, and the second baseball specific document, summarizes the laboratory procedures for baseball/softball batter's helmet certification.

3.4. NOCSAE DOC ND-023

The objective of 'Laboratory Procedural Guide for Certifying Newly Manufactured Baseball/Softball Batter's Helmets' or ND-023 is to establish recommended practices for baseball/softball batter's helmet certification.

Similar to ND-022, the majority of the information in ND-023, such as laboratory environment, equipment calibration, and test set-up, is referenced from ND-001 and ND-021. The pertinent material is the list of required test equipment. Sections 3.1~3.7 itemize the necessary test equipment for helmet certification including the twin guide rods for the drop tower, headforms, ball propelling device, accelerometers, and other miscellaneous equipment. Primarily, ND-023 is a compendium of the information detailed in ND-001, ND-021, and ND-022. The standards and test methods covered in this section form a partial basis for the NOCSAE helmet

22

testing protocols. However, as will be discussed in the next chapter, in the context of this experimental analysis they served as peripheral guidelines for the generation of supplemental information.

4. CHAPTER 4 – HELMET TESTING STRUCTURE (HYBRID TOWER)

An examination of NOCSAE's catalogue revealed that load cells were not listed on the instrument lists and force measurement was not a requirement in the data acquisition process. It was in the need to fill that void where the aspiration of this experimental analysis resided, which was to enact minor modifications to the test method in order to generate beneficial quantitative data that could form a basis for comparison. The modifications included positioning accelerometers in strategic locations on the test structure with the intent of collecting readings to derive transfer functions. As previously mentioned, the alterations in the test method were implemented within the scope of the NOCSAE standards, and were intended to supplement those methods not take away from them. The following sections detail the design and construction of the helmet test structure and test method procedure.

4.1. Helmet Test Structure

The concept of this design was an apparatus which provided the capability to conduct both drop impact and projectile impact helmet tests. Essentially, the notion was to create a device that incorporated the test methods of ND-001 and ND-021. The embodiment of the design was a free standing hybrid drop-tower-pendulum structure.

The primary structural components of the device were the four-post tower with a base plate and a top plate, the modified I-beam pendulum attached to the top plate, a pedestal, and a linear bearing table. The secondary elements included the twin-rod guide assembly, the carriage, the DC powered hoist, and an anvil. Most of the structural components were fabricated from 6000 series aluminum including the carriage and the furnishings used to affix and secure the components. However, some minor elements, such as the guide rods were made of mild steel. To avoid metal deformation and to facilitate disassembly, the hybrid tower was constructed using gussets and bolts in place of welding techniques.

24

A 9-foot, 2 inch square post was attached to each corner of the base plate using two gussets and a 9-bolt pattern and to each corner of the top plate with two gussets and a 6-bolt pattern. The base plate was a 2 foot square, 1½ inch thick aluminum slab. Three T-slots were channeled along the entire width of the base plate. In addition, bolt holes machined through the entire depth of the plate were strategically located across its surface area. The T-slots were used to secure the linear bearing table, the pedestal, and the anvil to the base plate. The T-slots allowed the pedestal and the anvil to be moved laterally to the left and right of the structure's centerline. Also, the slots permitted the front edge of the linear bearing table to be adjusted within five inches of the front edge of the base plate. The bolt holes in the base plate were used to attach the tower to a granite pediment. This was in accordance with ND-001 which requires the base of the drop tower to be securely mounted on a stone foundation. The top plate was a 2 foot square, 1 inch thick aluminum slab with a square pattern of holes spaced 5 inches apart across its surface area. The holes were used to attach the DC powered hoist and the gussets for the pendulum to the top plate. Figure 4-1 is a SolidWorks® schematic of the conceptual tower design and Figure 4-2 is a full length view of the Hybrid drop tower without the pendulum attached.
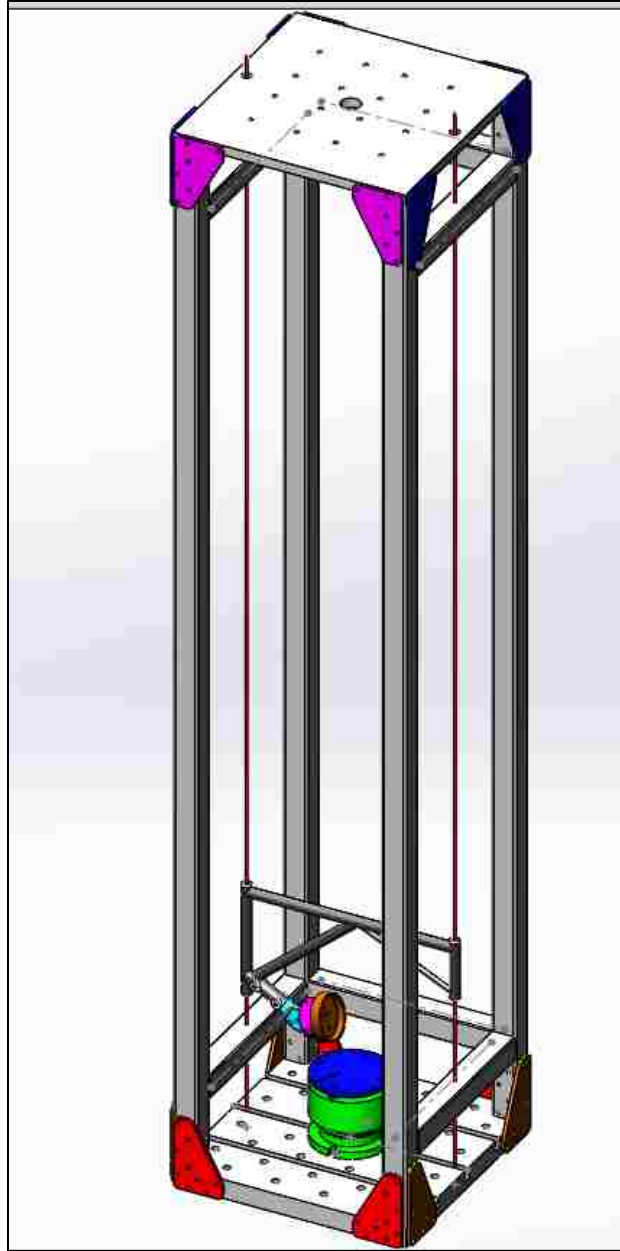
Figure 4-1: SolidWorks Conceptual Hybrid Tower Design

Figure 4-2: Full Length View of Hybrid Impact Tower

4.2. T-beam Pendulum

The pendulum was a modified I-beam device intended to simulate the projectile test method of ND-021.

The completed pendulum consisted of a 7½ feet long tapered 6000 series aluminum T-beam with a flange width of 3.44 inches and a thickness of 0.34 inches. The tapered T-beam was created by removing one of the flanges of a six foot I-beam and then cutting an 18 inch angled wedge from the end. The tip of the wedge was machined to create a smooth flat surface on the 'T' side; this end would serve as the free end of the pendulum. Subsequently, the wedge was welded edge to edge to the same end from which it was cut in order to bring the beam to the required length of 7½ feet (90 inches). In its mounted position, the top of the beam was attached to a rod which was supported by two gussets bolted to the top plate of the tower. Linear bushings were used to fit the bolt to the gussets thus allowing the pendulum to swing through the front plane of the tower. The total mass of the T-beam was 19.21lb (8.71kg).

A four inch slot was cut through the free end to provide a means to secure measurement instruments, the baseball, and other devices to the end of the pendulum. A bolt fastened through the slot was the anchor for the attachments. The non-impact side of the bolt was threaded and used to bolster the pendulum bob, which could also serve as the added mass of the pendulum. The head of the impact segment of the bolt was tapped to accommodate the screw on the non-impact face of the load cell. Finally, a specially fabricated concave adapter designed to cradle the baseball was coupled to the threaded hole on the impact face of the load cell. The physical arrangement of those components was pivotal in the execution of the experimental analysis mainly because it provided a means to mount a load cell between the baseball and the free end of the pendulum. In addition, an accelerometer could be mounted to the adapter.

The significance of this strategy was the ability to measure the acceleration of the pendulum, hence the baseball, but more importantly the force of the impact into the baseball and subsequently into the helmet-headform assembly. To iterate, the measurement of the force of the impact albeit central to the analysis, is not a requirement under NOCSAE standards. The effective mass of the pendulum was 11.0 lb. (4.989 kg). Figure 4-3 is a SolidWorks® illustration of the T-beam. Figure 4-4 depicts the pendulum suspended from the top plate of the tower, and Figure 4-5 is a close up view of the free end of the pendulum showing the adapter and the load cell. The two other major elements, the pedestal and the linear bearing table, were designed to be interchangeable depending on the capacity in which the hybrid tower was being used.
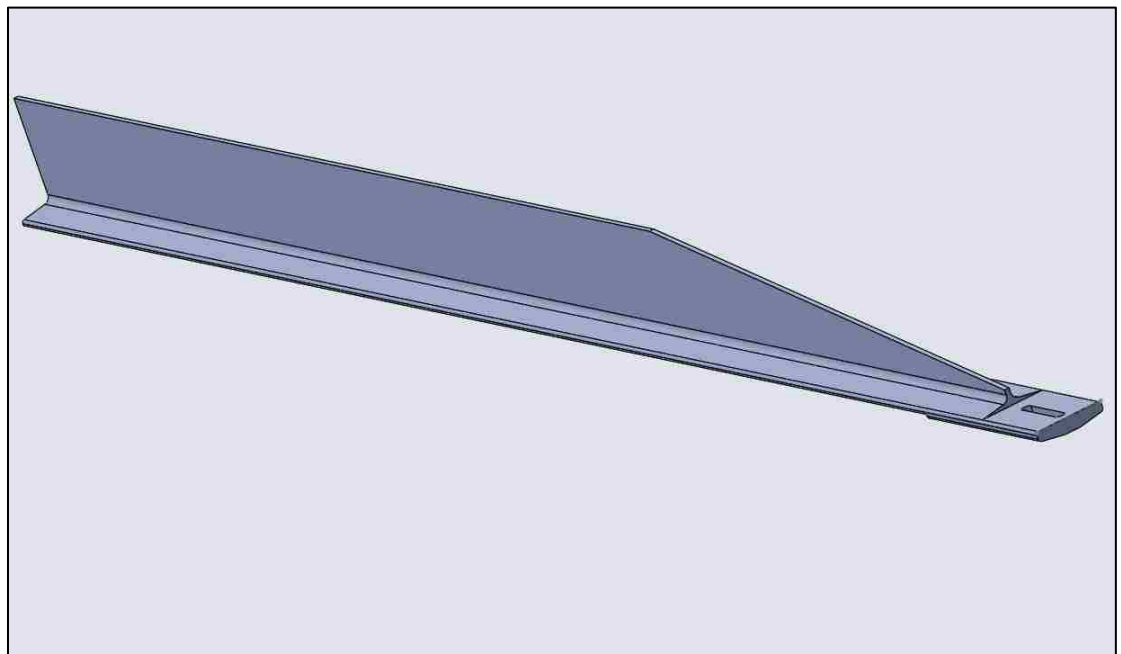
Figure 4-3: SolidWorks Illustration of Tapered T-Beam

Figure 4-4: Pendulum Suspended from Top Plate of Hybrid Tower

Figure 4-5: Free End of Pendulum with Load Cell & baseball Adapter

4.3. The Pedestal

The pedestal was designed to be utilized in either the drop tower or pendulum application. The pedestal could be used to accommodate a second headform fitted with a helmet. Ergo, in the drop tower capacity a helmet on helmet impact can be implemented, which as alluded to earlier, represents a more realistic simulation of the impacts that occur in football.

The primary components of the pedestal included four ¾ inch thick gussets and a two inch square center post, all made of 6000 series aluminum. Each gusset was secured to a face of the center post with four bolts and extended four inches beyond the post.

31

A 1.1 inch diameter vertical hole was machined through most of the length of the center post. In addition, two horizontal holes were machined through the entire width of the center post, and in the corresponding location on two of the gussets. The vertical hole was used to accommodate the headform rotator shaft and the horizontal holes were for the bolts used to secure the rotator shaft to the pedestal. The pedestal was secured to the tower with the use of clamps and the T-slots in the baseplate. However, it could be rotated to change the impact location on the headform. The mass of the pedestal was 9.10lb (4.128 kg).

During pendulum testing, the pedestal was used to position and hold the headform in place for static impacts. The pedestal did not allow the headform to move after impact, as required by ND-021, hence the collision was partially inelastic and enabled a more accurate measurement of the force of the impact. Figure 4-6 is the SolidWorks® schematic of the pedestal with the headform rotator shaft, and Figure 4-7 depicts the pedestal mounted to the baseplate of the tower (inset: Pedestal). The third primary structural component of the tower, the linear bearing, table facilitated pendulum testing as well and it was consistent with the type of collision dictated by ND-021.
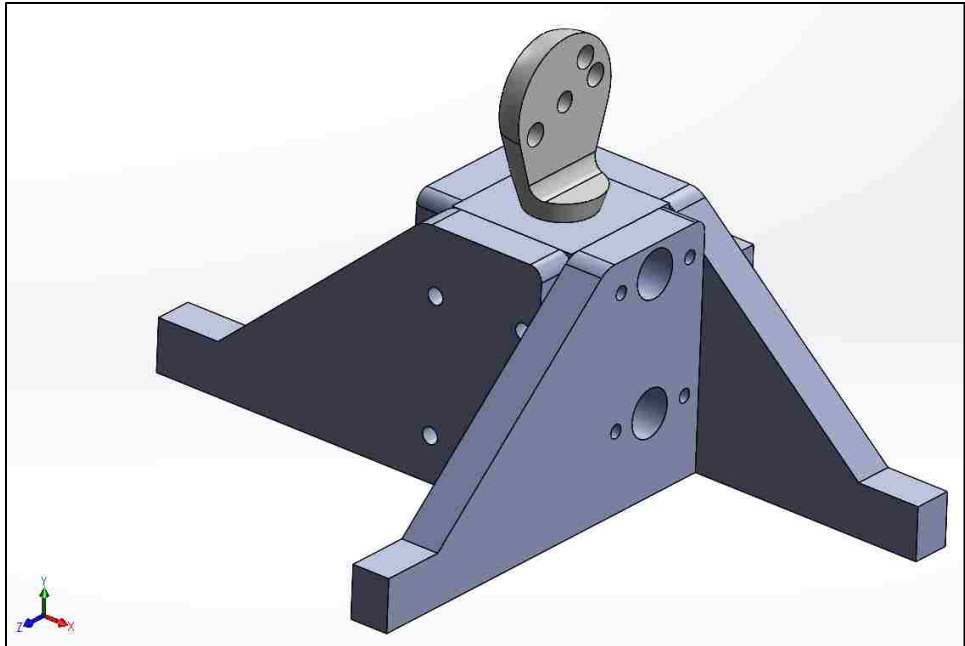
Figure 4-6: SolidWorks Illustration of Pedestal
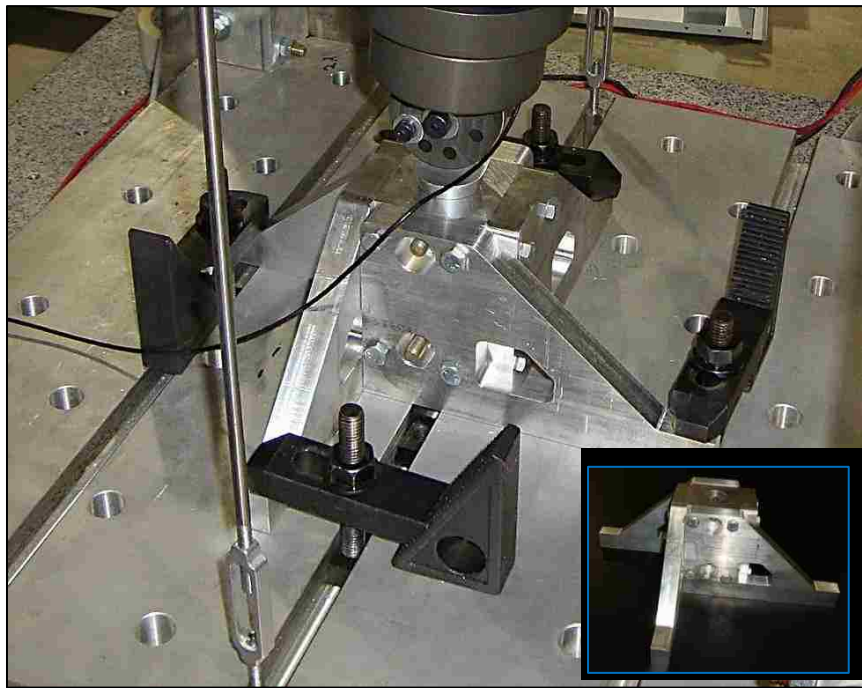
Figure 4-7: Pedestal Mounted to Baseplate of Tower (Inset: Pedestal)

4.4. The Linear Bearing Table

The Linear Bearing Table (LBT) possessed a design very similar to the concept illustrated in ND-021 and Figure 3-7. The top and base plates were fabricated from ½ inch thick 6000 series aluminum. The base plate was 10 inches by 36 inches and the top plate, used to support the headform, was 10 inches by 12 inches. A ¼ inch deep, 2 inch square hole was machined in the center of the top plate. This hole was used to secure the center post that housed the headform rotator shaft. The center post possessed the same characteristics as the one used for the pedestal. Linear bushings housed in pillow-blocks permitted the top plate, thus the headform, to traverse along the 36 inch long, ¾ inch diameter steel rods mounted to the base plate. Consequently, the movement of the headform after impact was more consistent with the somewhat elastic collision recommended by ND-021.

In order to keep the alignment of the headform with the baseball consistent between pedestal and LBT testing, the clearance between the top and base plates was 1/8 inch. However, this proved to be a challenge for securing the LBT to the base plate of the tower because the space did not allow the top plate to clear the heads of the bolts. Therefore, three measures were taken to alleviate the problem. First the grooves in the base plate used to hold the bolts were inset ¼ inch from the top surface of the base plate. Second, two 1/8 inch deep channels were cut along the entire length of the bottom of the top plate directly above the location of the grooves in the base plate. Finally, the heads of the bolts were machined down approximately one sixteenth of an inch. Ultimately, enough room was created to remove any impediment between the two plates. The mass of the top plate of the LBT was 9.23lb (4.187kg). Figure 4-8 is a SolidWorks® illustration of the linear bearing table, and Figures 4-9 and 4-10 depict the linear bearing table alone and as it was mounted to the base plate of the tower respectively.
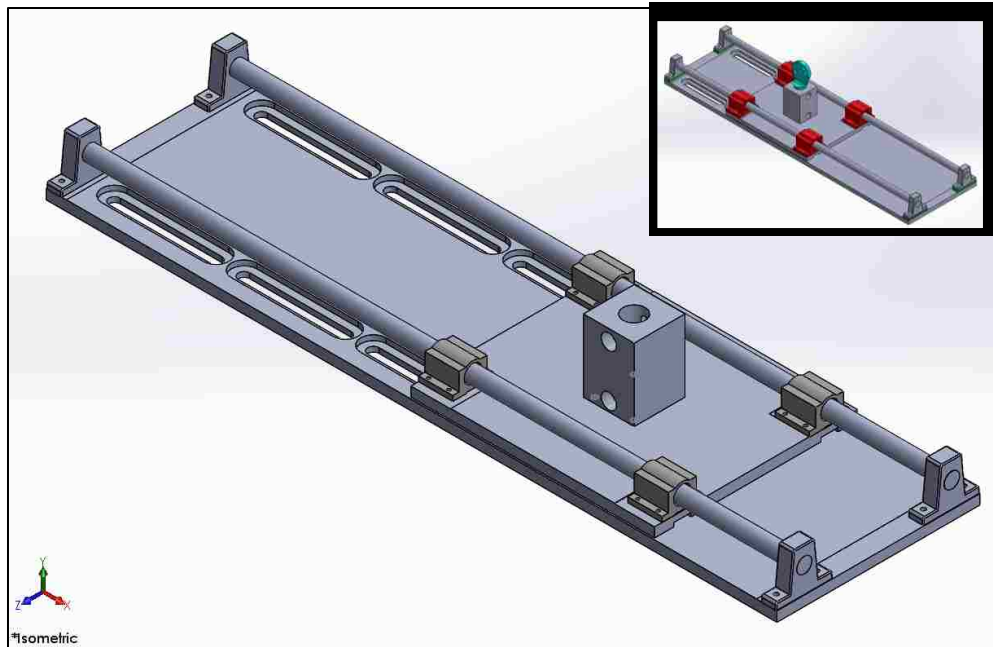
Figure 4-8: SolidWorks Illustration of the Linear Bearing Table Conceptual Design
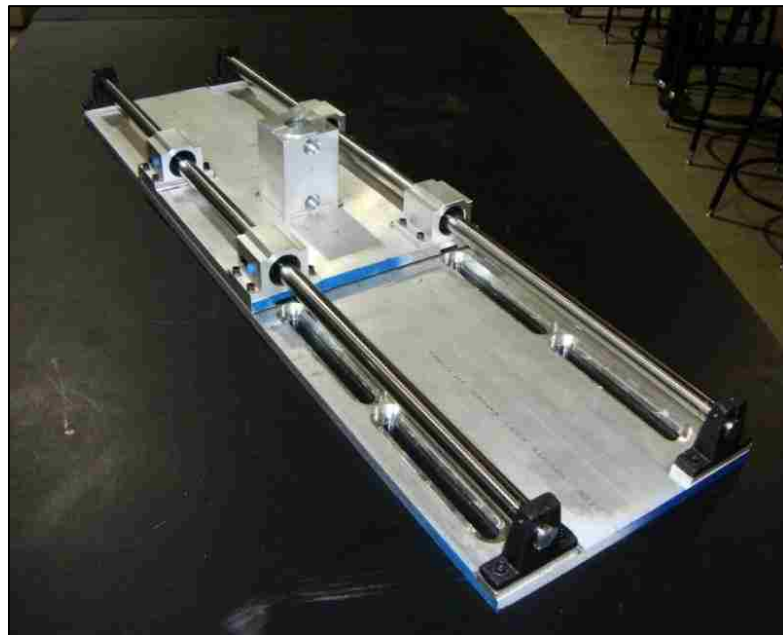
Figure 4-9: Linear Bearing Table (LBT)
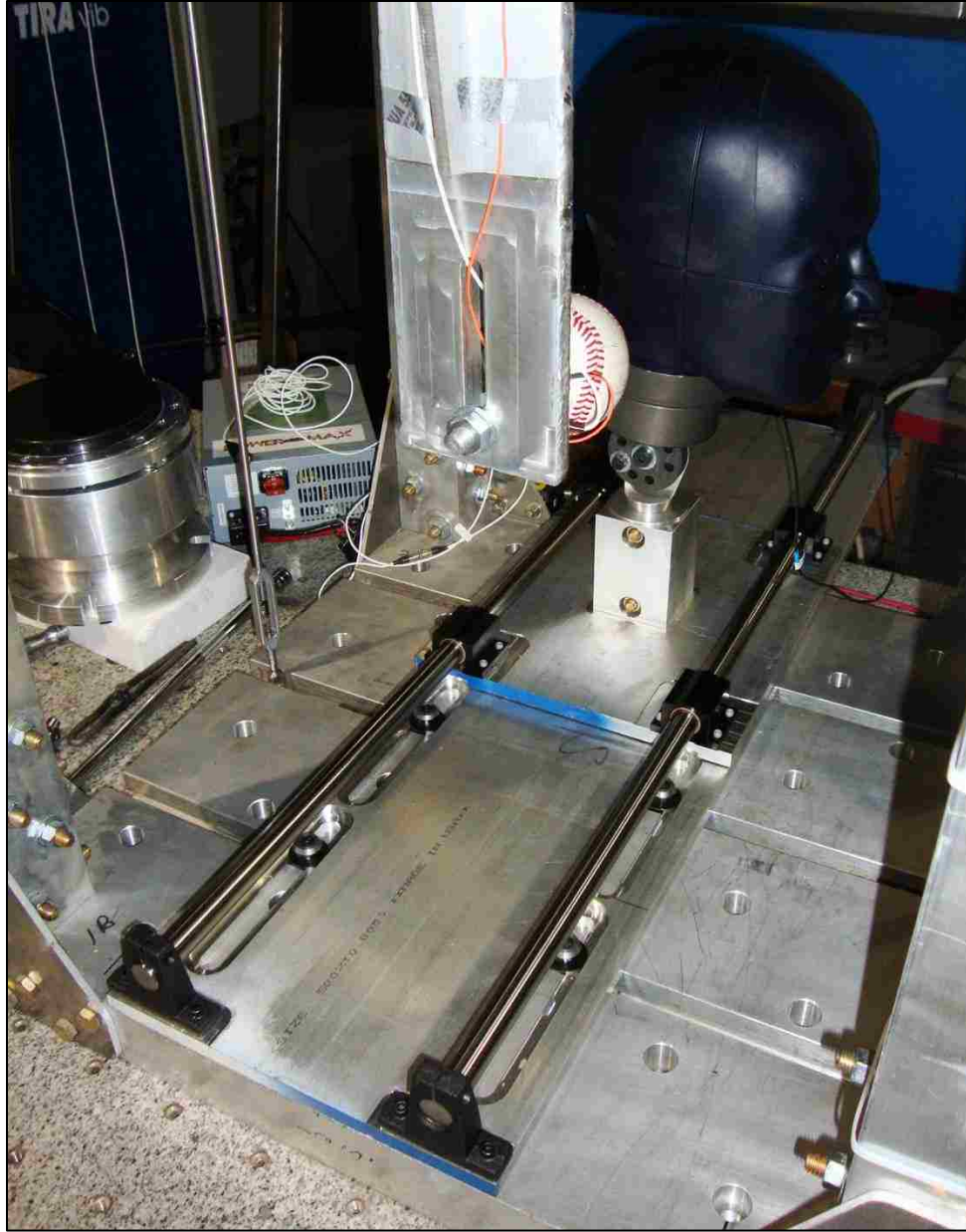
Figure 4-10: LBT Mounted to Baseplate of Tower

4.5. Secondary Components

The secondary elements of the hybrid tower, such as the twin-rod guide assembly, the carriage, the anvil, and the DC powered hoist, were all consistent with test method of ND-001.

The anvil however was slightly altered. A tapped hole, used to attach a load cell, was inserted on the top surface of the anvil. Also, some clearance space was machined on the bottom surface of the plate holding the MEP pad to ensure that the load cell would not be damaged during an impact. These modifications allowed the force of the impact of the helmet with the anvil to be measured. The force measurement provided supplemental data not required by ND-001. Figures 4-11, 4-12, and 4-13 are pictures of the twin-rod guide assembly/carriage, the anvil, and the DC powered hoist respectively.

This section revealed that there were some comparable and contrasting hardware characteristics of the hybrid tower with NOCSAE's drop tower and projectile method. Table 4-1 itemizes the similarities and differences in those characteristics. In the upcoming   chapters the topic delves into the testing procedures including the software and hardware (chapter 5), and test helmets (chapter 6). Wherever it was relevant, the differences or similarities between the test method used in this analysis, including the impact properties that were measured and acquired, and those prescribed by NOCSAE were be highlighted.
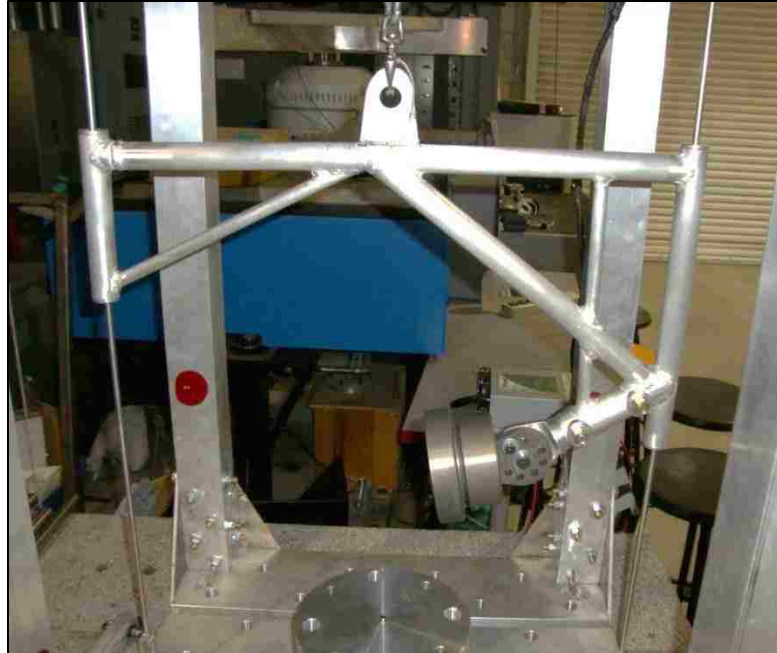
Figure 4-11: Twin-Rod Guide Assembly with Carriage

Figure 4-12: Anvil (Inset: Anvil with MEP Pad)
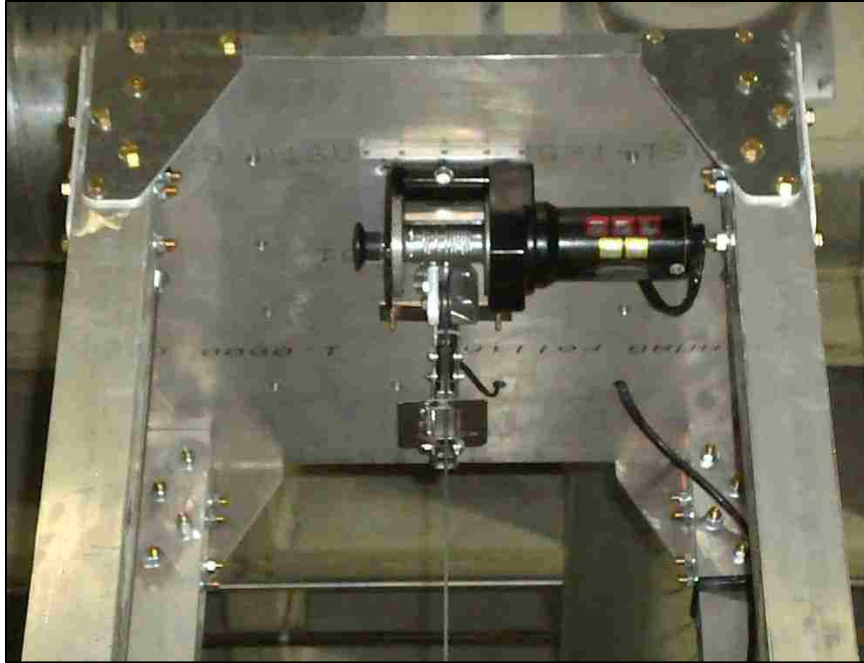
Figure 4-13: DC Powered Hoist

Table 4-1: Characteristics of Hybrid vs. NOCSAE Tower & Projectile Impact Test

Characteristic	Hybrid Tower	NOCSAE Drop Tower	NOCSAE Projectile Impact
Mount	Free Standing, Anchored to Granite Pediment	Attached to Wall, Anchored to Concrete Surface	Housed on Rack
Impact Type	• Drop • Pendulum (Projectile)	• Drop	• Air Cannon (Projectile)
Helmet Testing Capability	• Football Helmet to Anvil • Football Helmet to Football Helmet • Baseball to Baseball Batter's Helmet	• Football Helmet to Anvil	• Baseball to Baseball Batter's Helmet
Measurement Instruments	• Tri-Axial Accelerometer • Piezoelectric Miniature Accelerometer • IEPE Force Sensor	• Tri-Axial Accelerometer	• Tri-Axial Accelerometer • Velocity Sensor

5. CHAPTER 5 – ANALYSIS SOFTWARE AND HARDWARE TOOLS

Comprehensively, this experimental analysis was developed to acquire data to supplement the information produced when the test methods of ND-001 and ND-021 are conducted. NOCSAE uses the KME 200 Data Analyzer for post-processing data, and the standards do not endorse a system by a specific manufacturer. However, the standards do require that a data analyzer with capabilities equivalent to the KME 200 and a computer equipped with the appropriate software be employed. As with most empirical research, the backbone of this experimental analysis was the software and hardware devices that comprised the data acquisition system. Consequently, this chapter provides an account of the software and hardware constituents of the system.

5.1. The Data Acquisition System

Brüel & Kjær's PULSE® is an analyzer platform used in Vibroacoustic, Electroacoustic, and Structural Dynamic applications. The system possesses real-time data acquisition, data management, and post-processing capabilities. The PULSE® platform contains software and hardware facets, both of which were utilized in this analysis. The following sections expound on these two elements citing equipment specific to this experiment.

5.1.1. PULSE® Software

Most experimental measurement procedures can be disseminated into a logical sequence of events. The logical sequence of events includes transducer conditioning, basic measurement analysis, post-processing of analyzed data, and the display of results. For this analysis the PULSE® graphic user interface was used to initiate and carry-out the logical sequence of events. In PULSE® each event within the sequence is implemented with an Organizer function. The event and its corresponding Organizer function within PULSE® were as follows:

- Transducer Conditioning: Implemented with the 'Configuration Organizer'

- Basic Measurement Analysis: Implemented with the 'Measurement Organizer'

- Post-processing of Analyzed Data: Implemented with the 'Function Organizer'

- Display of results: Implemented with the 'Display Organizer'

Within the PULSE® environment, the Organizer functions are located in the dropdown menu of the 'Organizer' tab on the toolbar and are outlined in the following sections.

5.1.1a. Configuration Organizer

The Configuration Organizer was used to set-up the front-end configuration of PULSE®. This tool was used to select the accelerometers from the 'Transducer Database'. The accelerometers were listed by serial number in the database. There is also an option to add accelerometers to the transducer database if they are not already listed. In addition, accelerometer properties such as sensitivity can be adjusted in the transducer database dialog box. Once the accelerometers were selected (or added) the serial number appeared in the dropdown queue of the 'Configuration Organizer'. Right clicking on the highlighted accelerometer serial number opens the Configuration Properties window, which provides a summary of the accelerometer settings and properties. As with most windows based software, the accelerometer can be renamed by double clicking on its icon in the dropdown queue.

Four accelerometers and the load cell were added to the database for testing including the tri-axial accelerometer in the headform and the miniature accelerometer for the baseball adapter. The miniature accelerometer was positioned on the baseball adapter during pedestal and LBT testing and could be positioned on the proposed headform adapter during drop tests. The headform adapter is discussed further in Chapter 8. Figure 5-1 illustrates the Configuration Organizer and the Configuration Properties while Figure 5-2 depicts the Transducer Database window.

41
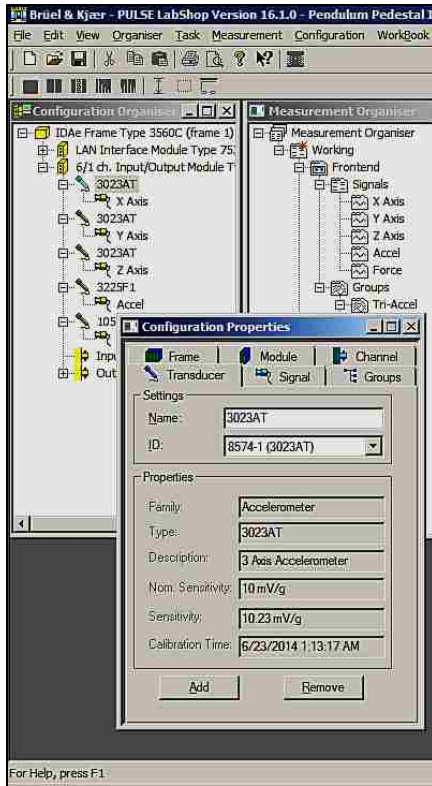
Figure 5-1: PULSE Transducer Configuration Organizer/Properties
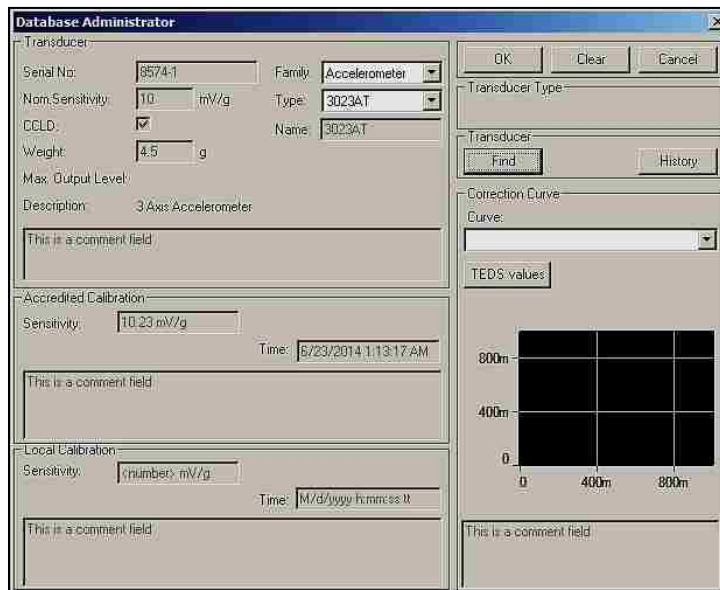
Figure 5-2: PULSE Transducer Database Administrator

5.1.1b. Measurement Organizer

The Measurement Organizer provided basic auto and cross-spectral data, and time functions when available. This function was used to group the accelerometers as well as to select and assign the type of analyzer used to evaluate the accelerometer signals. In the dropdown queue of the measurement organizer the accelerometers were arranged in logical groups by right clicking the word 'Group' choosing 'Insert signal' and selecting the appropriate accelerometer. Further, one or more analyzers could be assigned to each group based on the type of analysis required. The FFT analyzer was used for this analysis and it was applied to the accelerometer and the force signals. It uses the Fast Fourier Transformation algorithm to calculate a spectrum from a time domain signal.

Right clicking on an accelerometer in the queue opened the properties window for that particular accelerometer. In this window the sensitivity, offset, and gain of the accelerometer could be adjusted. Likewise, right clicking on an analyzer opened the properties window for that analyzer. Properties such as frequency lines, bandwidth, and averaging mode were adjusted in this window. In addition to assigning analyzers, the Measurement Organizer was also used to set-up the test trigger. The trigger was a system feature that allowed the system to start and stop collecting data at a specified time or event. For each test, the trigger was assigned to the load (force signal) cell and set to start collecting data 5 milliseconds before impact and stop collecting data after the impact. Figure 5-3 is a screenshot of the Measurement Organizer queue displaying the Accelerometer and Force (load cell) groups, Figure 5-4 is the properties box for an accelerometer, Figure 5-5 shows the FFT analyzer property box, and Figure 5-6 illustrates the Trigger setup box.

43
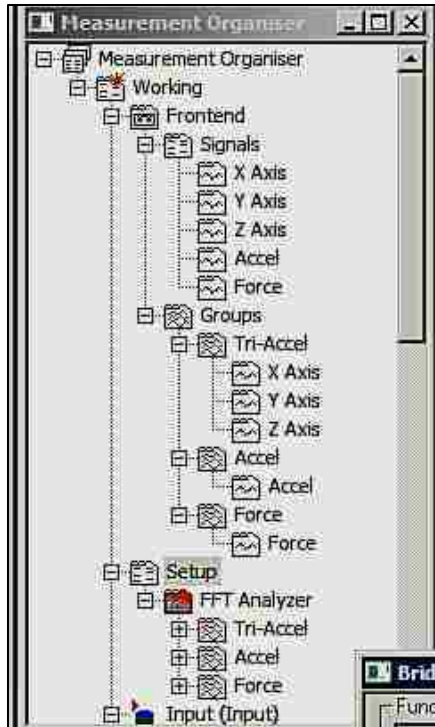
Figure 5-3: PULSE Measurement Organizer
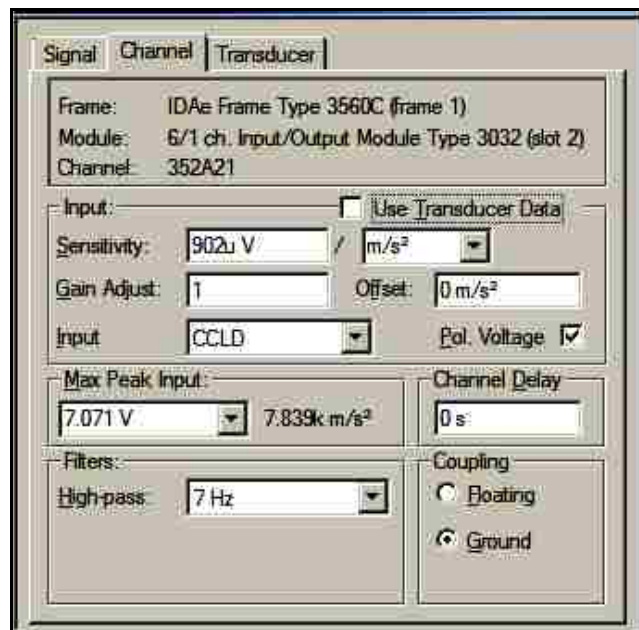
Figure 5-4: PULSE Signal/Transducer Measurement Property Box
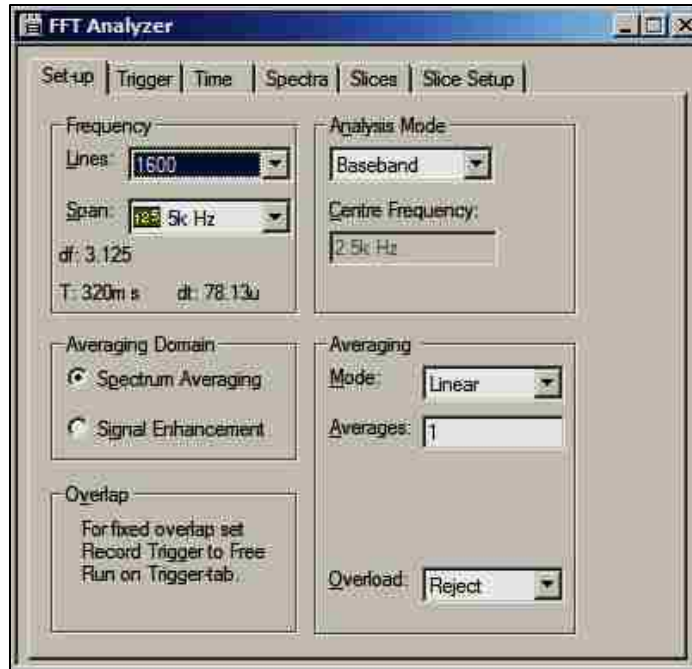
Figure 5-5: PULSE FFT Analyzer Property Box
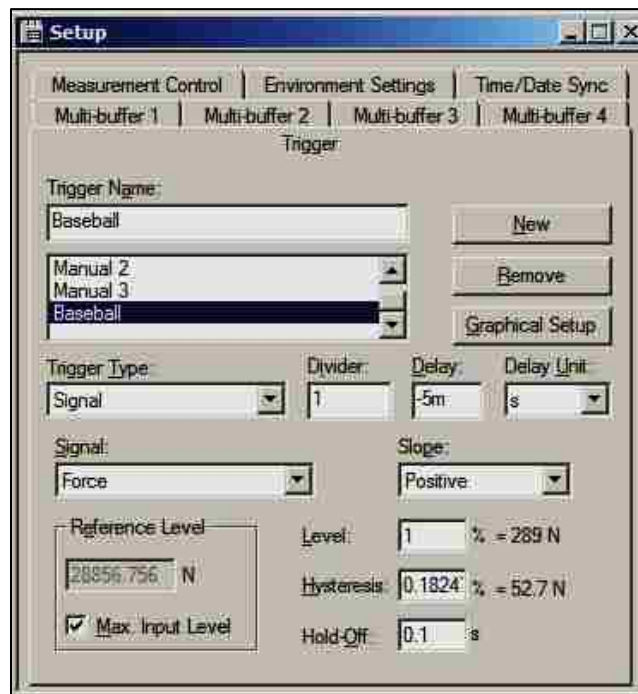
Figure 5-6: Trigger Properties Set-up Box

45

5.1.1c. Function Organizer

As the name implies, this tool was used to implement various functions used to analyze the signals measured by the load cell and the accelerometers, and its main use was the post-processing of the data. Analyzers were used to apply the selected function to the accelerometers. For each test in this analysis the Time function was applied to each axis of the Tri-Axial accelerometer in the headform, to the accelerometer attached to the baseball adapter, and to the load cell. In addition, the Frequency Response H2 function was applied to each axis of the Tri-Axial accelerometer in the headform.

The Time function allowed measurements to be acquired as a unit of measure versus time. Hence, in the case of the load cell the data was represented as Newton (N) versus time (sec). Accordingly, the accelerometer data was exhibited as acceleration (m/s^2) versus time (sec).

The Frequency Response H2 generated a mathematical representation, in terms of spatial or temporal frequency, of the relation between the input and output of a linear time-invariant system, commonly referred to as a Transfer Function. The Transfer Function of interest in this analysis was the ratio of the output acceleration to the input acceleration. The corporeal embodiment of this was the ratio of the acceleration of the Y axis of the headform with the baseball adapter acceleration. The value of the resulting Transfer Function was of course a unit less (m/s^2/ m/s^2) number. Right clicking on a function in the queue opened the 'Function' window in which the function could be applied to a signal (accelerometer or load cell) and implemented by an analyzer. Figure 5-7 displays a screenshot of the Function Organizer with the Frequency Response H-2 property window visible.
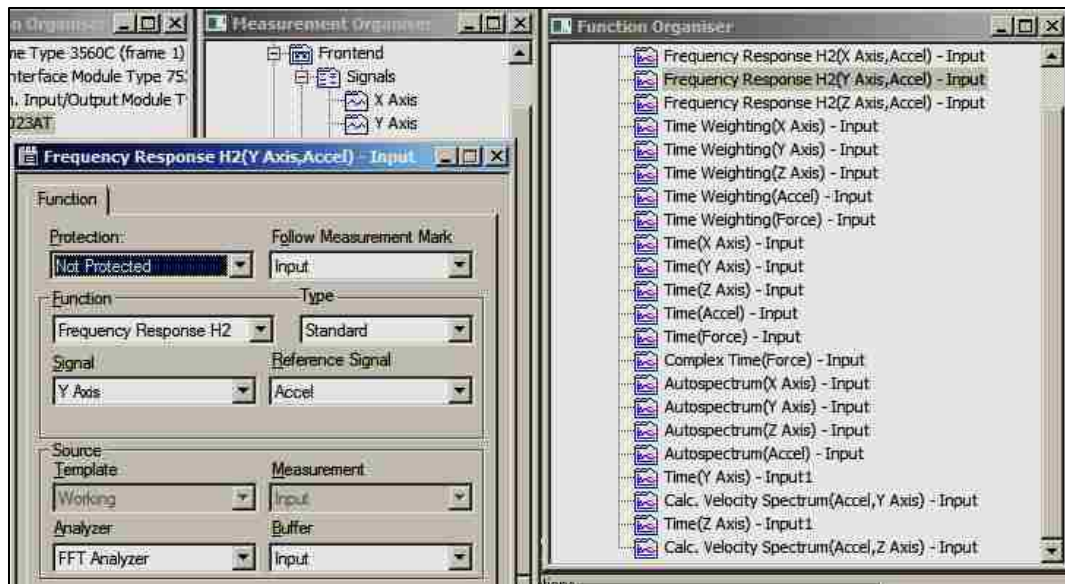
Figure 5-7: Function Organizer with Frequency Response H-2 Property Window

5.1.1d. Display Organizer and Workbook

The two remaining features that finalized the logical sequence of events were the Display Organizer and the Workbook. The Display Organizer was used to create and display graphical representations of the data processed by the functions. Right clicking on a function display in the queue opened the window used to format properties of the graph such as axis units, coordinates, and color palettes. The Workbook tool provided a way to save a desired screen layout. Once the organizers and displays were arranged in the desired setting, the layout could be saved in the Workbook dropdown queue. In addition, each layout could be uniquely named. Double clicking on the layout name in the Workbook queue opened that particular layout. Figure 5-8 depicts the Display organizer with the Workbook queue to the right.

Figure 5-8: Display Organizer and Workbook Queue

5.2. Hardware Components

The hardware components consisted of the measurement devices and the data acquisition module coupled to a computer equipped with PULSE®. The measurement devices included the PCB Piezotronics Type 352A21 accelerometer and the Dytran Model 1051V4 IEPE Force Sensor (load cell). The data acquisition module was the Brüel & Kjær Type 3560-C. The accelerometer was attached to the outer surface of the concave adapter used to cradle the baseball, while the load cell was bolted between the pendulum and the concave adapter with the use of tapped holes. The data acquisition module was capable of supporting six input channels, five of which were utilized. Channels 1 through 3 were used for the headform tri-axial accelerometer, channel four was occupied by the adapter accelerometer, and the load cell was connected through channel five. Figure 5-9 illustrates the accelerometer and the load cell in relation to the concave adapter and Table 5-1 itemizes the specifications of the hardware components used during the analysis.

48

This chapter covered the software and hardware tools used to conduct the impact testing analysis, in the subsequent chapter the discussion targets the test methods and procedures that were implemented using these tools. Further, the validation of each method is assessed by virtue of its adherence to the corresponding NOCSAE procedure.
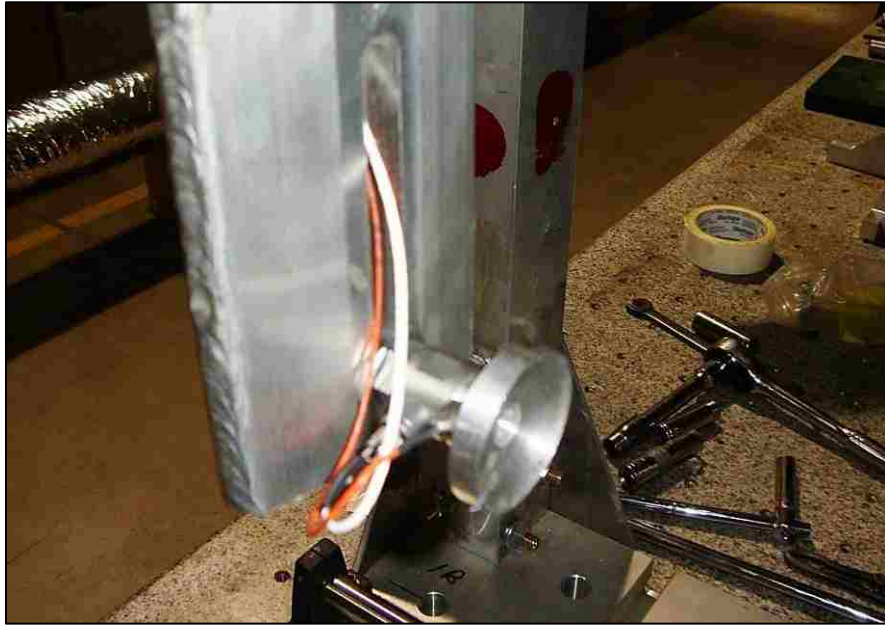
Figure 5-9: Load Cell & Accelerometer Attached to Concave Baseball Adapter

Table 5-1: Specifications of Data Acquisition Hardware Components

Component	Manufacturer /Purpose	Specifications
	PCB Piezotronics/ Measurement Device: Accelerometer placed on baseball adapter.	Sens. (±15 %) =0.25 mV/(m/s²) Meas. Range = ±19600 m/s² pk Freq. Range (±5 %) = 1.0 to 10000 Hz Freq. Range (±10 %) = 0.7 to 13 kHz Freq. Range (±3 dB) = 0.3 to 20000 Hz Res. Freq. = ≥80 kHz Brdband. Res. (1) = 0.1 m/s² rms Temp. Range = -65 to 250 °F Excitation Voltage = 18 ~ 30 VDC Current Excitation = 2~20 mA Height/Weight = .14in/.02oz
	Dytran/ Measurement Device: Dytran model 1051V4 is an IEPE force sensor. Placed between Pendulum and baseball.	10 mV/lbf sensitivity 500 lbf compression range 500 lbf tension range 10,000 lbf maximum compression 500 lbf maximum tension 10-32 radial connector 1/4-28 tapped holes top and bottom 28 grams, Stainless steel High natural frequency IEPE
	Brüel & Kjær / Data Acquisition Module. Link between measurement devices and analysis software.	25 kHz analysis frequency range Six input channels Two generators with 25 kHz frequency range

6. CHAPTER 6 - HYBRID TOWER IMPACT TEST METHODS AND ROCEDURES

Initially, this analysis was inspired by the motivation to build and validate a drop impact tower to examine and quantify shock to the head through reliable and repeatable testing procedures. The tentative proposal involved conducting drop impact tests on football helmets using the anvil as the impact surface. However, the unpredictable nature of building and testing an experimental structure and the incongruences between predicted results and observed results altered the trajectory of the inquiry. As a result the latest embodiment of the project focused on a different objective and encompassed greater detail than the original proposal.

The evolved mission still included validating the tower, but projectile impact testing of baseball batter's helmets became the centric theme. Indeed, the methods of ND-001 & ND-021 and the specifications of ND-022 & ND-023 remained the governing statutes. Ergo, test protocols such as helmet impact locations and baseball properties were consistent with those standards. In general, the only significant modifications included using a pendulum to deliver the projectile impact, adding static impacts using the pedestal, and the acquisition of force data. The following sections outline the test methods in the same order as each of the relevant NOCSAE standard in the continuing effort to exhibit the similarities and or differences in each approach.

6.1. Hybrid Tower Helmet Test Methods

In the spirit of order and completeness, the methods and specifications used in this analysis will be outlined as they applied to each standard successively from ND-001 through ND-023.

6.1.1. Test Methods As They Applied To ND-001

Most of the information covered in ND-001governs the administration of football helmet drop impact testing and manufacturers' responsibilities for helmet certification, which was

outside the scope of this analysis. The regulations that were common to all helmets tested including conditioning environment, instrument calibration, and system checks were adhered to and are addressed below.

Conditioning Environment

a) The standard requires helmets to be exposed to the testing environment a minimum of four hours prior to testing. During testing, the helmets were placed in the test environment within twenty-four hours, but no less than twelve hours prior to testing.

b) In accordance with the standard, the temperature in the testing environment was maintained within the stipulated range of 72 F° ±5 F° (22 C° ±2 C°). Note*: Low temperature [32 F° (-3 C°)] and High temperature [115 F° (46 C°)] tests were not conducted.

 Instrument Calibration

a) The only calibration requirement was that the data acquisition system correctly calculated Severity Index (SI) values ±3% across a range of 300 SI to 2495 SI. It must be noted that SI values were not determined by the data acquisition system, but by post-processing of the data acquired by the system.

System Checks

a) Trial runs were conducted before each battery of tests to ensure connections were secure and to verify that PULSE® was functioning as required. System checks were also performed after a software crash or an anomalous test result.

6.1.2. Test Methods As They Applied To ND-021

ND-021 outlines the method for protective headgear and projectile impact testing. Therefore, at this point it is fitting to address the differences in the method of the experimental

analysis and this standard. First, although the analysis complied with the regulation regarding the properties of the baseball, the projectile itself was not evaluated. Second, a pendulum was used to deliver the baseball to the headform in contrast to an air cannon. Finally, in addition to mounting the headform on a linear bearing table, the headform was also tested in a static position using the pedestal. The following stipulations were respected as they applied to this analysis.

Headgear/Baseball Construction, Labeling, and Position

a) The headgear used during testing was fabricated to remain on the wearer's head during impact. The two batter's helmets were made of rigid, durable material that would be considered resistant to weather elements. Helmet A was made of carbon fiber and Helmet B was made of plastic. The Pitcher hat however, was constructed of fabric and could not be considered resistant to weather elements. Helmet A and the Pitcher hat were clearly labeled with the name of the manufacturer, but only Helmet B, considered an amateur helmet, and the Pitcher hat were labeled with the size.

b) The headgear was placed on the headform as per the standard, but the experiment deviated from the standard in regards to the distance between the projectile and the headform prior to executing a test. In tests using the pedestal and the linear bearing table, the headform was positioned so as to barely touch the baseball as the pendulum hung in its unimpeded vertical position. On the other hand, ND-021 requires the headform to be at or within twenty-four inches from the nozzle of the air cannon prior to the initiation of a test. Figure 6-1 is a picture of the three-sample headgear that was tested and Figures 6-2 through 6-4 are views of the inside of each headgear. The padded inner lining of the Pitcher hat significantly affects the value of the measured impact velocity, as will be stated later.

Figure 6-1: Sampled Headgear: Helmet A, Helmet B, and Pitcher Hat

Figure 6-2: Inner Surface of Carbon Fiber Helmet A

Figure 6-3: Inner Surface of Plastic Helmet B

Figure 6-4: Inner Surface of Fabric Pitcher Hat

c) The baseball was a Rawlings® Corked/Rubber Pill Yarn Wound Core ball. The ball was within the physical property guidelines with a weight of 141.7 grams and a circumference of 9 inches. Determining the Compression-Deflection and Coefficient of Restitution (COR) for the baseball was not within the scope of this analysis. However, NOCSAE standard ND-027 recommends using the guidelines stipulated by the American Society of Testing and Materials (ASTM) regulation F1887/1888 for calculating those values.

Test Instruments and Equipment

a) The list of suggested equipment included a projectile launching device, strike plate, electronic speed monitors, and a compression measuring device. In addition the standard required that the combined weight of the moving top layer of the LBT and the post to support the headform be no greater than 5.7 kg ±0.5 kg (12.57 lb. ± 1.1 lb.) As previously mentioned, the pendulum was used in place of an air cannon and the compression-deflection was not determined. Also, neither a strike plate nor electronic speed monitors were utilized. However, the combined weight of the top plate of the LBT and the headform support post was within the prescribed weight at 9.23 1b.

6.1.3. Test Methods As They Applied To ND-022

The crucial aspects of ND-022 that the experimental analysis abided by included impact locations and test requirements.

Impact Locations

a) The benefit of delivering the impacts to the helmet locations specified by ND-022 was the ability to form a congruent basis for comparison of results with findings of other analyses. However, during pedestal and linear bearing table testing only right side 90° impacts were delivered to the headform and each headgear. Figure 6-5 is a sketch taken form ND-022

showing the impact locations on the baseball batter's helmet and Figure 6-6 depicts the position of the head for right side impacts on a linear bearing table.
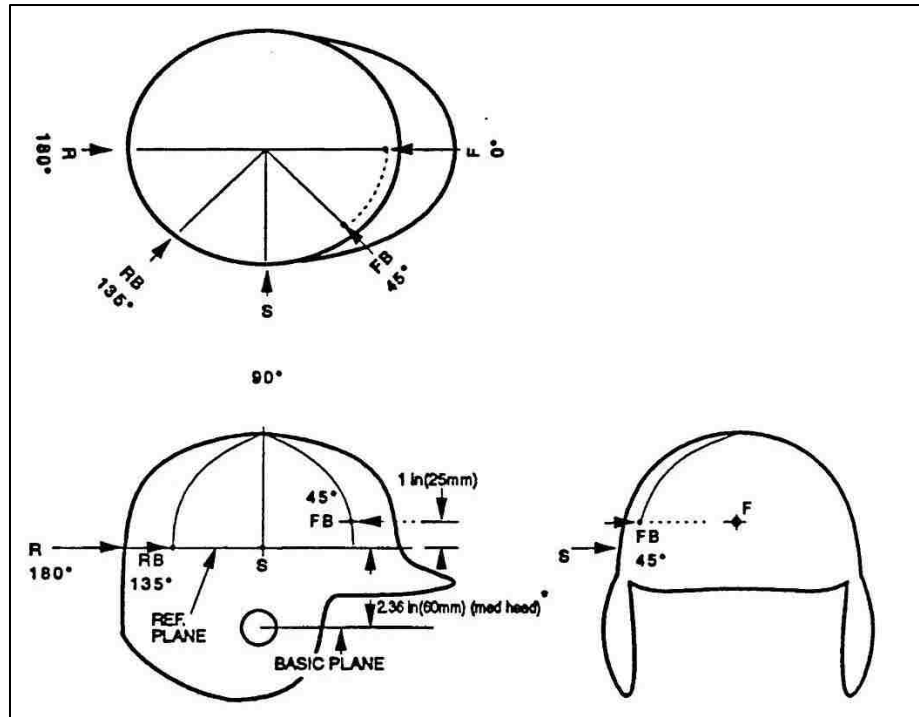
Figure 6-5: NOCSAE Impact Locations for Baseball Batter's Helmet
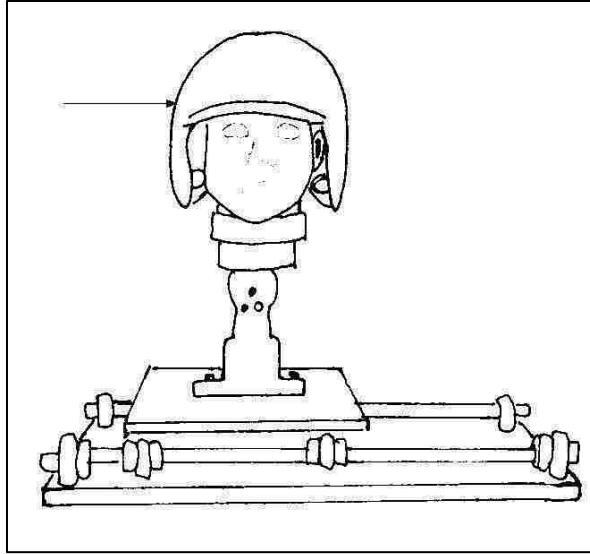
Figure 6-6: Right Side Helmet Impact on Linear Bearing Table

Test Requirements

a) Helmets may shimmy out of position after an impact; fortunately the standard allows the repositioning of helmets for proper fit after impact. Although the headform and each helmet was impacted several times (at least 5) during any particular test, only one sample of each helmet model was tested. In contrast, ND-022 requires three of each helmet model to be tested.

6.1.4. Test Methods As They Applied To ND-023

ND-023 is a laboratory procedural guide for certifying newly manufactured baseball helmets. Essentially, it is a concise itemized list referencing the various stipulations put forward in ND-001, ND-021, and ND-022. Hence, the applicability that governed the other standards was pertinent to ND-023 as well.

6.2. Hybrid Tower Test Procedures

In Chapter 3 an overview of the four NOCSAE standards relevant to this experimental analysis was presented. In the previous section, the elements of the methods covered in those standards that were implemented in this project were presented. Those sections served as a backdrop for the focal point of this endeavor, which was the test procedure. In the upcoming sections the two primary elements of the test procedure are mapped, including the theoretical applications administered to the acquired data and the test process, which is covered in a subsequent section.

6.2.1. Theoretical Applications Administered to the Acquired Data

Applying theoretical equations to the data was guided by the paramount aspiration of the entire analysis, which was to discern and quantify certain empirical data for comparison with theoretical values. Empirical data was collected by two means, instrument and observed. Through the use of the load cell and the accelerometers, instrument collected data included the impact force and the impact acceleration of the pendulum and the Y axis of the headform. Observable collected data included the pendulum rebound height during pedestal tests and the LBT travel distance (which was not used for reasons forthcoming) after impact. In addition to the energy equations used to derive the theoretical values, two more equation driven values were calculated including the Severity Index (SI) and the Head Impact Criterion (HIC). In the succeeding sections the context will hone in on illuminating the details of the theoretical applications beginning with the development of the energy equations.

6.2.1a. Energy Equations as Applied to the Pedestal

As stated earlier, the energy equations were used to quantify the empirical data for comparison with theoretical values, the most important value being the impact velocity of the

baseball. Frankly, determining the actual value of the velocity of the baseball was the crux of the experimental analysis.

A sum-of-the-forces theoretical analysis of the pendulum to determine the baseball impact velocity would require calculating the moment of inertia of the T-beam relative to its point of rotation. Also, the corresponding equation would require taking the rotational viscous friction into account. Finally, the analysis would involve determining the applied torque. The resulting equation would yield angular acceleration and would be represented by the following equation;

$$\dot{\omega} = \frac{1}{ML^2} \left[-MgL\sin\theta - B\omega + \tau_a \right]$$
(6-1)

where **ML** is the moment of inertia of the T-Beam based on the assumption of a concentrated mass at the end, **B** is the rotational viscous friction of the bearings, τ_a is the applied torque, and $\dot{\omega}$ is the angular acceleration. Technical constraints precluded the calculation of the inertia and friction terms on the right hand side of equation 6-1 for the pendulum in the hybrid tower's test configuration. Therefore, in order to decipher what lay ahead and to move forward with the experimental analysis, a simplified assumption was made in regards to the pendulum analysis.

The decision was made to treat the pendulum not as a continuous beam, but as a massless rod with a lumped mass at the end. The starting point for the assumption was based on applying the energy equation using the moment of inertia of the pendulum about its point of rotation 'a'. In addition, to corroborate the assumption, the relationship between the angle that a pendulum arm subtends during its motion and the height above the equilibrium point was used in the starting derivation. Figure 6-7 is a picture displaying the relationship between the angle of the pendulum arm and the height above its vertical resting equilibrium point. The derivation of the energy equation that governed the pendulum based on the assumption follows Figure 6-7.

60
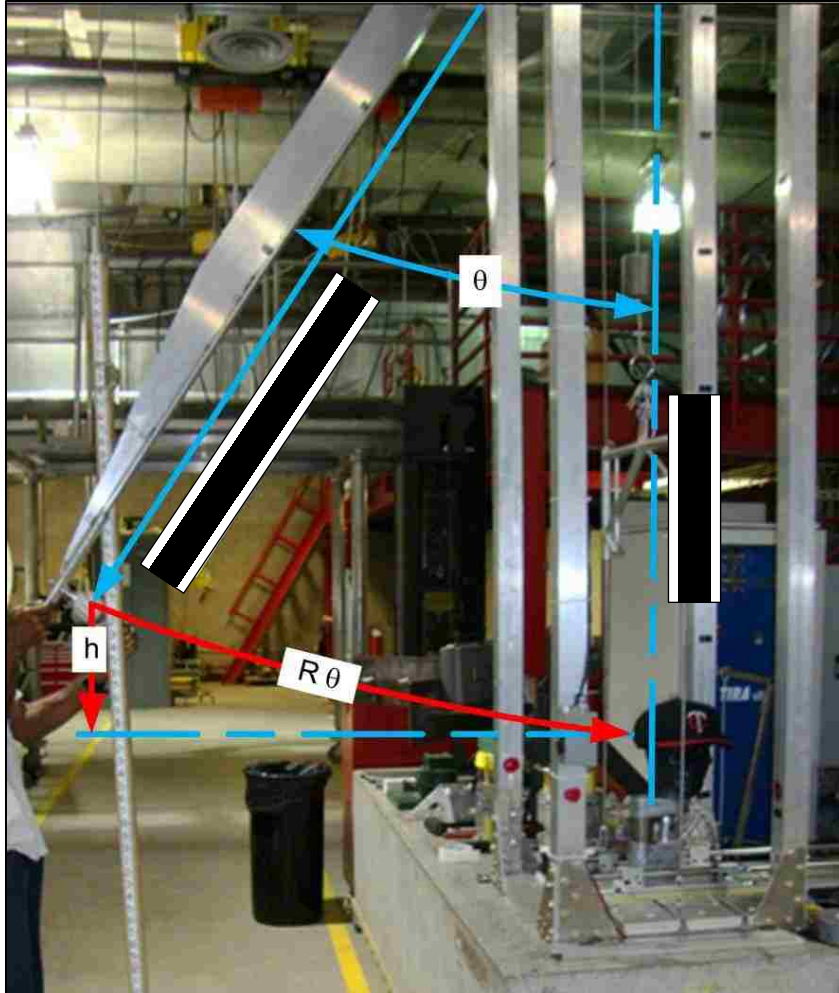
Figure 6-7: Simple Pendulum Physics as Applied to the Hybrid Tower

$$\frac{1}{2}J_a\omega^2 = mgL(1-\cos\theta) \tag{6-2}$$

$$\omega^2 = 2\frac{mgL}{J_a}(1-\cos\theta)$$

$$\omega = \sqrt{2\frac{mgL}{J_a}(1-\cos\theta)} \tag{6-3}$$

where $\mathbf{J_a}$ was the moment of inertia of the pendulum about its point of rotation 'a', $\mathbf{m}$ was the mass at the centroid of the pendulum, $\boldsymbol{\omega}$ was angular velocity, and $\mathbf{g}$ was the acceleration due to gravity.

In general, the principle that forms the foundation for the assumption is based on a simple pendulum with the mass concentrated at the end in an environment that neglects friction and air resistance as is shown in Figure 6-8.
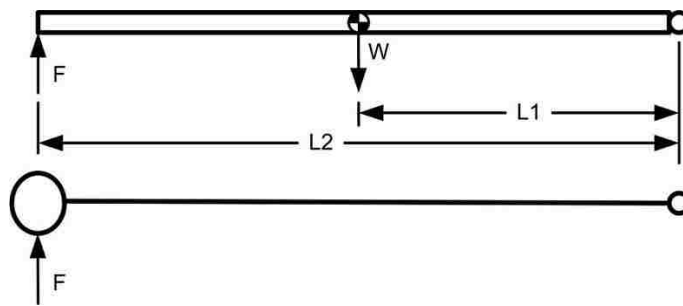
Figure 6-8: Rotation of a Uniformed Rod About its Center of Gravity

From Figure 6-8 it can be seen that the force required to rotate the rod can be determined by the following equation:

$$F = W\frac{L2}{L1} = m_P\, g \qquad\qquad (6\text{-}4)$$

where $\mathbf{F}$ is the required force, $\mathbf{W}$ is the weight measured at the center of gravity of the rod, $\mathbf{L1}$ is the distance from the end of the rod to the center of gravity, and $\mathbf{L2}$ is the entire length of the rod. The term on the right hand side of the equation ($\mathbf{m_p g}$) is the corresponding equation for force as applied to a massless rod with the mass concentrated at the end. In this case, the force ($\mathbf{F}$) was measured with the load cell and the effective mass of the pendulum, which was used for the value

of $\mathbf{m_p}$ was calculated by measuring the weight of the pendulum with a digital force gauge and then dividing that value by the acceleration due to gravity.

Once equation 6-4 was developed, proceeding with the analysis was simply a matter of using the appropriate values based on the set-up of the test system. Therefore with the assumption of a concentrated mass at the end the pendulum's moment of inertia about the pivot was $J = mL^2$. The rest of the derivation was as follows:

$$\omega = \sqrt{2\frac{m_p g L}{m_p L^2}(1 - \cos\theta)} \qquad (6\text{-}5)$$

$$\omega = \sqrt{2\frac{g}{L}(1 - \cos\theta)}$$

$$\text{Since } v^2 = L^2\omega^2$$

$$v^2 = L^2 2\frac{g}{L}(1 - \cos\theta) = 2gL(1 - \cos\theta)$$

$$v = \sqrt{2gL(1 - \cos\theta)}$$

$$v = \sqrt{2gh} \qquad (6\text{-}6)$$

where $\mathbf{v}$ was the theoretical tangential impact velocity of the pendulum and $\mathbf{h}$ was the vertical linear height measured from the tip of the pendulum to its equilibrium point at its resting position at the bottom, $\mathbf{m_P}$ was the effective mass of the pendulum, and $\mathbf{L}$ was the length of the pendulum. As the pedestal was a fixed structure, there was some rebound of the pendulum after impact. The hypothesis was that the sum of the rebound potential energy of the pendulum plus the kinetic energy of the baseball was equal to the potential energy of the initial position of the pendulum. Using energy equations, this hypothesis could be represented by implementing the following

derivation in which equation 6-6 could be modified to calculate the baseball velocity by incorporating the rebound height to yield the following equation:

$$m_P \, g \, h_1 = m_P \, g \, h_2 + \frac{1}{2} m_b \, v_b^2$$

$$v_b = \sqrt{\frac{m_P}{m_b} \left[2g \left(h_1 - h_2 \right) \right]} \qquad (6\text{-}7)$$

where m_b was the mass of the baseball and h_2 was the rebound height of the pendulum. Equations 6-6 and 6-7 served as the foundation for the analytical analysis of the pendulum, and both equations emerged from the assumption illustrated in Figure 6-8.

Obviously, this procedure constituted a rudimentary way of determining the theoretical velocity. However, the main tenet was to bear in mind that the length of a pendulum and the angle determine the maximum achievable tangential velocity at the base.

6.2.1b. Energy Equations as Applied to the LBT

The final desired destination when the energy equations were applied to the LBT was the same as for the pedestal with one adjustment. As the top plate of the LBT moved after impact, the pendulum did not rebound; consequently the assumption was that the total work energy performed by the pendulum was equal to the sum of the work done by the travel of the top plate of the LBT and the impact kinetic energy of the baseball.

It is well known that work energy is the product of force and distance traveled. Hence, an important factor was to consider if the work performed by the pendulum should have been calculated using the height (h) distance, which was the vertical linear path-independent distance traveled, or arc length, which was the rotational non-linear path-dependent distance traveled. Arc length was calculated as the product of the distance from the center of rotation to the point of interest (R), which in this case was the length of the pendulum and the angle θ, which was the

angle subtended by the pendulum arm. Unfortunately, many attempts to create a reasonably accurate model of the LBT using the energy equations based on the assumption were unsuccessful. One of the implications that may have precluded developing a justifiable model of the LBT is discussed further in chapter 8. Next the Severity Index (SI) is covered.

6.2.1c. Severity Index (SI)

The SI value is a unit less measure of the severity of impact with respect to the instantaneous acceleration experienced by the headform as it is impacted [8]. NOCSAE standard ND-021 requires that the headforms pass through a specific SI value within a specific impact velocity range. The data entered into the SI equation (2-1) was the x and y coordinate, time and acceleration values acquired by PULSE®.

The impact acceleration values calculated by PULSE® were represented in meters per second squared by default. As a result, each value was divided by 9.8067 m/s^2 to derive the acceleration due to gravity g. The imported value for time was the time duration from the zero acceleration value just after the trigger to the point when the first impact peak returned to zero or within a reasonable approximation of zero at that time stamp. The aim was to determine the SI value of the pulse, which was essentially the area under the peak point of the acceleration curve. The integration was executed in Matlab®, and it was carried out for each of the five drops for the adapter accelerometer and for the Y axis of the tri-axial accelerometer in the headform. The values for the Y-initial response of the headform tri-axial accelerometer were multiplied by -1 because they were negative due to its placement in the headform. An average SI was calculated for the four heights. Presently, it is worth mentioning that during pedestal testing an observable phenomenon lead to additional calculations.

After examining the graphs of the pedestal test results it was evident that for the Y tri-axial accelerometer in the headform, the area under the rebound acceleration peak appeared

greater than the initial impact acceleration peak. This observation inspired the decision to calculate the SI values for the second acceleration peak for the headform accelerometer. The Y-rebound acceleration values were positive and did not require multiplication by -1. The time duration, however was taken between the second and third time values at which the acceleration was zero. In the following chapters the hypothesis driven by the rebound phenomenon is explored in greater detail.

The reason for formulating the SI values during this analytical experiment was simply to form a compatible basis for comparison with NOCSAE standards. ND-021 requires that an appropriate response for the medium headform, the size used during testing, is to pass through 1200 SI within the velocity range of 36-44 mph. The ambition of the experiment was not to prove this criterion, but simply not to operate beyond it. Also, as mentioned in Chapter 2, studies by Pellman et al. have shown that concussions occur in athletes at an approximate SI value of 300 [6]. The other impact value derived was the HIC, which is discussed next.

6.2.1d. Head Injury Criterion (HIC)

The Head Injury Criterion (HIC) is a measure of the likelihood of head injury arising from an impact. It is a unit less value calculated using an average of the acceleration over a period of time during the impact. The HIC is a derivative of the Wayne State Tolerance Curve (WSTC), which was conceived to quantify head injury acceleration thresholds in vehicular impacts. However, the WSTC uses skull fracture as a criterion in contrast to brain injury or the onset of a concussion. Similar to the SI, the HIC is based on linear acceleration versus impact time duration. The time frame is usually between 3ms to 36ms with 15ms being the accepted standard. Also, the time frame is set to include the maximum acceleration pulse. The HIC is considered to be a more accurate measure of the severity of an impact because it is weighted with a time duration factor.

The same procedure applied to the data for the SI values was used to formulate the HIC equation (2-2) values. The x and y coordinates were imported into Matlab® for the integration step. Further, all the measures taken during pedestal testing to calculate the rebound SI values were repeated for the rebound HIC values. NOCSAE baseball standards do not make any provisions for calculating the HIC. However, research has shown that in general athletes suffer concussions around an HIC value of 250 [6]. Consequently, obtaining the HIC values was another way of creating a basis for comparison with other research findings. The succeeding section covers the test procedure. The curve for HIC_{15} is shown in the Appendix (A-3).

6.2.2. Drop Heights and Test Technique

The testing procedure was simple, which was to impact the headform and the headform fitted with a helmet multiple times from varying heights while it was attached to either the pedestal or the LBT.

Drop Heights

The headform and each helmet were impacted from four different drop heights five times each. Each height corresponded to a particular angle of the pendulum from its vertical equilibrium position and was represented by the vertical distance from the center of the headform up to the horizontal plane parallel to the end of the pendulum at the point where the baseball was attached. The height of the pendulum above the equilibrium position could be determined by implementing the principles of Figure 6-7 and equation 6-6. Table 6-1 itemizes the five heights including the four drop heights and the maximum height (not tested), the corresponding angles, and the resulting theoretical tangential velocity based on simple pendulum kinematics.

Table 6-1: Maximum Velocity of Pendulum Based on Height Above Equilibrium Point

Theoretical Velocity At Equilibrium Position Based on Pendulum Length of 90in				
Degrees	**Height* (in)**	**Velocity (mi/hr.)**	**Velocity (ft./sec)**	**Velocity (m/s)**
30	12	5.48	8.04	2.45
45	26.36	8.1	11.88	3.62
50	32.14	8.95	13.13	4.00
60	45	10.59	15.53	4.73
90	90	14.98	21.97	6.70

Test Technique

The test technique consisted of five straightforward steps which were repeated five times at each height and are outlined below.

1) Assure that the pendulum was hanging in its equilibrium position. Also, the pedestal or the LBT was secured in such a manner that the baseball attached to the end of the pendulum was barely touching the headform or helmet at the equilibrium position. After impacts a helmet may shim out of position. Hence, verify that the helmet fit the headform the way it was intended to be worn.

2) Elevate and maintain the pendulum at the desired drop height using the 6-foot extendable slide rule as shown in Figure 6-7

3) Verify that the trigger in PULSE® was set, and then initiate the data collection sequence.

4) Release the pendulum.

   a) Catch the pendulum at its maximum rebound height after it strikes the headform during pedestal tests and measure and record the height.

   b) Measure and record the travel distance of the LBT after impact (12in. & 26.36in.)

5) Save and then export the data from PULSE®

The same test technique was used for both the pedestal and the LBT with one exception. Impacts were not conducted at the 32.14 in. and 45 in. drop heights. At those two heights the energy imparted to the system caused the LBT to impact the shaft supports at the far end and then rebound. Ultimately, it was determined that the data from those tests would be inconclusive. In the final section of this chapter the naming convention of each signal used during testing and the significance of the name is discussed. Also, the details of which signal response values were calculated and compared are outlined.

6.2.3. Response Names and Comparison of Results

Prior to the testing phase of the experimental analysis, there was no preset plan to adopt a particular naming convention for the signal responses. In fact, the response names are reminiscent of the location of the sensor or the observed phenomenon associated with that response during testing. Five sensors were used during testing including the load cell, miniature accelerometer, and the headform tri-axial accelerometer. The results for the load cell were not factored into the analysis, so in the spirit of clarification the names of the accelerometers are addressed next.

The miniature accelerometer was placed on the baseball adapter, which was located on the end of the pendulum. For this reason, the response for that accelerometer was titled the 'Adapter' accelerometer. Henceforth, any discussion that pertains to the acceleration or velocity of the adapter is in direct reference to the accelerometer on the baseball adapter located at the end of the pendulum. The significance of the adapter accelerometer was to determine the velocity of the pendulum on initial impact. The term 'rebound height' as it is used in this analysis, is strictly in reference to the height the pendulum achieved after it rebounded from striking the headform during pedestal testing. Rebound height is represented by h_2 in equation 6-7 and is not associated with the rebound of the headform itself. The other two names of significance were Y-initial and Y-rebound.

69

In chapter 1 it was mentioned that the NOCSAE headform is a reasonable model of the human head and that it is fitted with a tri-axial accelerometer. Also, it seems feasible to assume that the accelerometer is an analog of the human brain. Therefore, the response of the accelerometer to an impact could simulate the response of the brain to an impact. This was the logic that drove the decision to use the names Y-initial and Y-rebound. The direction of the impact during testing required that only the Y axis response of the tri-axial accelerometer located inside the headform could be used for the analysis. Y-initial was perceived to be the initial movement of the brain in the direction of the impact upon impact. Y-rebound was perceived to be the movement of the brain in the direction opposite to impact during the head's recoil from an impact. To clarify, Y-initial and Y-rebound represented the initial response peak and the recoil response peak respectively on the same signal response, which was the Y axis of the tri-axial accelerometer located inside the headform. This distinction is further explained in Figures 8-1 and 8-2 in chapter 8. Table 6-2 itemizes the signal response titles, location, and significance.

Table 6-2: Signal Response Titles and Significance

Signal Response Titles and Significance			
Response Title	**Sensor Location**	**Sensor Type**	**Significance**
Adapter	Baseball adapter at the end of the pendulum.	Miniature accelerometer	Pendulum acceleration/ velocity
Y-initial	Y axis of tri-axial accelerometer inside headform.	Tri-axial accelerometer	Headform (brain) initial accel./ velocity in direction of impact
Y-rebound	Y axis of tri-axial accelerometer inside headform	Tri-axial accelerometer	Headform (brain) recoil accel./ velocity in opposite direction of impact

The result values generated in this analysis were either measured or calculated and then compared. The strategy was the same for both the pedestal and the LBT. The only difference was the comparisons for the LBT were restricted to the equivalent response for the pedestal.

The measured values for each were the force, adapter accelerometer, and Y-initial and Y-rebound. The calculated values for each were the pendulum velocity, the headform velocity, the SI and the HIC. For the pedestal the calculated velocities were compared to each other and to the velocities derived by equation 6-6 and 6-7. In addition, for the pedestal the SI and HIC values for the bare headform were compared with those with the headform fitted with each of the headgear and for the Y-initial versus Y-rebound. For the LBT, the calculated velocities were only compared to the velocity of the corresponding response for the pedestal. All the velocities, with the exception of equations 6-6 and 6-7, and the SI and HIC values were calculated using Matlab®. Table 6-3 lists the calculated and compared velocity values and the SI and HIC values for the experimental analysis.

In chapter 7 the results of the tests are examined. As the details of the tests unfurl, it is important to remember that the main objective was not to create a method that seamlessly translated empirical data into theoretical values. It was, however, intended to validate the hybrid tower by developing a basis for comparison of the collected data with established findings.

Table 6-3: Calculated and Compared Velocity, SI, and HIC Values

Calculated and Compared Velocity, SI, and HIC Values			
Title	**Calculated**	**Represented**	**Compared with**
Adapter	Integrate adapter Accelerometer curve.	Pendulum Velocity.	Y-init./ Y-reb./ Eqns. 6-6/6-7
Y-initial	Integrate Y axis Accelerometer initial peak.	Headform velocity From initial impact.	Adapter/ Y-reb./ Eqns. 6-6/6-7
Y-rebound	Integrate Y axis Accelerometer recoil peak.	Headform velocity From recoil of initial impact.	Adapter/ Y-init./ Eqns. 6-6/6-7
SI (not a velocity)	Equation 2-1	Threshold value for occurrence of concussion as stated by Pellman.	Bare headform vs. Protected headform
HIC (not a velocity)	Equation 2-2	Threshold value for occurrence of concussion as stated by Pellman.	Bare headform vs. Protected headform
Theoretical Velocity[5]	Equation 6-6	Theoretical velocity of a pendulum with the dimensions as that of the hybrid tower.	Adapter/ Y-init./ Y-rebound
Theoretical Velocity[5]	Equation 6-7	Hypothetical velocity of baseball based on the dimensions of pendulum and hypothesis.	Adapter/ Y-init./ Y-rebound

7. CHAPTER 7 - TEST RESULTS

Earlier the discussion alluded that multiple variables alter the trajectory of an experimental analysis as it is conducted. The variables range from manufacturing setbacks, if building a system is involved, to unforeseen shortfalls in the test method. However, an important component in the process is whether the results remain consistent within the scope of adjustments. As the test results are examined the presence of consistency within them will be emphasized. In each case the headform was used as the base value. In each section the review of the results begin with the pedestal test results followed by the test results of the LBT. However, the tables will have the results for both structures to facilitate comparison.

7.1. Pedestal and LBT Test Results

7.1.1. Measured Velocities vs. Energy Equation Derived Velocity Values

For the pedestal, the headform and each helmet were impacted at the four drop heights five times each. At each height the adapter velocity value for the headform was the closest to the value derived by equation 6-6. The adapter velocities for Helmet-B had the second closest values followed by the adapters for Helmet-A, and then the Pitcher hat. These results seemed plausible in the sense that the bare headform offered no deflection while the Pitcher hat, which had the most padding, offered significantly more energy absorption. In each instance the velocity of Y-initial in the headform was less than the adapter velocity, as it should have been. However the second peak, which was classified earlier as the Y-rebound, was the highest of the velocities including those derived by equation 6-6. This phenomenon may be related to the fact that more energy might be associated with the rebound of the impact than the impact itself. These trends were consistent for Y-rebound for the headform and the headgear at each drop height for equation 6-6.

In contrast, the velocity values generated by equations 6-7 differed significantly from the measured values. They were much larger values. The adapter for the headform had the highest of these values, followed by the adapter for Helmet A, but surprisingly the values for the adapter for the Pitcher Hat were slightly higher than those for Helmet B's adapter values. The focus now shifts to the LBT.

NOCSAE does not have a standard that uses a pedestal for testing baseball headgear, therefore the pedestal tests in this experimental analysis was one of the test method modifications mentioned earlier. The use of a LBT is the prescribed method for testing baseball headgear.

The data pool for the LBT tests was half that of the pedestal because tests were not conducted at 32.14in and 45in. drop heights. The test results were not in accordance with what was expected. The results for Helmet B turned out to be inconclusive. The measured velocity values for the adapter were very low for Helmet B. There must have been an arbitrary occurrence which affected the instrument readings. That incident constituted one of the unforeseen developments that can arise in an experimental analysis. The adapter velocities were not as high as those of the pedestal, but they were consistent in the sense that the adapter headform had the highest values while the adapter Pitcher hat had the lowest. Unlike the pedestal results, the Y-rebound velocities were smaller in value than the adapter velocities, but greater than the Y-initial velocities. Those findings were found to be more closely aligned with general intuition. The aforementioned results were consistent for the headform and each headgear at both heights with the exception of Helmet B.

In section 6.2.1b it was mentioned that attempts to reasonably model the LBT using the energy equations involving work were unsuccessful. One of the possibilities for this could have been the rods on which the LBT travelled. Maybe there was some bending in the rods due to the combined weight of the LBT and the headform (23.2lb) that could have absorbed some energy

74

from the system. Of course, this notion is purely conjecture. Figure 7-1 itemizes the average

velocity values of each drop height for the headform and each headgear. The cells bordered in

black are measured velocities, the green text compares measured velocity with equation 6-6 and

the red text is a comparison with equation 6-7.

AVERAGE VELOCITY OF 5 TEST RUNS						
Test Element	PEDESTAL				LBT	
	12 inch	26.36 inch	32.14 inch	45 inch	12 inch	26.36 inch
	mi/hr	mi/hr	mi/hr	mi/hr	mi/hr	mi/hr
Headform						
Adapter	**5.165**	**7.939**	**9.089**	**10.735**	**4.976**	**7.704**
Engy. Eqn. (6-6)	**5.470**	**8.107**	**8.951**	**10.592**	N/A	N/A
Engy. Eqn. (6-7)	**28.003**	**42.984**	**47.601**	**57.179**	N/A	N/A
Y-Initial	3.329	4.660	5.109	5.872	3.361	4.735
Y- Rebound	6.871	9.886	10.851	12.451	4.260	6.274
Helmet A						
Adapter	**4.455**	**6.568**	**7.383**	**8.514**	**4.395**	**6.255**
Engy. Eqn. (6-6)	**5.470**	**8.107**	**8.951**	**10.592**	N/A	N/A
Engy. Eqn. (6-7)	**28.155**	**42.382**	**46.508**	**55.312**	N/A	N/A
Y-Initial	3.141	4.378	4.733	5.430	3.213	4.524
Y- Rebound	6.307	8.990	9.861	11.431	3.510	5.331
Helmet B						
Adapter	**3.849**	**7.490**	**8.375**	**10.036**	**0.817**	**1.383**
Engy. Eqn. (6-6)	**5.470**	**8.107**	**8.951**	**10.592**	N/A	N/A
Engy. Eqn. (6-7)	**27.384**	**40.469**	**45.010**	**54.335**	N/A	N/A
Y-Initial	3.368	4.616	5.017	5.784	3.289	4.649
Y- Rebound	6.999	9.688	10.574	12.117	3.974	5.919
Pitcher Hat						
Adapter	**4.024**	**5.924**	**6.682**	**7.825**	**3.887**	**5.850**
Engy. Eqn. (6-6)	**5.470**	**8.107**	**8.951**	**10.592**	N/A	N/A
Engy. Eqn. (6-7)	**28.458**	**42.584**	**46.646**	**55.235**	N/A	N/A
Y-Initial	3.028	4.306	4.736	5.465	3.049	4.386
Y- Rebound	5.969	8.517	9.440	11.002	3.472	5.405

Figure 7-1: Measured Velocities vs. Velocities Derived by Energy Eqns. for Pedestal & LBT

7.1.2. Severity Index (SI) & Head Injury Criterion (HIC)

The central theme for the SI and HIC values was the same as it was for the velocity value, which was consistency. In the pedestal results, once again the adapter for the headform yielded the highest values in both the SI and HIC categories. There were two instances where the headform adapter SI value stood out. First at the 32.14in drop height the SI value came very close to the NOCSAE recommended value of 1200 for the medium headform. Second, at the 45in. drop height the SI value exceeded the NOCSAE recommended value of 1200 for the medium headform. The NOCSAE value only pertains to the response of the tri-axial accelerometer in the headform, but if the true baseball velocity is close to those adapter values, then this may be an indication that the test went beyond the 36-44 mph range. Those results seemed feasible because at those two drop heights the theoretical baseball velocity derived by using equation 6-7 consistently exceeded the NOCSAE maximum velocity value range of 36-44mph. Also, the bare headform offers no impact mitigation. This result did seem to add some validity to the premise that the hybrid tower could be used to form a basis for comparison of collected data with established findings. Also, it raised the question of whether the energy equations were catering for system properties that the sensors were not.

Consistent with the velocity results, the Pitcher hat values were the lowest, but in this batch of results Helmet A generated higher values than Helmet B for most of the adapter and Y-initial accelerometers values. Helmet A was composed of carbon fiber which is a sturdier material than the plastic used for Helmet B. Yet, Helmet B yielded lower SI and HIC values for some of the initial impact velocities. This may have quite possibly been related to the restitution energy of the helmet materials.

As evident in Figure 6-4, the Pitcher hat was the most padded of the three headgears thus its low SI and HIC values were congruent with the physics of the experiment. In terms of crossing

the SI (300) and HIC (250) concussion threshold for most athletes, neither the Y-initial nor the Y-rebound responses exceeded the threshold values. The velocity values for these responses were relatively low, so the low SI and HIC numbers made sense.

Finally, one more consistent trend was observed in the pedestal results. Identical to the velocity results, the SI and HIC values for the headform Y-rebound was greater than the SI and HIC values of the Y-initial for each headgear at every drop height. This fact was exemplified by plotting the Y-initial and Y-rebound SI and HIC values for the bare headform and the headform with each headgear and extrapolating the curve. Also, the theoretical SI and HIC values at which concussions occur according to Pellman were represented by a horizontal line on the plot as well.

For the bare headform and for the headform fitted with each headgear the Y-rebound curve was steeper and reached the SI and HIC horizontal line faster than Y-initial. The values when the headgear was fitted with Helmet A and Helmet B were close, but Y-rebound was consistently a steeper curve compared to Y-initial. Further, as with all the results, the curve for the Pitcher hat was the shallowest. Y-rebound for the bare headform crossed the SI line in the range of 70~75 mph. For Helmet A the range was 80~90 mph, and for Helmet B and the Pitcher hat the range was 75~80 mph. The Y-rebound HIC ranges were similar to the SI values. The range for the bare headform was of 70~75 mph. For Helmet A and the Pitcher hat the range was 80~90 mph, and for Helmet B the range was 80~85 mph. Those observations lend further credence that the rebound of the impact may have more energy than the impact itself.

There were only two observations that could be gleaned from the LBT SI and HIC values. Again, this was due to the elimination of two drop heights.

First, it was obvious that with such small impact velocity values the occurrence of SI values above the NOCSAE standard for the medium headform would disappear. Second, unlike the pedestal, for the most part the Y-initial SI values were greater than those of the Y-rebound. As

before, the adapter accelerometer SI and HIC values were the highest. Figures 7-2 and 7-3 list the average SI and HIC values respectively for all the test elements. The cell outlined in black exceeds the NOCSAE SI standard of 1200 for the medium headform. Figures 7-4 ~ 7-15 illustrate the extrapolated plots of the Y-initial and Y-rebound SI and HIC curves for the bare headform and the headform fitted with each headgear. Figures 7-16 ~ 7-27 display the average adapter and headform Y axis acceleration responses at each drop height for the pedestal and LBT respectively. The peaks of the Y-initial response and the Y-rebound response are reversed on the Y tri-axial acceleration graphs due to the headform tri-axial accelerometer placement during testing. In general the Y-initial peak should have been positive and the Y-rebound peak should have been negative. Also, the wider area under the Y-rebound peak is clearly evident on the Y tri-axial plots.

In the closing chapter the significance of the results are discussed. In addition, the short comings of the hybrid tower and the applied test method are addressed. Finally, the suggestions for future work are covered.

AVERAGE SI OF 5 TEST RUNS						
Test Element	PEDESTAL				LBT	
	12 inch	26.36 inch	32.14 inch	45 inch	12 inch	26.36 inch
Headform						
Adapter	246.844	816.160	1163.440	**1876.760**	199.213	662.903
Y-Initial	19.860	52.209	67.664	101.729	17.185	46.930
Y- Rebound	38.084	99.011	125.075	175.801	10.892	32.669
Helmet A						
Adapter	82.972	313.306	460.798	673.804	89.121	321.084
Y-Initial	15.365	38.417	49.048	72.074	14.336	37.208
Y- Rebound	27.018	69.265	87.235	126.071	6.882	21.044
Helmet B						
Adapter	56.859	264.987	378.633	697.093	6.234	25.162
Y-Initial	13.813	37.759	49.309	75.745	11.906	35.765
Y- Rebound	33.975	82.662	104.393	147.909	8.722	26.041
Pitcher Hat						
Adapter	48.711	146.003	198.179	314.875	48.722	161.712
Y-Initial	9.507	24.787	32.423	48.851	9.570	25.802
Y- Rebound	25.958	67.227	87.418	128.734	6.609	23.786

Figure 7-2: Average Severity Index (SI) Values for Pedestal & LBT Tests

AVERAGE HIC OF 5 TEST RUNS						
Test Element	**PEDESTAL**				**LBT**	
	12 inch	26.36 inch	32.14 inch	45 inch	12 inch	26.36 inch
Headform						
Adapter	103.931	313.377	439.360	690.511	37.236	116.613
Y-Initial	10.141	23.205	29.955	42.428	5.910	14.709
Y- Rebound	27.705	73.076	92.236	130.070	6.847	18.771
Helmet A						
Adapter	38.032	121.460	204.850	299.939	18.279	61.420
Y-Initial	6.638	15.895	18.906	27.532	4.259	10.762
Y- Rebound	20.799	53.848	68.860	98.148	4.497	11.994
Helmet B						
Adapter	8.353	132.873	182.331	309.557	0.603	2.374
Y-Initial	6.864	16.849	21.637	32.242	4.115	11.100
Y- Rebound	24.508	60.816	76.726	108.681	5.878	16.754
Pitcher Hat						
Adapter	27.147	72.631	96.350	148.270	13.441	38.786
Y-Initial	5.751	15.592	20.225	29.314	4.011	10.085
Y- Rebound	18.842	46.341	59.949	88.540	3.944	14.089

Figure 7-3: Average Head Injury Criterion (HIC) for Pedestal & LBT Tests
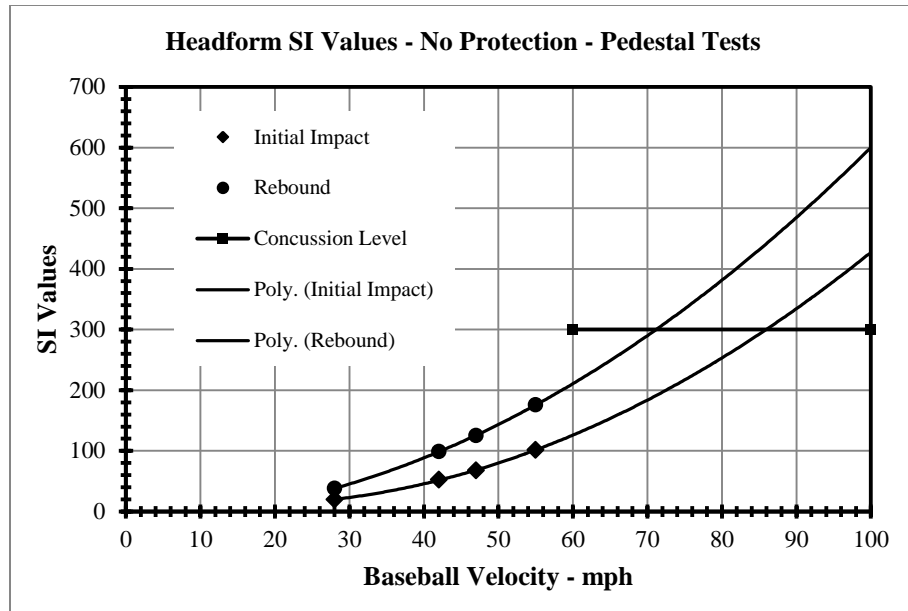
Figure 7-4: Headform SI Values - No Protection - Pedestal Tests
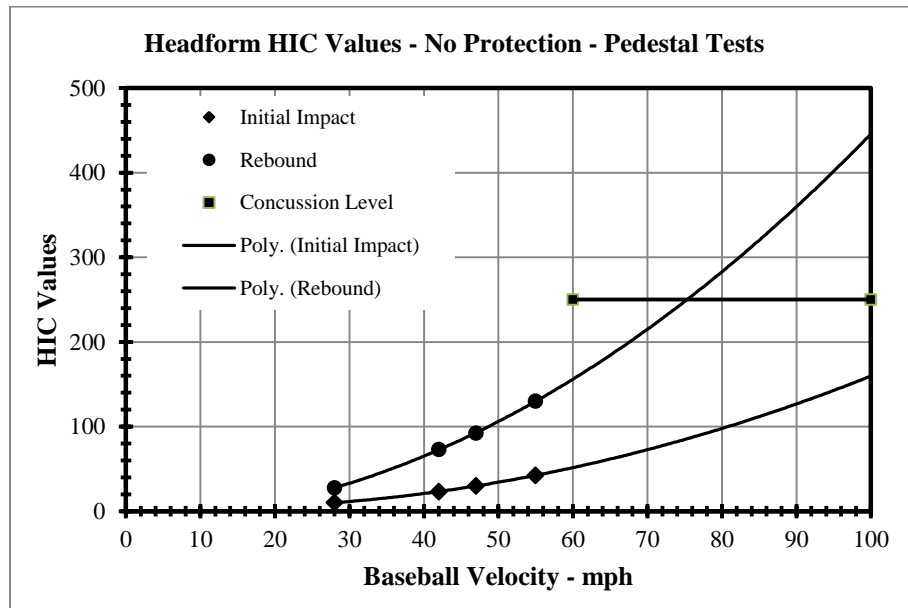
Figure 7-5: Headform HIC Values - No Protection - Pedestal Tests

Headform SI Values - Helmet A - Pedestal Tests
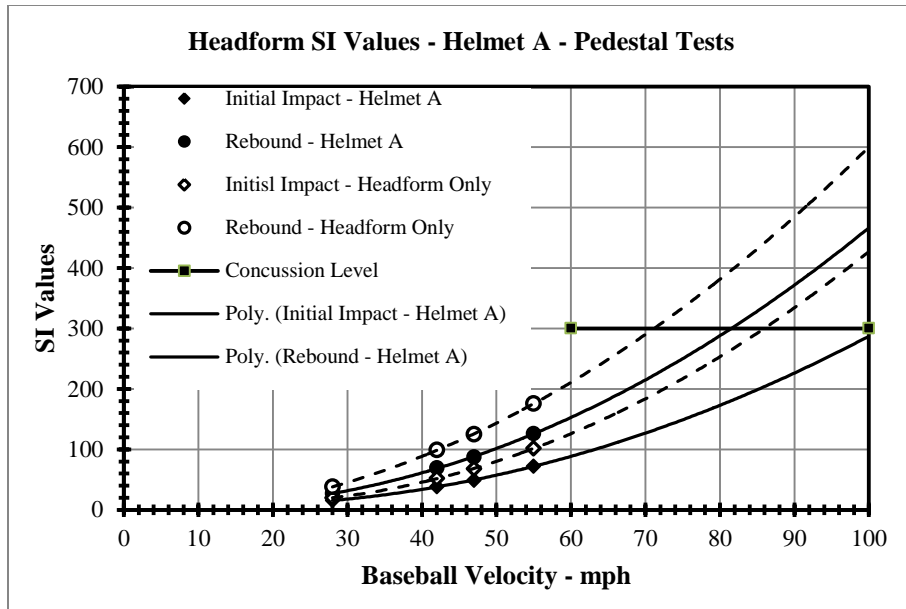
Figure 7-6: Headform SI Values - Helmet A - Pedestal Tests

Headform HIC Values - Helmet A - Pedestal Tests
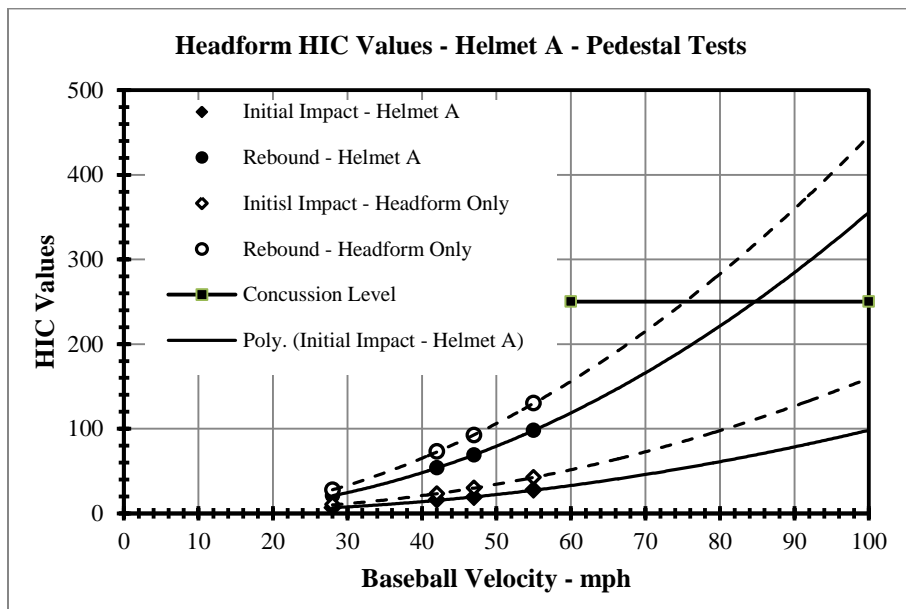
Figure 7-7: Headform HIC Values - Helmet A - Pedestal Tests
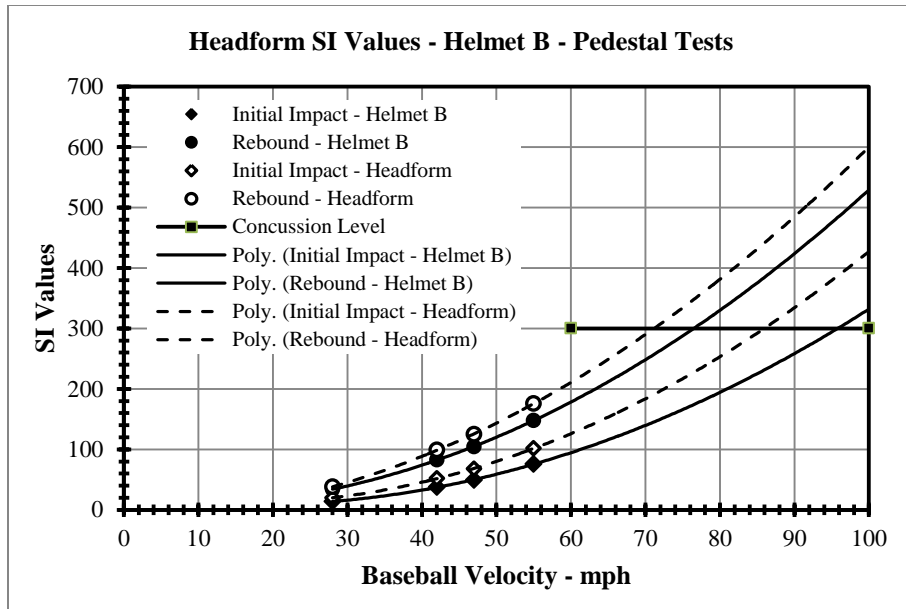
Figure 7-8: Headform SI Values - Helmet B - Pedestal Tests
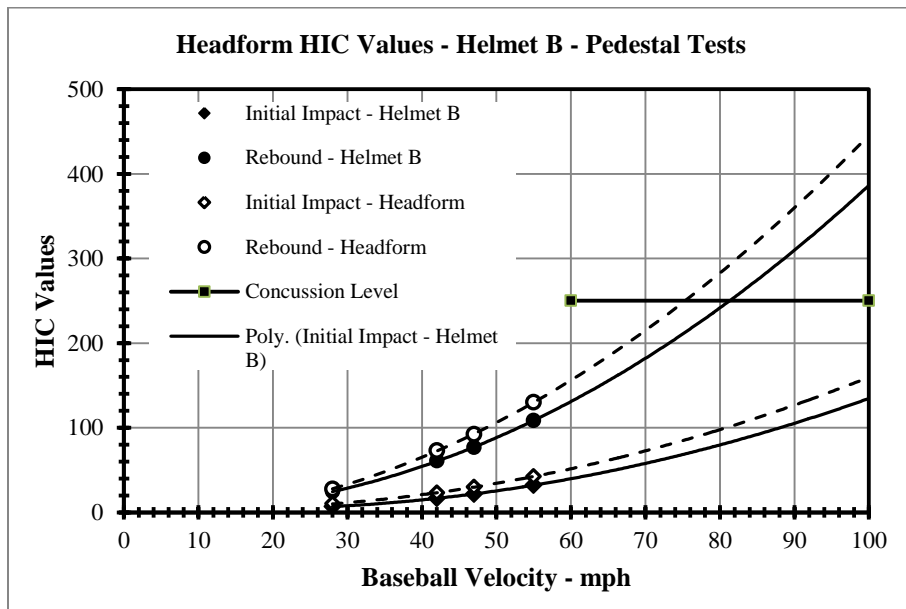
Figure 7-9: Headform HIC Values - Helmet B - Pedestal Tests

Headform SI Values Pitcher Hat- Pedestal Tests
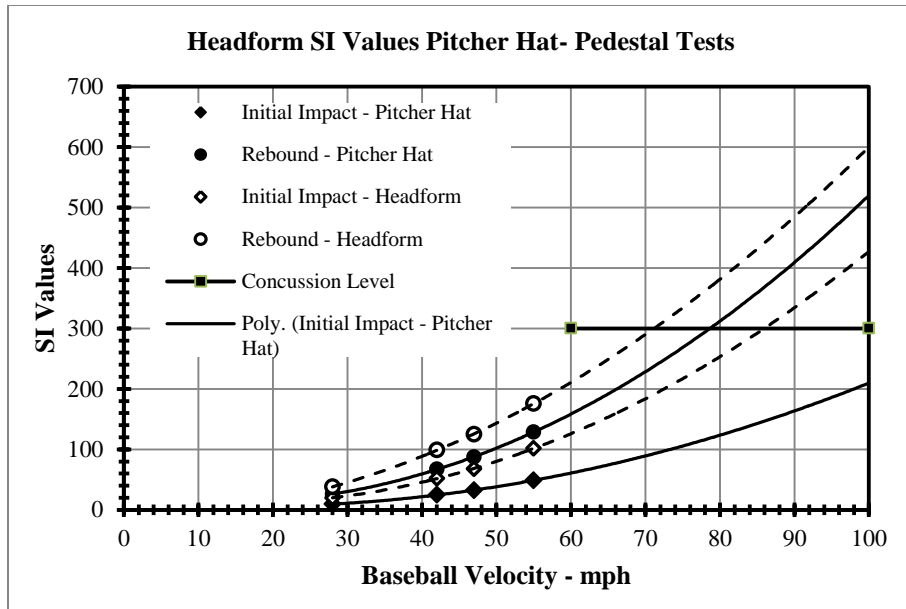
Figure 7-10: Headform SI Values Pitcher Hat - Pedestal Tests

Headform HIC Values - Pitcher Hat - Pedestal Tests
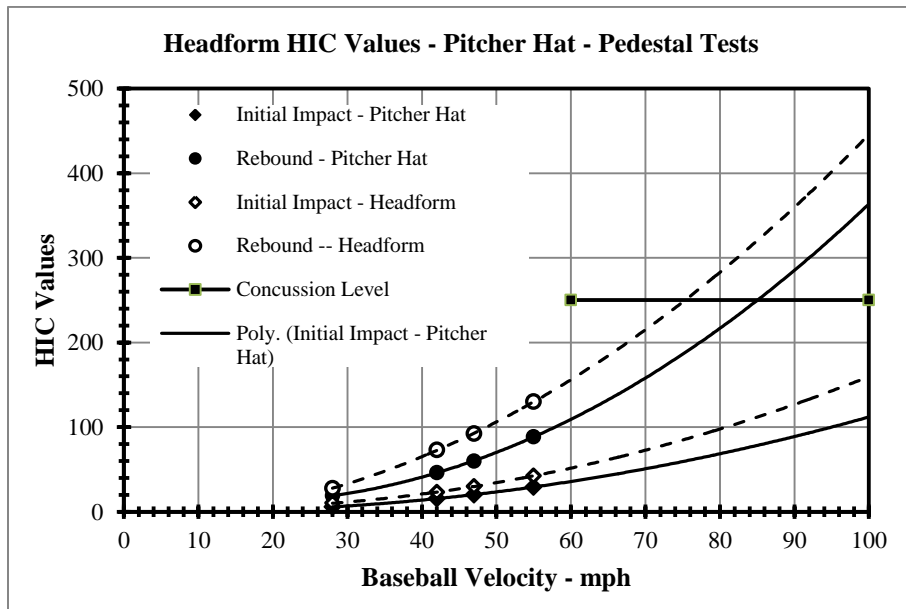
Figure 7-11: Headform HIC Values - Pitcher Hat - Pedestal

84

Headform SI Values - Initial Impact - Pedestal Tests
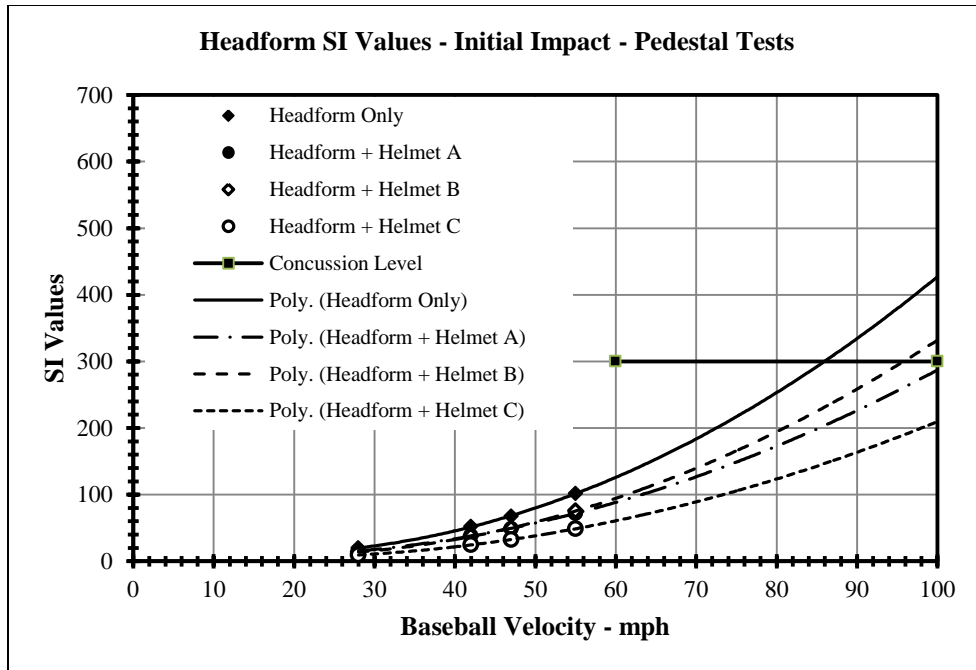
Figure 7-12: Headform SI Values - Initial Impact - Pedestal Tests

Headform SI Values - Rebound- Pedestal Tests
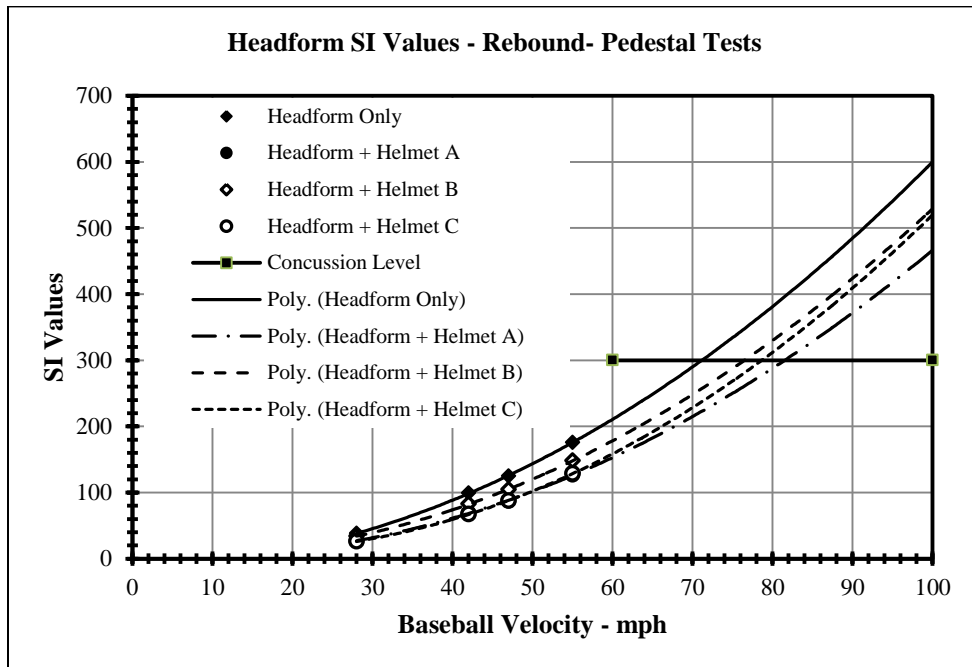
Figure 7-13: Headform SI values - rebound - Pedestal Tests

85
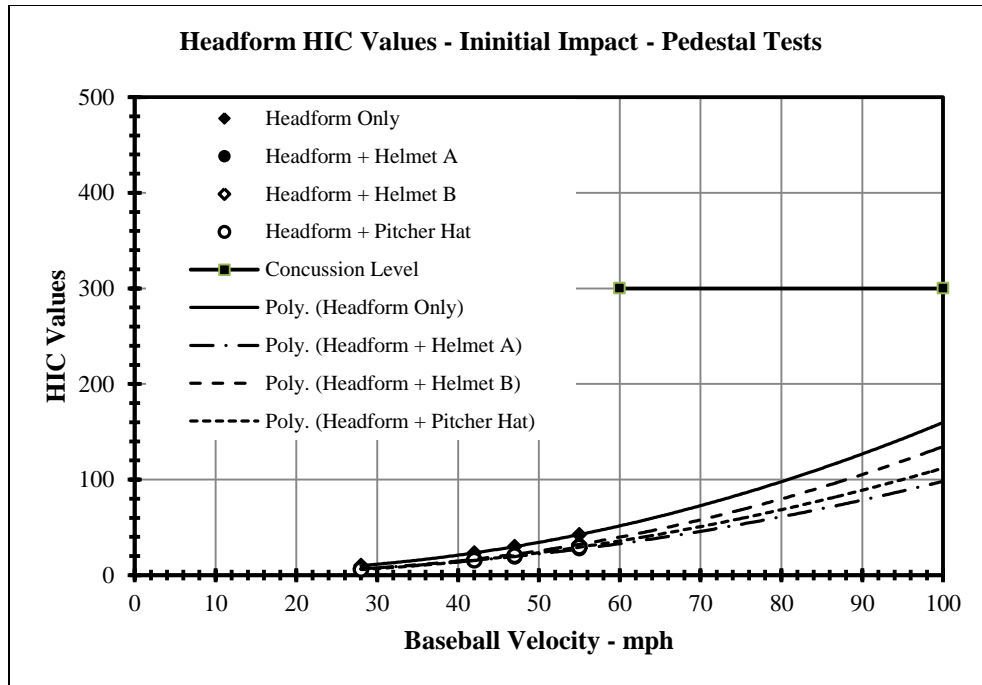
Figure 7-14: Headform HIC Values - Initial Impact - Pedestal Tests
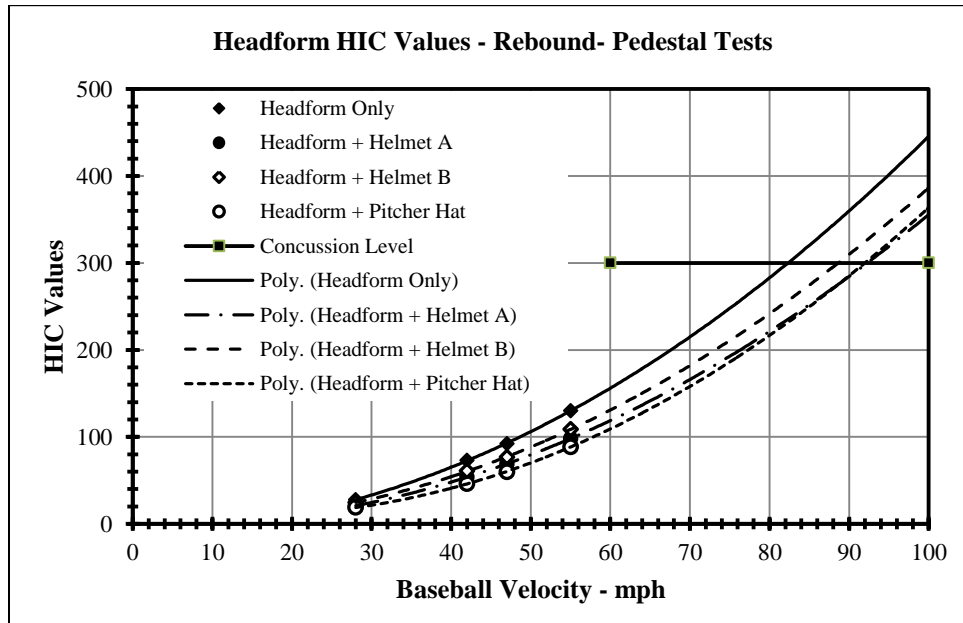
Figure 7-15: Headform HIC Values - Rebound - Pedestal Tests

86
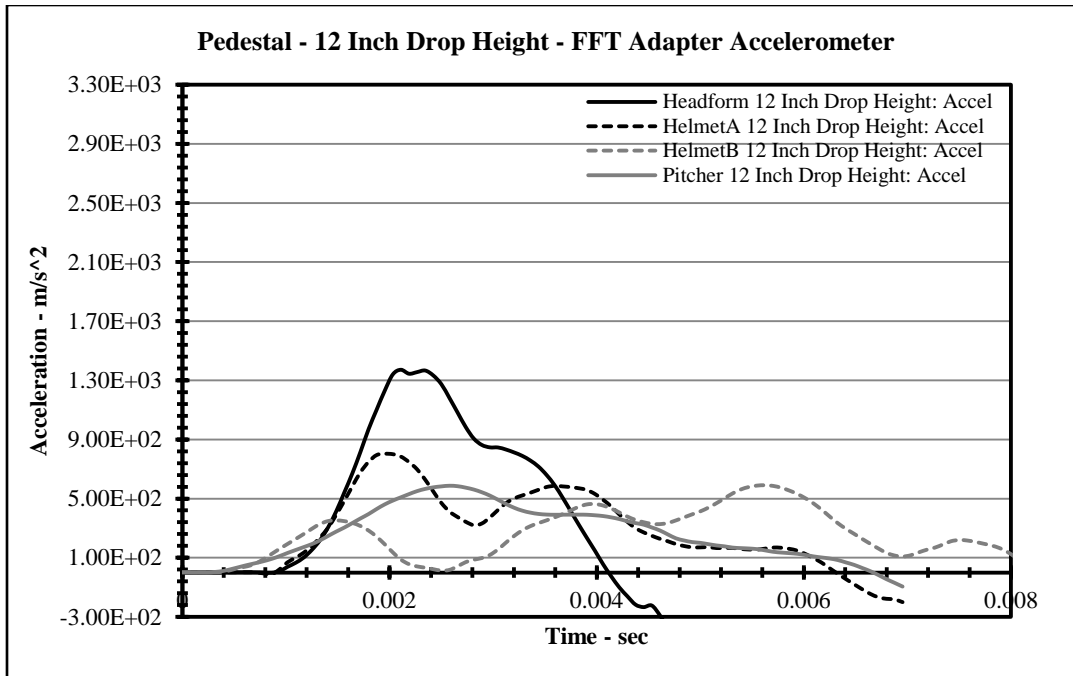
Figure 7-16: Pendulum Impact Acceleration for 12 Inch Drop Height
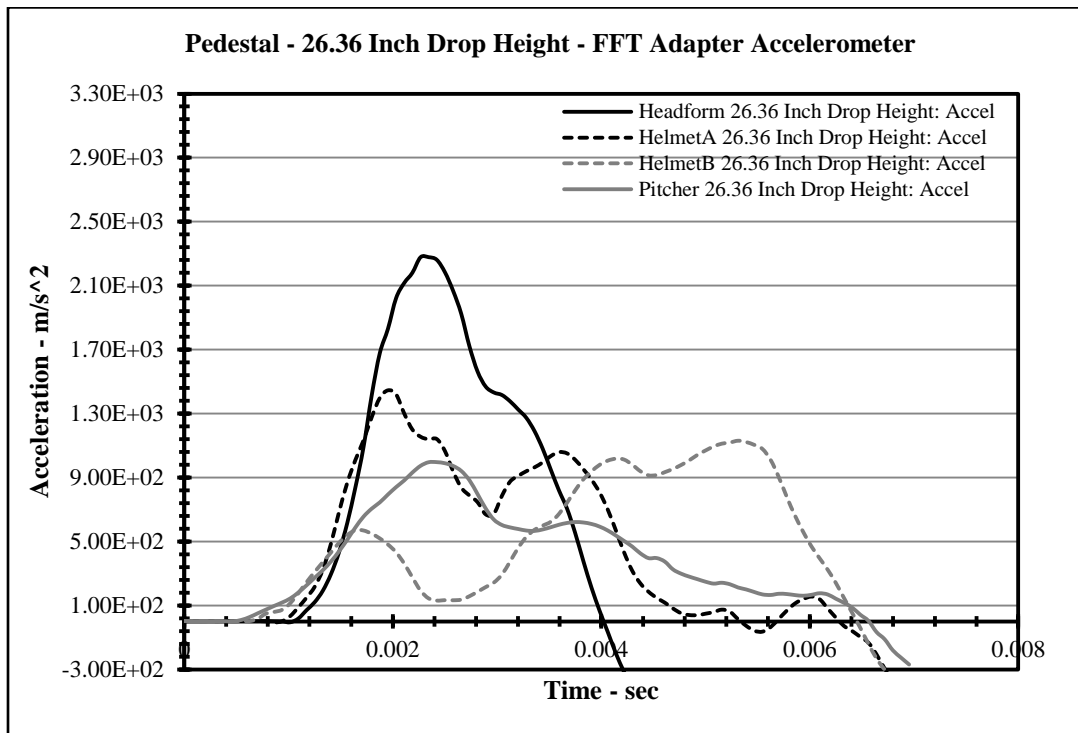
Figure 7-17: Pendulum Impact Acceleration for 26.36 Inch Drop Height

87
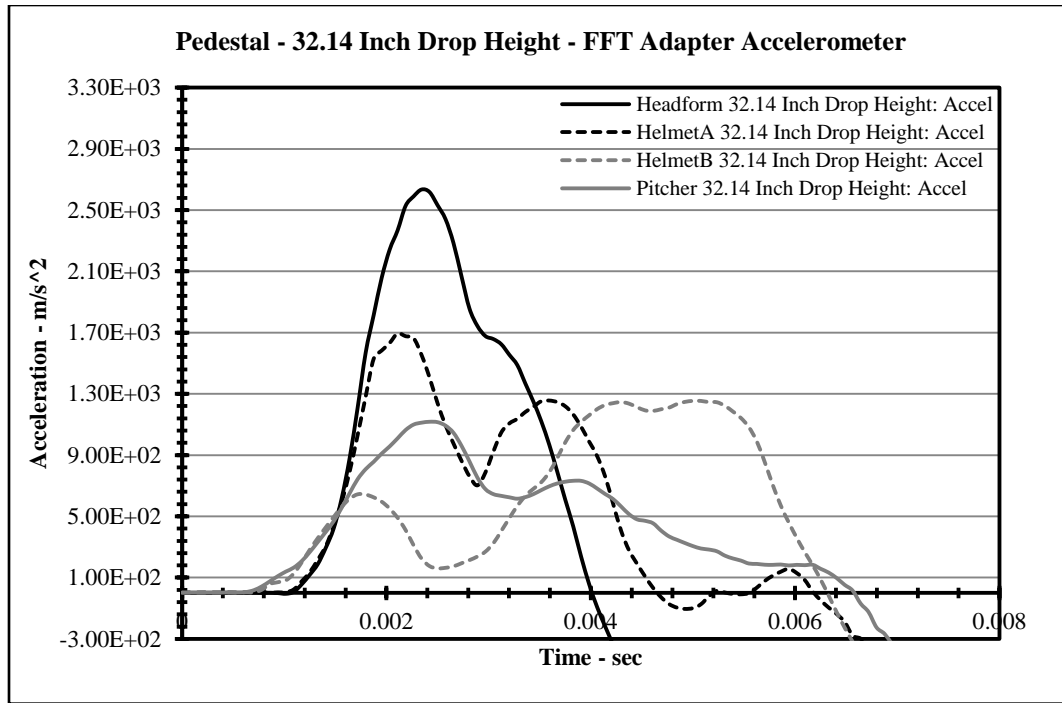
Figure 7-18: Pendulum Impact Acceleration for 32.14 Inch Drop Height
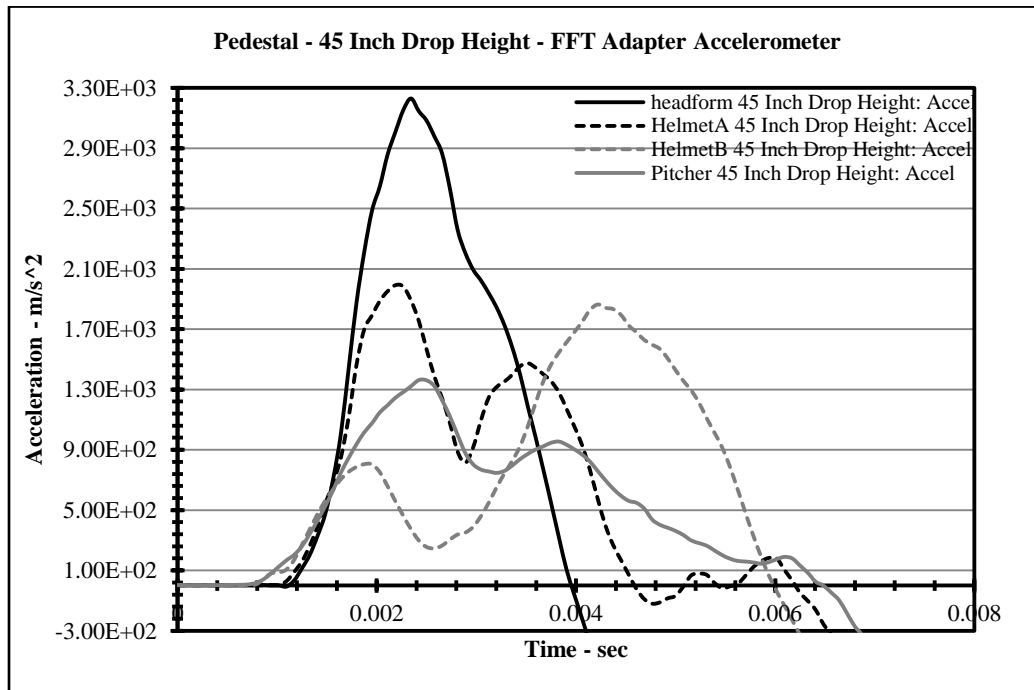
Figure 7-19: Pendulum Impact Acceleration for 45 Inch Drop Height

88
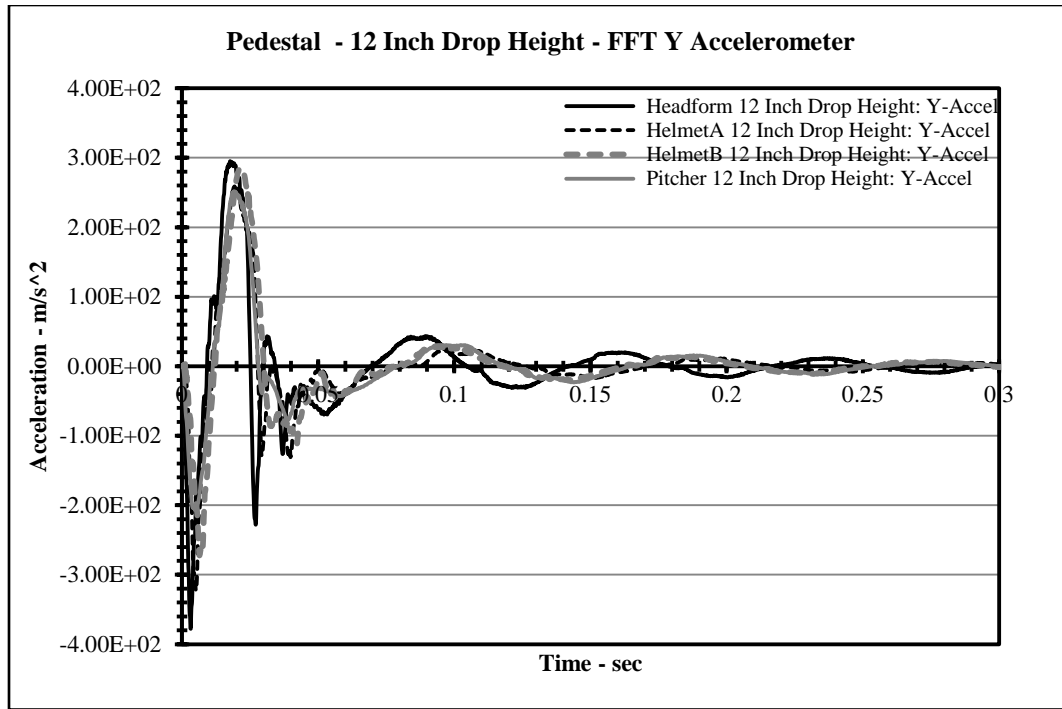
Figure 7-20: Acceleration Plot for Y Axis of Headform Tri-Axial at 12 Inch
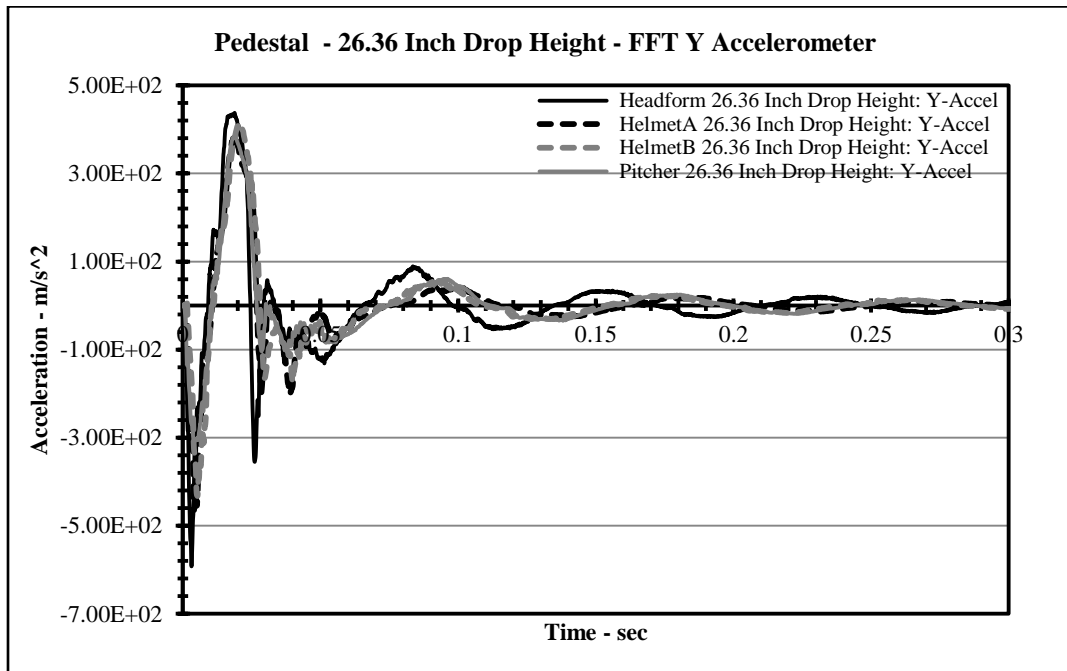
Figure 7-21: Acceleration Plot for Y Axis of Headform Tri-Axial at 26.36 Inch

89
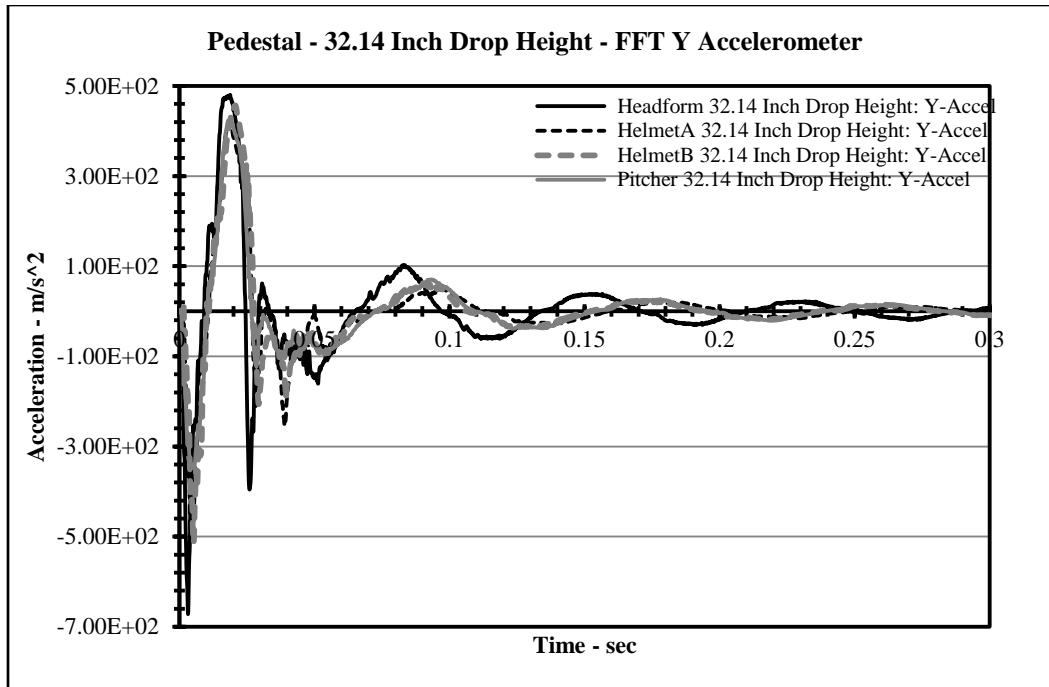
Figure 7-22: Acceleration Plot for Y Axis of Headform Tri-Axial at 32.14 Inch
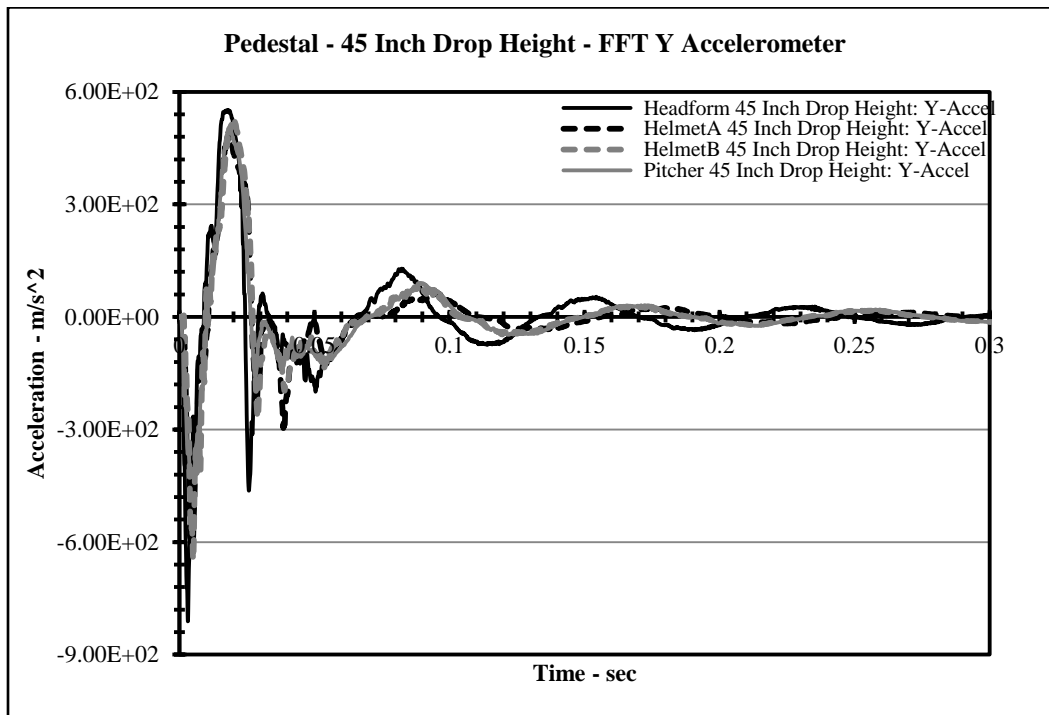
Figure 7-23: Acceleration Plot for Y Axis of Headform Tri-Axial at 45 Inch

90
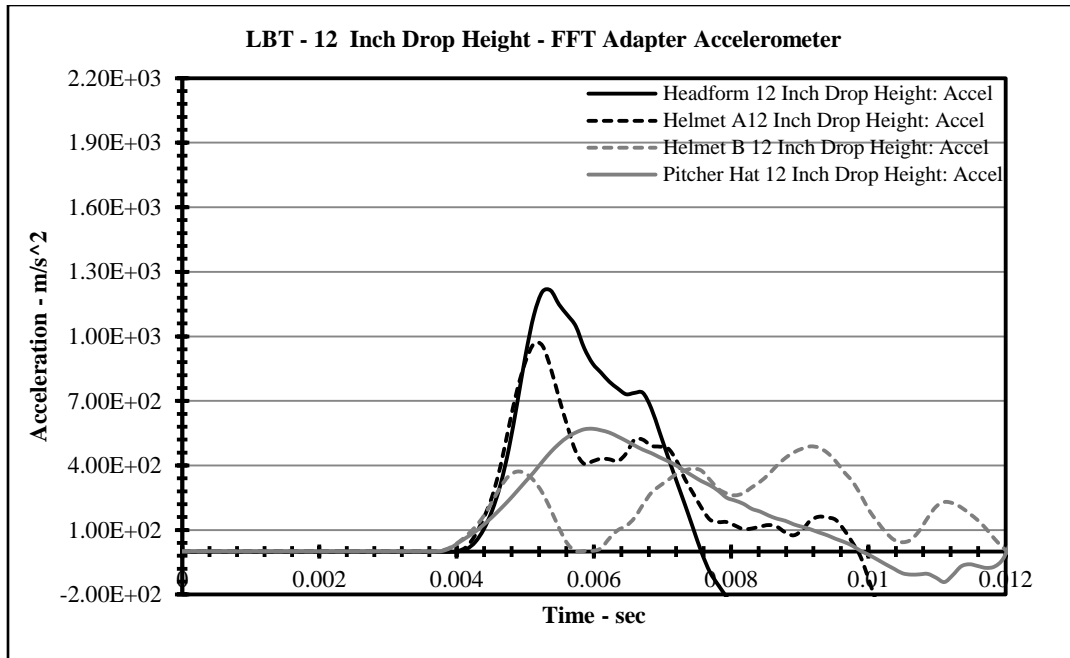
Figure 7-24: Pendulum Impact Acceleration for 12 Inch Drop Height
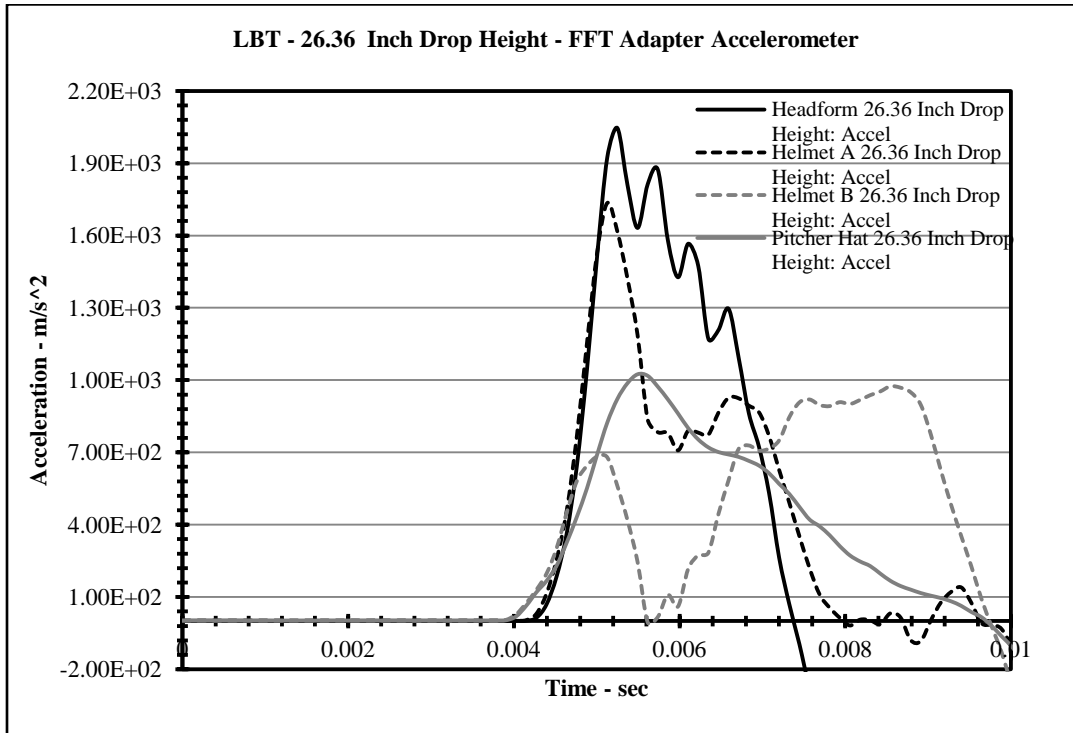
Figure 7-25: Pendulum Impact Acceleration for 26.36 Inch Drop Height

91
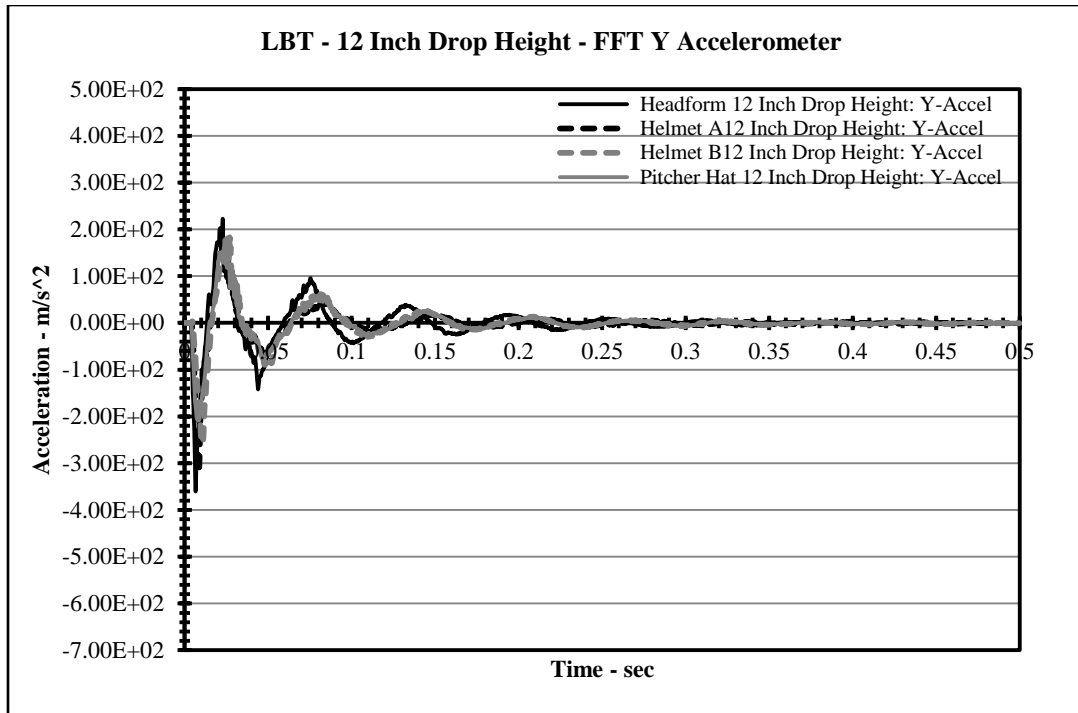
Figure 7-26: Acceleration Plot for y Axis of Headform Tri-Axial for 12 Inch
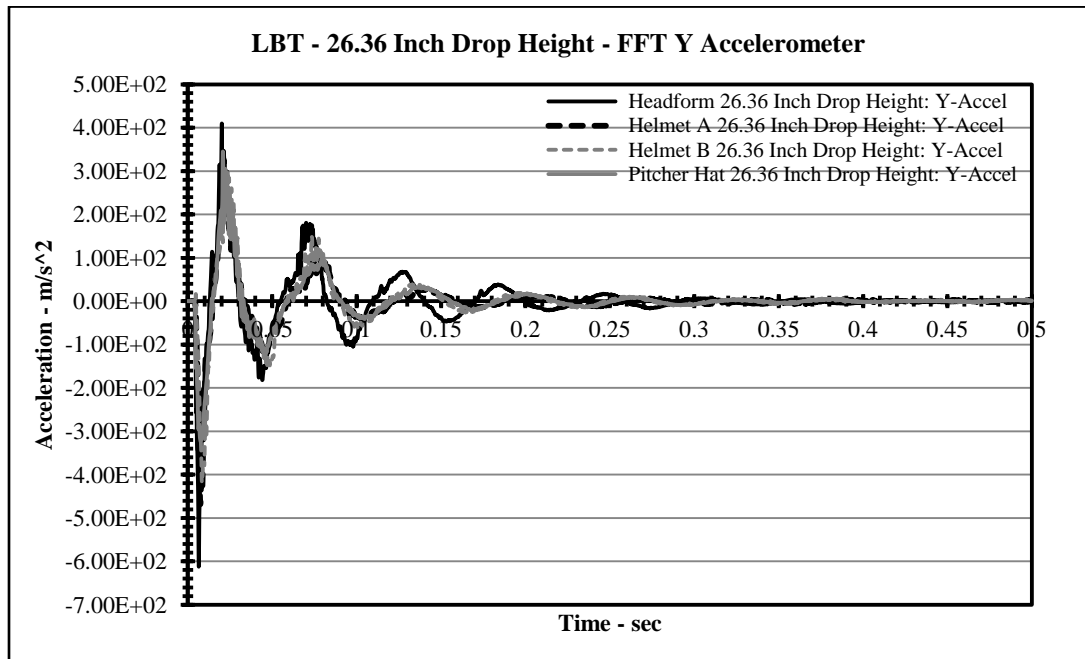
Figure 7-27: Acceleration Plot for Y Axis of Headform Tri-Axial for 26.36 Inch

8. CHAPTER 8 - CONCLUSIONS

At the onset of this academic quest the fundamental goal was to develop a means to more reasonably quantify head shock due to impact. The targeted approach to achieving this objective was to modify existing NOCSAE test methods. The telescopic outlook was to generate results that could possibly be added to existing findings geared towards a better understanding of the contributing factors of TBIs. However, although the unpredictable nature of hands-on experimentation may have changed the trajectory of this experimental analysis, the final destination was still achieved. As the results are discussed the examiner must remain vigilant to realize the accomplishments as measures of success.

8.1. Discussion of Results

As mentioned in one of the opening chapters of this report, this experimental analysis was a dual faceted endeavor with physical and theoretical aspects. Hence, the synopsis of the results covers the theoretical application, as well as the physical phase. The physical phase is addressed first.

8.1.1. Results of Physical Component

Considering the logistics that were involved in its fabrication and assembly, the physical embodiment of the hybrid tower itself was an accomplishment. The customizable design of the hybrid tower provided the ability to conduct both static and LBT tests. During static tests the headform was attached to the pedestal which was secured to the base plate. Conversely, with a slight modification the pedestal could be removed and the LBT could be installed. Installation of the LBT provided the ability to conduct tests comparable to those proposed by ND-021 and ND-022.

In each configuration the pendulum was used to deliver the impacts. Drop tests were not conducted, but the baseplate was designed to accommodate installation of the anvil used in drop tests. In general, the hybrid tower could be configured to execute baseball to helmet, helmet to helmet, and helmet to anvil impact tests. Also, the proposal to use a pendulum could be further validated by the fact that Withnall and Bayne chose to patent the pendulum concept that they introduced into their design. Finally, NOCSAE itself is in the process of evaluating the proposal for a test method in which a Pneumatic Ram may replace the drop and projectile impact methods [8]. Taken as a whole, the aforementioned factors help validate the hybrid tower and serve to establish it as the first measure of success for this experiment. An illustration of NOCSAE's proposed Pneumatic Ram can be viewed in Appendix A-1.

8.1.2. Results of Theoretical Component

The destination of this experimental analysis during its latest iteration remained the same as the original ideology. Therefore, as the theoretical results are scrutinized the intent was to concentrate on the factors that helped realize that goal.

The pedestal test results revealed that the rebound acceleration of the headform from an impact was greater than the initial headform impact acceleration. This observation may form a basis for the consideration that rebound energy may be a greater contributor to TBIs than the initial impact energy. The pedestal tests may not be relevant to the glancing impacts that occur in football, but in a stationary setting, such as a batter in baseball they seem applicable. Further, when the Y-initial and Y-rebound SI and HIC values were plotted and extrapolated it was evident that the curves for Y-rebound values were steeper and reached the threshold for concussion point as stated by Pellman faster than the Y-initial curve. This was true for the bare headform and the headform fitted with each helmet. Those results make a claim that based on the limited velocity values achieved during testing, and relative to the comparison of the data generated by this

experiment with that of Pellman as illustrated in Figures 7-4 ~ 7-15, it appears that helmets do not remove the potential for injury.

Figure 8-1 illustrates the first 30 milliseconds of the Y axis of the headform tri-axial at a drop height of 45 inch for the pedestal. Notice the greater area under the Y-rebound peak compared to the Y-initial impact peak. To build on the discussion in 6.2.3, Y-initial and Y-rebound are simply the first and second peaks respectively of the response of the Y axis of the tri-axial accelerometer located inside the headform. Figure 8-2 inverses the Y-initial peak so it can be compared side-by-side with the Y-rebound peak.
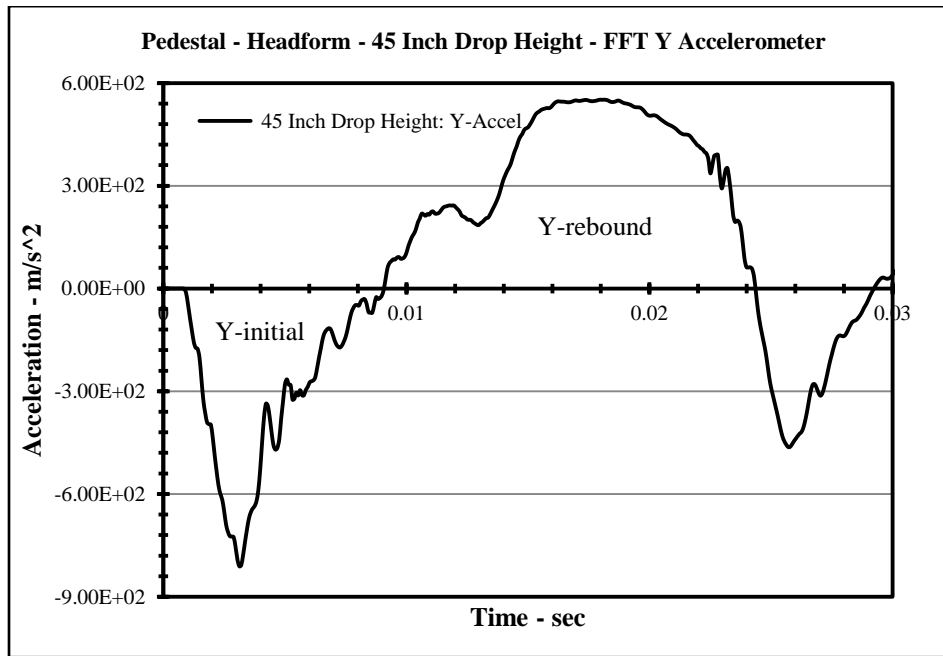
Figure 8-1: First 30 msec of Headform Y Axis Response at 45 Inch for Pedestal
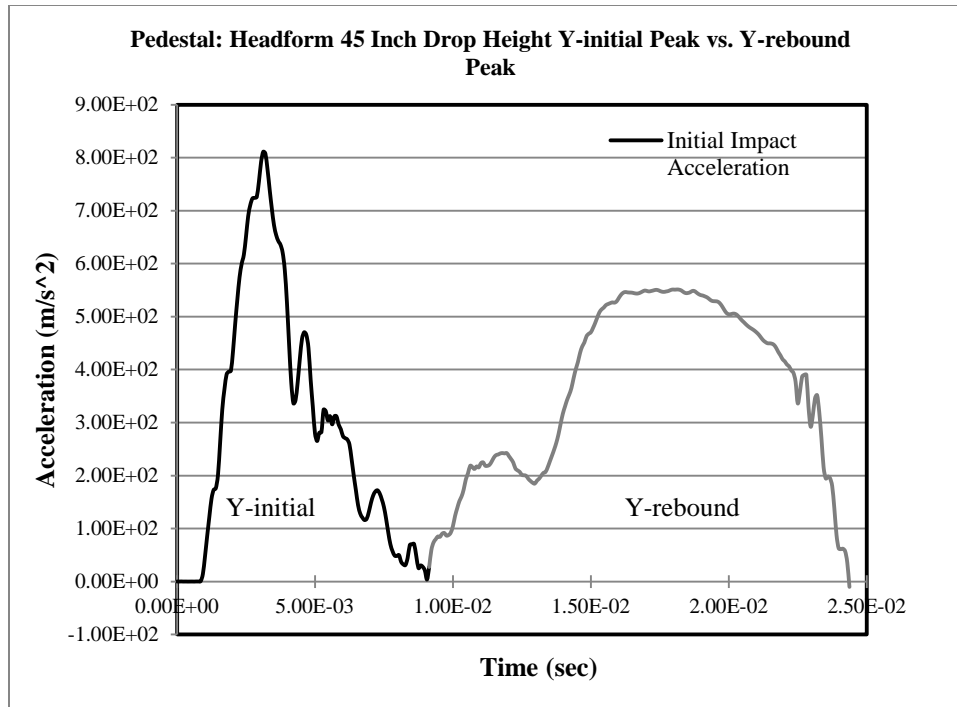
Figure 8-2: Greater Area under Rebound Peak than Initial Impact Peak

Of the two equations derived from the assumption of equations 6-2 & 6-4, the values generated by equation 6-6 were the values most in accordance with the calculated values. Equation 6-7 yielded exaggerated values.

For the most part, the pedestal results were consistent with general intuition except for the slightly higher average SI and HIC values for Helmet A over Helmet B. In Chapter 6 restitution was attributed to the baseball, but it can be applied to any element in a collision. In PULSE® it was represented by the transfer function. The restitution value is the ratio of the outbound velocity and the inbound velocity, and in the transfer function it is assigned a value between 0 and 1. On an average the transfer function values during pedestal testing were slightly lower for Helmet B than for Helmet A. Physically, this meant Helmet B was slightly more effective at deflecting the impact. This made sense since Helmet B's less sturdy plastic design

possessed more 'give', whereas Helmet A's rigid carbon fiber design 'transferred' more of the energy. This was the hypothesis that seemed plausible to explain the slightly higher SI and HIC values for Helmet A during pedestal tests.

There were some anomalies in the LBT results as well. The most obvious of these were the unusually low values for the pendulum (adapter) accelerometer for Helmet B, which may have been attributed to instrument or system error.

The hypothesis concerning the LBT was that the difference between the work performed by the pendulum and the work performed by the top slide of the LBT should result in the baseball impact energy. This speculation seemed reasonable, but the notion to use the arc distance as opposed to the linear (height) distance was debatable. Unfortunately, preliminary analysis of the LBT resulted in conflicting results that were not resolved. Consequently, it was evident that there was some energy that went unaccounted for during LBT tests. One area that seemed suspect was the rods on which the LBT travelled. Maybe there was some bending in the rods due to the combined weight of the LBT and the headform (23.2lb) that could have absorbed some energy from the system.

Based on the constraint of the fixed length of the pendulum, an actual impact velocity of 70 mi/hr. may have been unattainable. However, some of the velocity values determined using equations 6-7 did reach 55 mi/hr., and since these are energy equations it proves that the Hybrid tower is capable of imparting energy values equal to or greater than those delivered in NOCSAE tests.

As stated, some of the unaccounted energy could have been in the form of the helmet material restitution energy. The restitution energy was not calculated in the analysis. However, some of the energy loss could have been determined by calculating the value of the following equation:

$$\frac{1}{2} m_P \left(v_1^2 - v_2^2 \right) \tag{8-1}$$

where $\mathbf{m_p}$ was the effective mass of the pendulum and $\mathbf{v_1}$ and $\mathbf{v_2}$ were its velocities before and after impact respectively. Ultimately, the consistent average transfer function value of .9 for the headform verified that as long as the impact angle or height could be measured, the assumption that gave rise to the implementation of equation 6-6 was sufficient. The bottom line is that the input energy can be quantified using the pedestal rebound energy and the LBT kinetic energy and whatever energy is left over minus system damping is equivalent to the kinetic energy of the baseball.

Perhaps there were no groundbreaking revelations made during the theoretical applications of the data. However, the observance that the rebound from the impact carries more energy and may cause more damage than the initial impact itself, and the congruency between the measured impact velocities and the velocities derived using equation 6-6 do help to signify a measure of success.

8.2. Moving Forward

In certain situations to move forward successfully requires looking back. Consequently, before advocacy for future tests can be proposed, this section opens with a retrospective examination of the areas for improvement with the experimental analysis.

8.2.1. Areas for Improvement

There were two concerns that arose during testing. First, the procedure to position the baseball at the drop height was flawed. Lifting the pendulum to the desired height was acceptable, but manually holding it in place before the drop was not. One possible solution would be to design a ruled or calibrated stand with a removable pin or locking mechanism on which the end of the pendulum could be placed. In order to release the pendulum, the pin would be removed or

the locking mechanism would be released. This concept would remove the possibility of human error by ensuring that the same height is achieved each time. The second concern was the length and stability of the LBT. Test conducted using the LBT were restricted to the 12in and 26.36in drop heights because the top slide of the LBT impacted the shaft supports at the higher drop heights. Increasing the LBT from three feet to possibly six feet could alleviate that problem. Also adding more shaft supports and placing the bearings in a position which would allow the table to slide above the shafts may yield better results.

8.2.2. Recommendations for Future Test

The drop impact test method was not evaluated during this experimental analysis, for this reason that may be an appropriate starting point for future test. One possible adaptation to the NOCSAE drop test method could be to record the acceleration of the impact by positioning an accelerometer at the point of impact between the headform and the anvil. This modification to the method would add an extra stream of data. To facilitate accelerometer placement a headform adapter could be designed. The headform adapter would be attached to the headform at the point where the headform makes contact with the anvil. Basically, the adapter would serve the same purpose that the baseball adapter did in this analysis. Figure 8-3 is a conceptual model of the headform adapter and there are two more illustrations of the adapter in appendix section A-2. Finally, future testing could also involve testing the effectiveness of different shock attenuation materials. These fabrics could either be used as helmet inserts or they could be used to construct the helmet itself. Essentially, boundless options lie on the horizon.
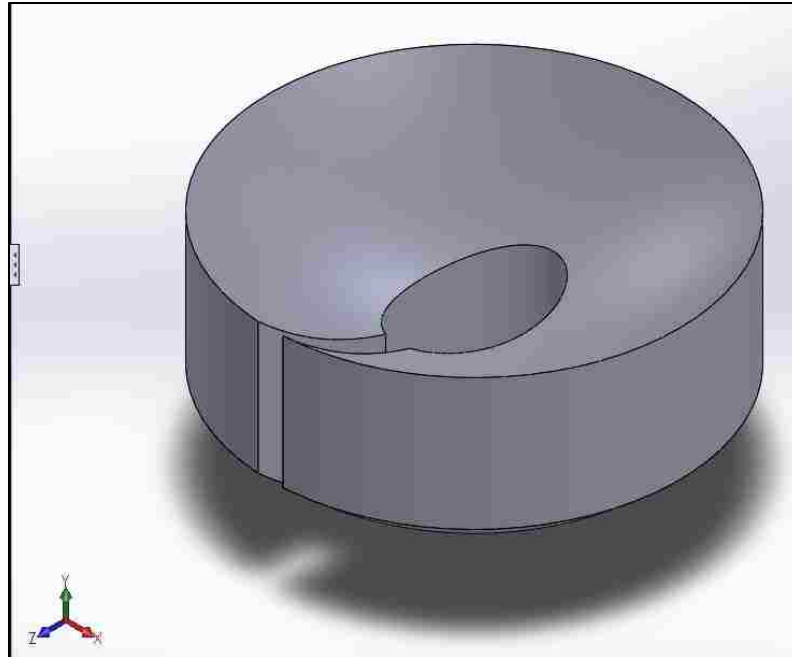
Figure 8-3: Conceptual design of Headform Adapter for Drop Impact Tests

The work performed in this experimental analysis can be used as the foundation for research of much broader latitude. Most of the objectives that were laid out were achieved and information that could possibly be added to the current knowledge base aimed at TBI research was generated. As the work progresses, the focus should be to propose a model to help understand what is occurring at the point of impact and not what is measured due to the impact. This would be necessary to develop effective shock mitigating methodologies. Ultimately, if the two factors necessary to validate an experiment of this nature are to one conceive, design, build, and test an impact test structure with a concept similar to a future NOCSAE proposal and to two help elucidate the characteristics of the contributing biomechanical factors of TBIs, then this experimental analysis was a triumph.

9. APPENDIX

A-1. NOCSAE Proposed Pneumatic Ram
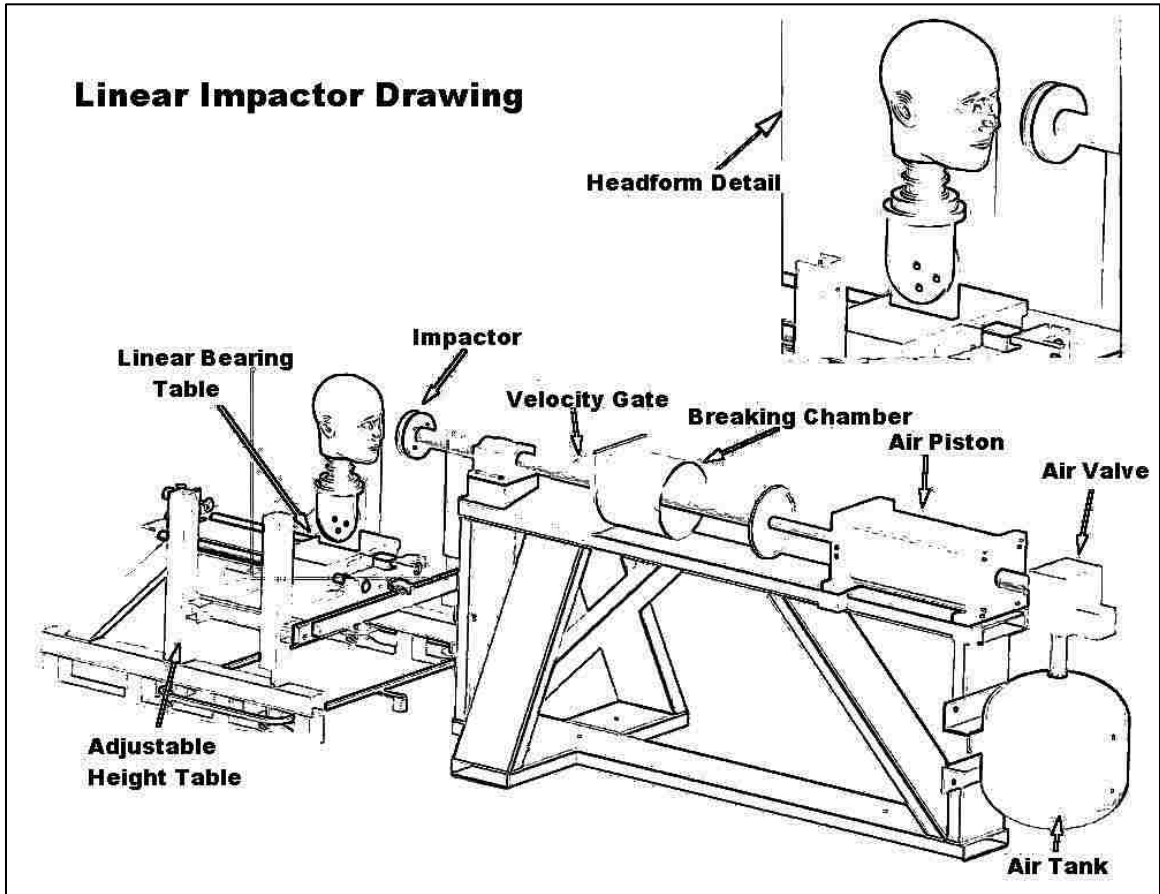
Figure 9-1: NOCSAE's Proposed Pneumatic Ram [8]

A-2. Proposed Headform Adapter
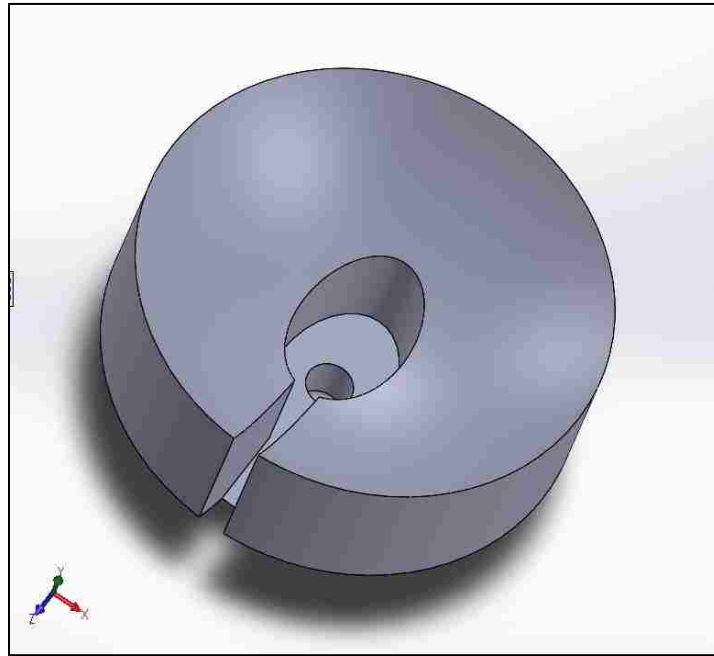
Figure 9-2: Inner Surface of Proposed Headform Adapter for Drop Tests
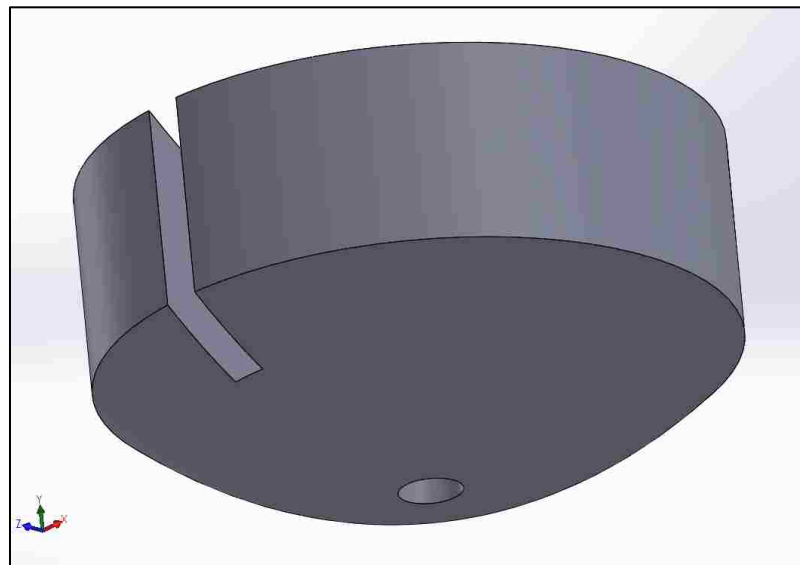
Figure 9-3: Impact Surface of Proposed Headform Adapter

A-3. HIC 15 Curve
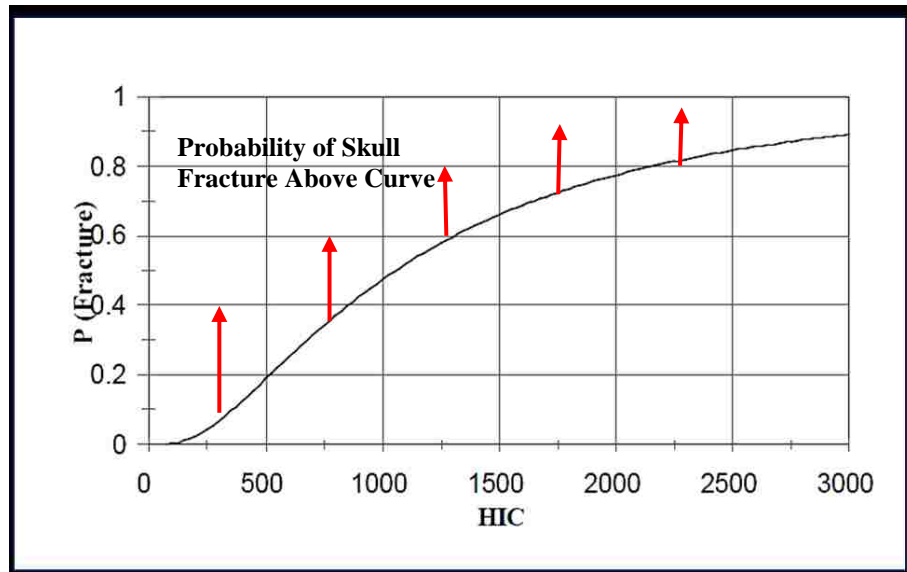
Figure 9-4: Skull Fracture Curve for HIC 15 [16]

A-4. Sample Matlab® Code

```
%% Head Injury Criteria Y-Tri-Axial 2nd Peak
%% LBT Right Side Impacts (Feb 19 2015)Weighted/Non-Weighted
%% Drop Tower/Pendulum Thesis
%% MAR 1 2015
 %% Importing Data Points from Excel for Helmet A
****************************************************************************************************
%%  LBT HelmetA Y-Tri-Axial Accelerometers 2nd Peak
****************************************************
 %% ************************ WEIGHTED ***************************************************************
 %% 12 Y-Tri-------------------------------------------------------------------------------
HelmetA_12A_trix = xlsread('Velocity HelmetA 19 FEB.xlsx','12','X3:X172');
HelmetA_12A_triy = xlsread('Velocity HelmetA 19 FEB.xlsx','12','Y3:Y172');
HelmetA_12B_trix = xlsread('Velocity HelmetA 19 FEB.xlsx','12','X3:X172');
HelmetA_12B_triy = xlsread('Velocity HelmetA 19 FEB.xlsx','12','Z3:Z172');
HelmetA_12C_trix = xlsread('Velocity HelmetA 19 FEB.xlsx','12','X3:X172');
HelmetA_12C_triy = xlsread('Velocity HelmetA 19 FEB.xlsx','12','AA3:AA172');
HelmetA_12D_trix = xlsread('Velocity HelmetA 19 FEB.xlsx','12','X3:X172');
HelmetA_12D_triy = xlsread('Velocity HelmetA 19 FEB.xlsx','12','AB3:AB172');
HelmetA_12E_trix = xlsread('Velocity HelmetA 19 FEB.xlsx','12','X3:X172');
HelmetA_12E_triy = xlsread('Velocity HelmetA 19 FEB.xlsx','12','AC3:AC172');
HelmetA_12avg_trix = xlsread('Velocity HelmetA 19 FEB.xlsx','12','X3:X172');
HelmetA_12avg_triy = xlsread('Velocity HelmetA 19 FEB.xlsx','12','AD3:AD172');


 %% 26 Y-Tri-------------------------------------------------------------------------------
HelmetA_26A_trix = xlsread('Velocity HelmetA 19 FEB.xlsx','26.36','X3:X153');
HelmetA_26A_triy = xlsread('Velocity HelmetA 19 FEB.xlsx','26.36','Y3:Y153');
HelmetA_26B_trix = xlsread('Velocity HelmetA 19 FEB.xlsx','26.36','X3:X153');
HelmetA_26B_triy = xlsread('Velocity HelmetA 19 FEB.xlsx','26.36','Z3:Z153');
HelmetA_26C_trix = xlsread('Velocity HelmetA 19 FEB.xlsx','26.36','X3:X153');
HelmetA_26C_triy = xlsread('Velocity HelmetA 19 FEB.xlsx','26.36','AA3:AA153');
HelmetA_26D_trix = xlsread('Velocity HelmetA 19 FEB.xlsx','26.36','X3:X153');
HelmetA_26D_triy = xlsread('Velocity HelmetA 19 FEB.xlsx','26.36','AB3:AB153');
HelmetA_26E_trix = xlsread('Velocity HelmetA 19 FEB.xlsx','26.36','X3:X153');
HelmetA_26E_triy = xlsread('Velocity HelmetA 19 FEB.xlsx','26.36','AC3:AC153');
HelmetA_26avg_trix = xlsread('Velocity HelmetA 19 FEB.xlsx','26.36','X3:X153');
HelmetA_26avg_triy = xlsread('Velocity HelmetA 19 FEB.xlsx','26.36','AD3:AD153');

 %% **************************** NON - WEIGHTED
*************************************************************
 %% 12 Y-Tri-------------------------------------------------------------------------------
HelmetA_12A_trixNW = xlsread('Velocity HelmetA 19 FEB.xlsx','12NW','X3:X145');
HelmetA_12A_triyNW = xlsread('Velocity HelmetA 19 FEB.xlsx','12NW','Y3:Y145');
HelmetA_12B_trixNW = xlsread('Velocity HelmetA 19 FEB.xlsx','12NW','X3:X145');
HelmetA_12B_triyNW = xlsread('Velocity HelmetA 19 FEB.xlsx','12NW','Z3:Z145');
HelmetA_12C_trixNW = xlsread('Velocity HelmetA 19 FEB.xlsx','12NW','X3:X145');
HelmetA_12C_triyNW = xlsread('Velocity HelmetA 19 FEB.xlsx','12NW','AA3:AA145');
HelmetA_12D_trixNW = xlsread('Velocity HelmetA 19 FEB.xlsx','12NW','X3:X145');
HelmetA_12D_triyNW = xlsread('Velocity HelmetA 19 FEB.xlsx','12NW','AB3:AB145');
HelmetA_12E_trixNW = xlsread('Velocity HelmetA 19 FEB.xlsx','12NW','X3:X145');
HelmetA_12E_triyNW = xlsread('Velocity HelmetA 19 FEB.xlsx','12NW','AC3:AC145');
HelmetA_12avg_trixNW = xlsread('Velocity HelmetA 19 FEB.xlsx','12NW','X3:X145');
HelmetA_12avg_triyNW = xlsread('Velocity HelmetA 19 FEB.xlsx','12NW','AD3:AD145');
 %% 26 Y-Tri-------------------------------------------------------------------------------
HelmetA_26A_trixNW = xlsread('Velocity HelmetA 19 FEB.xlsx','26.36NW','X3:X151');
HelmetA_26A_triyNW = xlsread('Velocity HelmetA 19 FEB.xlsx','26.36NW','Y3:Y151');
HelmetA_26B_trixNW = xlsread('Velocity HelmetA 19 FEB.xlsx','26.36NW','X3:X151');
HelmetA_26B_triyNW = xlsread('Velocity HelmetA 19 FEB.xlsx','26.36NW','Z3:Z151');
HelmetA_26C_trixNW = xlsread('Velocity HelmetA 19 FEB.xlsx','26.36NW','X3:X151');
HelmetA_26C_triyNW = xlsread('Velocity HelmetA 19 FEB.xlsx','26.36NW','AA3:AA151');
HelmetA_26D_trixNW = xlsread('Velocity HelmetA 19 FEB.xlsx','26.36NW','X3:X151');
HelmetA_26D_triyNW = xlsread('Velocity HelmetA 19 FEB.xlsx','26.36NW','AB3:AB151');
HelmetA_26E_trixNW = xlsread('Velocity HelmetA 19 FEB.xlsx','26.36NW','X3:X151');
HelmetA_26E_triyNW = xlsread('Velocity HelmetA 19 FEB.xlsx','26.36NW','AC3:AC151');
HelmetA_26avg_trixNW = xlsread('Velocity HelmetA 19 FEB.xlsx','26.36NW','X3:X151');
HelmetA_26avg_triyNW = xlsread('Velocity HelmetA 19 FEB.xlsx','26.36NW','AD3:AD151');

 %% Importing Data Points from Excel for Helmet B
****************************************************************************************************
%% LBT HelmetB Y-Tri-Axial Accelerometers 2nd Peak
****************************************************
```

```matlab
%% ************************WEIGHTED
************************************************************************
%% 12 Y-Tri-----------------------------------------------------------------------------------
HelmetB_12A_trix = xlsread('Velocity HelmetB 19 FEB.xlsx','12','X3:X146');
HelmetB_12A_triy = xlsread('Velocity HelmetB 19 FEB.xlsx','12','Y3:Y146');
HelmetB_12B_trix = xlsread('Velocity HelmetB 19 FEB.xlsx','12','X3:X146');
HelmetB_12B_triy = xlsread('Velocity HelmetB 19 FEB.xlsx','12','Z3:Z146');
HelmetB_12C_trix = xlsread('Velocity HelmetB 19 FEB.xlsx','12','X3:X146');
HelmetB_12C_triy = xlsread('Velocity HelmetB 19 FEB.xlsx','12','AA3:AA146');
HelmetB_12D_trix = xlsread('Velocity HelmetB 19 FEB.xlsx','12','X3:X146');
HelmetB_12D_triy = xlsread('Velocity HelmetB 19 FEB.xlsx','12','AB3:AB146');
HelmetB_12E_trix = xlsread('Velocity HelmetB 19 FEB.xlsx','12','X3:X146');
HelmetB_12E_triy = xlsread('Velocity HelmetB 19 FEB.xlsx','12','AC3:AC146');
HelmetB_12avg_trix = xlsread('Velocity HelmetB 19 FEB.xlsx','12','X3:X146');
HelmetB_12avg_triy = xlsread('Velocity HelmetB 19 FEB.xlsx','12','AD3:AD146');
%% 26 Y-Tri-----------------------------------------------------------------------------------
HelmetB_26A_trix = xlsread('Velocity HelmetB 19 FEB.xlsx','26.36','X3:X140');
HelmetB_26A_triy = xlsread('Velocity HelmetB 19 FEB.xlsx','26.36','Y3:Y140');
HelmetB_26B_trix = xlsread('Velocity HelmetB 19 FEB.xlsx','26.36','X3:X140');
HelmetB_26B_triy = xlsread('Velocity HelmetB 19 FEB.xlsx','26.36','Z3:Z140');
HelmetB_26C_trix = xlsread('Velocity HelmetB 19 FEB.xlsx','26.36','X3:X140');
HelmetB_26C_triy = xlsread('Velocity HelmetB 19 FEB.xlsx','26.36','AA3:AA140');
HelmetB_26D_trix = xlsread('Velocity HelmetB 19 FEB.xlsx','26.36','X3:X140');
HelmetB_26D_triy = xlsread('Velocity HelmetB 19 FEB.xlsx','26.36','AB3:AB140');
HelmetB_26E_trix = xlsread('Velocity HelmetB 19 FEB.xlsx','26.36','X3:X140');
HelmetB_26E_triy = xlsread('Velocity HelmetB 19 FEB.xlsx','26.36','AC3:AC140');
HelmetB_26avg_trix = xlsread('Velocity HelmetB 19 FEB.xlsx','26.36','X3:X140');
HelmetB_26avg_triy = xlsread('Velocity HelmetB 19 FEB.xlsx','26.36','AD3:AD140');

%% ****************************  NON - WEIGHTED
*************************************************************
%% 12 Y-Tri-----------------------------------------------------------------------------------
HelmetB_12A_trixNW = xlsread('Velocity HelmetB 19 FEB.xlsx','12NW','X3:X149');
HelmetB_12A_triyNW = xlsread('Velocity HelmetB 19 FEB.xlsx','12NW','Y3:Y149');
HelmetB_12B_trixNW = xlsread('Velocity HelmetB 19 FEB.xlsx','12NW','X3:X149');
HelmetB_12B_triyNW = xlsread('Velocity HelmetB 19 FEB.xlsx','12NW','Z3:Z149');
HelmetB_12C_trixNW = xlsread('Velocity HelmetB 19 FEB.xlsx','12NW','X3:X149');
HelmetB_12C_triyNW = xlsread('Velocity HelmetB 19 FEB.xlsx','12NW','AA3:AA149');
HelmetB_12D_trixNW = xlsread('Velocity HelmetB 19 FEB.xlsx','12NW','X3:X149');
HelmetB_12D_triyNW = xlsread('Velocity HelmetB 19 FEB.xlsx','12NW','AB3:AB149');
HelmetB_12E_trixNW = xlsread('Velocity HelmetB 19 FEB.xlsx','12NW','X3:X149');
HelmetB_12E_triyNW = xlsread('Velocity HelmetB 19 FEB.xlsx','12NW','AC3:AC149');
HelmetB_12avg_trixNW = xlsread('Velocity HelmetB 19 FEB.xlsx','12NW','X3:X149');
HelmetB_12avg_triyNW = xlsread('Velocity HelmetB 19 FEB.xlsx','12NW','AD3:AD149');
%% 26 Y-Tri-----------------------------------------------------------------------------------
HelmetB_26A_trixNW = xlsread('Velocity HelmetB 19 FEB.xlsx','26.36NW','X3:X144');
HelmetB_26A_triyNW = xlsread('Velocity HelmetB 19 FEB.xlsx','26.36NW','Y3:Y144');
HelmetB_26B_trixNW = xlsread('Velocity HelmetB 19 FEB.xlsx','26.36NW','X3:X144');
HelmetB_26B_triyNW = xlsread('Velocity HelmetB 19 FEB.xlsx','26.36NW','Z3:Z144');
HelmetB_26C_trixNW = xlsread('Velocity HelmetB 19 FEB.xlsx','26.36NW','X3:X144');
HelmetB_26C_triyNW = xlsread('Velocity HelmetB 19 FEB.xlsx','26.36NW','AA3:AA144');
HelmetB_26D_trixNW = xlsread('Velocity HelmetB 19 FEB.xlsx','26.36NW','X3:X144');
HelmetB_26D_triyNW = xlsread('Velocity HelmetB 19 FEB.xlsx','26.36NW','AB3:AB144');
HelmetB_26E_trixNW = xlsread('Velocity HelmetB 19 FEB.xlsx','26.36NW','X3:X144');
HelmetB_26E_triyNW = xlsread('Velocity HelmetB 19 FEB.xlsx','26.36NW','AC3:AC144');
HelmetB_26avg_trixNW = xlsread('Velocity HelmetB 19 FEB.xlsx','26.36NW','X3:X144');
HelmetB_26avg_triyNW = xlsread('Velocity HelmetB 19 FEB.xlsx','26.36NW','AD3:AD144');

%% Importing Data Points from Excel for Headform
***********************************************************************************************
%% LBT Headform Y-Tri-Axial Accelerometers 2nd Peak
*******************************************************
%% ************************ WEIGHTED *************************************************************
%% 12 Y-Tri-----------------------------------------------------------------------------------
Headform_12A_trix = xlsread('Velocity Headform 19 FEB.xlsx','12','X3:X113');
Headform_12A_triy = xlsread('Velocity Headform 19 FEB.xlsx','12','Y3:Y113');
Headform_12B_trix = xlsread('Velocity Headform 19 FEB.xlsx','12','X3:X113');
Headform_12B_triy = xlsread('Velocity Headform 19 FEB.xlsx','12','Z3:Z113');
Headform_12C_trix = xlsread('Velocity Headform 19 FEB.xlsx','12','X3:X113');
Headform_12C_triy = xlsread('Velocity Headform 19 FEB.xlsx','12','AA3:AA113');
Headform_12D_trix = xlsread('Velocity Headform 19 FEB.xlsx','12','X3:X113');
Headform_12D_triy = xlsread('Velocity Headform 19 FEB.xlsx','12','AB3:AB113');
Headform_12E_trix = xlsread('Velocity Headform 19 FEB.xlsx','12','X3:X113');
Headform_12E_triy = xlsread('Velocity Headform 19 FEB.xlsx','12','AC3:AC113');
Headform_12avg_trix = xlsread('Velocity Headform 19 FEB.xlsx','12','X3:X113');
Headform_12avg_triy = xlsread('Velocity Headform 19 FEB.xlsx','12','AD3:AD113');
```

```matlab
%% 26 Y-Tri-----------------------------------------------------------------------------------
Headform_26A_trix = xlsread('Velocity Headform 19 FEB.xlsx','26.36','X3:X138');
Headform_26A_triy = xlsread('Velocity Headform 19 FEB.xlsx','26.36','Y3:Y138');
Headform_26B_trix = xlsread('Velocity Headform 19 FEB.xlsx','26.36','X3:X138');
Headform_26B_triy = xlsread('Velocity Headform 19 FEB.xlsx','26.36','Z3:Z138');
Headform_26C_trix = xlsread('Velocity Headform 19 FEB.xlsx','26.36','X3:X138');
Headform_26C_triy = xlsread('Velocity Headform 19 FEB.xlsx','26.36','AA3:AA138');
Headform_26D_trix = xlsread('Velocity Headform 19 FEB.xlsx','26.36','X3:X138');
Headform_26D_triy = xlsread('Velocity Headform 19 FEB.xlsx','26.36','AB3:AB138');
Headform_26E_trix = xlsread('Velocity Headform 19 FEB.xlsx','26.36','X3:X138');
Headform_26E_triy = xlsread('Velocity Headform 19 FEB.xlsx','26.36','AC3:AC138');
Headform_26avg_trix = xlsread('Velocity Headform 19 FEB.xlsx','26.36','X3:X138');
Headform_26avg_triy = xlsread('Velocity Headform 19 FEB.xlsx','26.36','AD3:AD138');
%% ****************************  NON - WEIGHTED
**********************************************************
%% 12 Y-Tri-----------------------------------------------------------------------------------
Headform_12A_trixNW = xlsread('Velocity Headform 19 FEB.xlsx','12NW','X3:X151');
Headform_12A_triyNW = xlsread('Velocity Headform 19 FEB.xlsx','12NW','Y3:Y151');
Headform_12B_trixNW = xlsread('Velocity Headform 19 FEB.xlsx','12NW','X3:X151');
Headform_12B_triyNW = xlsread('Velocity Headform 19 FEB.xlsx','12NW','Z3:Z151');
Headform_12C_trixNW = xlsread('Velocity Headform 19 FEB.xlsx','12NW','X3:X151');
Headform_12C_triyNW = xlsread('Velocity Headform 19 FEB.xlsx','12NW','AA3:AA151');
Headform_12D_trixNW = xlsread('Velocity Headform 19 FEB.xlsx','12NW','X3:X151');
Headform_12D_triyNW = xlsread('Velocity Headform 19 FEB.xlsx','12NW','AB3:AB151');
Headform_12E_trixNW = xlsread('Velocity Headform 19 FEB.xlsx','12NW','X3:X151');
Headform_12E_triyNW = xlsread('Velocity Headform 19 FEB.xlsx','12NW','AC3:AC151');
Headform_12avg_trixNW = xlsread('Velocity Headform 19 FEB.xlsx','12NW','X3:X151');
Headform_12avg_triyNW = xlsread('Velocity Headform 19 FEB.xlsx','12NW','AD3:AD151');
%% 26 Y-Tri-----------------------------------------------------------------------------------
Headform_26A_trixNW = xlsread('Velocity Headform 19 FEB.xlsx','26.36NW','X3:X147');
Headform_26A_triyNW = xlsread('Velocity Headform 19 FEB.xlsx','26.36NW','Y3:Y147');
Headform_26B_trixNW = xlsread('Velocity Headform 19 FEB.xlsx','26.36NW','X3:X147');
Headform_26B_triyNW = xlsread('Velocity Headform 19 FEB.xlsx','26.36NW','Z3:Z147');
Headform_26C_trixNW = xlsread('Velocity Headform 19 FEB.xlsx','26.36NW','X3:X147');
Headform_26C_triyNW = xlsread('Velocity Headform 19 FEB.xlsx','26.36NW','AA3:AA147');
Headform_26D_trixNW = xlsread('Velocity Headform 19 FEB.xlsx','26.36NW','X3:X147');
Headform_26D_triyNW = xlsread('Velocity Headform 19 FEB.xlsx','26.36NW','AB3:AB147');
Headform_26E_trixNW = xlsread('Velocity Headform 19 FEB.xlsx','26.36NW','X3:X147');
Headform_26E_triyNW = xlsread('Velocity Headform 19 FEB.xlsx','26.36NW','AC3:AC147');
Headform_26avg_trixNW = xlsread('Velocity Headform 19 FEB.xlsx','26.36NW','X3:X147');
Headform_26avg_triyNW = xlsread('Velocity Headform 19 FEB.xlsx','26.36NW','AD3:AD147');
%% Importing Data Points from Excel for
Pitcher*****************************************************************************************
%% ***********************  WEIGHTED ***************************************************
%% 12 Y-Tri-----------------------------------------------------------------------------------
Pitcher_12A_trix = xlsread('Velocity Pitcher 19 FEB.xlsx','12','X3:X145');
Pitcher_12A_triy = xlsread('Velocity Pitcher 19 FEB.xlsx','12','Y3:Y145');
Pitcher_12B_trix = xlsread('Velocity Pitcher 19 FEB.xlsx','12','X3:X145');
Pitcher_12B_triy = xlsread('Velocity Pitcher 19 FEB.xlsx','12','Z3:Z145');
Pitcher_12C_trix = xlsread('Velocity Pitcher 19 FEB.xlsx','12','X3:X145');
Pitcher_12C_triy = xlsread('Velocity Pitcher 19 FEB.xlsx','12','AA3:AA145');
Pitcher_12D_trix = xlsread('Velocity Pitcher 19 FEB.xlsx','12','X3:X145');
Pitcher_12D_triy = xlsread('Velocity Pitcher 19 FEB.xlsx','12','AB3:AB145');
Pitcher_12E_trix = xlsread('Velocity Pitcher 19 FEB.xlsx','12','X3:X145');
Pitcher_12E_triy = xlsread('Velocity Pitcher 19 FEB.xlsx','12','AC3:AC145');
Pitcher_12avg_trix = xlsread('Velocity Pitcher 19 FEB.xlsx','12','X3:X145');
Pitcher_12avg_triy = xlsread('Velocity Pitcher 19 FEB.xlsx','12','AD3:AD145');
%% 26 Y-Tri-----------------------------------------------------------------------------------
Pitcher_26A_trix = xlsread('Velocity Pitcher 19 FEB.xlsx','26.36','X3:X142');
Pitcher_26A_triy = xlsread('Velocity Pitcher 19 FEB.xlsx','26.36','Y3:Y142');
Pitcher_26B_trix = xlsread('Velocity Pitcher 19 FEB.xlsx','26.36','X3:X142');
Pitcher_26B_triy = xlsread('Velocity Pitcher 19 FEB.xlsx','26.36','Z3:Z142');
Pitcher_26C_trix = xlsread('Velocity Pitcher 19 FEB.xlsx','26.36','X3:X142');
Pitcher_26C_triy = xlsread('Velocity Pitcher 19 FEB.xlsx','26.36','AA3:AA142');
Pitcher_26D_trix = xlsread('Velocity Pitcher 19 FEB.xlsx','26.36','X3:X142');
Pitcher_26D_triy = xlsread('Velocity Pitcher 19 FEB.xlsx','26.36','AB3:AB142');
Pitcher_26E_trix = xlsread('Velocity Pitcher 19 FEB.xlsx','26.36','X3:X142');
Pitcher_26E_triy = xlsread('Velocity Pitcher 19 FEB.xlsx','26.36','AC3:AC142');
Pitcher_26avg_trix = xlsread('Velocity Pitcher 19 FEB.xlsx','26.36','X3:X142');
Pitcher_26avg_triy = xlsread('Velocity Pitcher 19 FEB.xlsx','26.36','AD3:AD142');
%% ****************************  NON - WEIGHTED
**********************************************************
%% 12 Y-Tri-----------------------------------------------------------------------------------
Pitcher_12A_trixNW = xlsread('Velocity Pitcher 19 FEB.xlsx','12NW','X3:X155');
Pitcher_12A_triyNW = xlsread('Velocity Pitcher 19 FEB.xlsx','12NW','Y3:Y155');
Pitcher_12B_trixNW = xlsread('Velocity Pitcher 19 FEB.xlsx','12NW','X3:X155');
```

```matlab
Pitcher_12B_triyNW = xlsread('Velocity Pitcher 19 FEB.xlsx','12NW','Z3:Z155');
Pitcher_12C_trixNW = xlsread('Velocity Pitcher 19 FEB.xlsx','12NW','X3:X155');
Pitcher_12C_triyNW = xlsread('Velocity Pitcher 19 FEB.xlsx','12NW','AA3:AA155');
Pitcher_12D_trixNW = xlsread('Velocity Pitcher 19 FEB.xlsx','12NW','X3:X155');
Pitcher_12D_triyNW = xlsread('Velocity Pitcher 19 FEB.xlsx','12NW','AB3:AB155');
Pitcher_12E_trixNW = xlsread('Velocity Pitcher 19 FEB.xlsx','12NW','X3:X155');
Pitcher_12E_triyNW = xlsread('Velocity Pitcher 19 FEB.xlsx','12NW','AC3:AC155');
Pitcher_12avg_trixNW = xlsread('Velocity Pitcher 19 FEB.xlsx','12NW','X3:X155');
Pitcher_12avg_triyNW = xlsread('Velocity Pitcher 19 FEB.xlsx','12NW','AD3:AD155');
%% 26 Y-Tri-----------------------------------------------------------------
Pitcher_26A_trixNW = xlsread('Velocity Pitcher 19 FEB.xlsx','26.36NW','X3:X139');
Pitcher_26A_triyNW = xlsread('Velocity Pitcher 19 FEB.xlsx','26.36NW','Y3:Y139');
Pitcher_26B_trixNW = xlsread('Velocity Pitcher 19 FEB.xlsx','26.36NW','X3:X139');
Pitcher_26B_triyNW = xlsread('Velocity Pitcher 19 FEB.xlsx','26.36NW','Z3:Z139');
Pitcher_26C_trixNW = xlsread('Velocity Pitcher 19 FEB.xlsx','26.36NW','X3:X139');
Pitcher_26C_triyNW = xlsread('Velocity Pitcher 19 FEB.xlsx','26.36NW','AA3:AA139');
Pitcher_26D_trixNW = xlsread('Velocity Pitcher 19 FEB.xlsx','26.36NW','X3:X139');
Pitcher_26D_triyNW = xlsread('Velocity Pitcher 19 FEB.xlsx','26.36NW','AB3:AB139');
Pitcher_26E_trixNW = xlsread('Velocity Pitcher 19 FEB.xlsx','26.36NW','X3:X139');
Pitcher_26E_triyNW = xlsread('Velocity Pitcher 19 FEB.xlsx','26.36NW','AC3:AC139');
Pitcher_26avg_trixNW = xlsread('Velocity Pitcher 19 FEB.xlsx','26.36NW','X3:X139');
Pitcher_26avg_triyNW = xlsread('Velocity Pitcher 19 FEB.xlsx','26.36NW','AD3:AD139');
 %% Getting time differences
 %% LBT Helmet A**************************************************************
 %% ******************  Weighted  ****************************************************
 %% 12 Y-Tri-----------------------------------------------------------------
 HelmetA_12A_trit1 = HelmetA_12A_trix(1);
HelmetA_12A_tritf = HelmetA_12A_trix(end);
HelmetA_12A_tridif = HelmetA_12A_tritf - HelmetA_12A_trit1;

HelmetA_12B_trit1 = HelmetA_12B_trix(1);
HelmetA_12B_tritf = HelmetA_12B_trix(end);
HelmetA_12B_tridif = HelmetA_12B_tritf - HelmetA_12B_trit1;

HelmetA_12C_trit1 = HelmetA_12C_trix(1);
HelmetA_12C_tritf = HelmetA_12C_trix(end);
HelmetA_12C_tridif = HelmetA_12C_tritf - HelmetA_12C_trit1;

HelmetA_12D_trit1 = HelmetA_12D_trix(1);
HelmetA_12D_tritf = HelmetA_12D_trix(end);
HelmetA_12D_tridif = HelmetA_12D_tritf - HelmetA_12D_trit1;

HelmetA_12E_trit1 = HelmetA_12E_trix(1);
HelmetA_12E_tritf = HelmetA_12E_trix(end);
HelmetA_12E_tridif = HelmetA_12E_tritf - HelmetA_12E_trit1;

HelmetA_12avg_trit1 = HelmetA_12avg_trix(1);
HelmetA_12avg_tritf = HelmetA_12avg_trix(end);
HelmetA_12avg_tridif = HelmetA_12avg_tritf - HelmetA_12avg_trit1;
 %% 26 Y-Tri-----------------------------------------------------------------

HelmetA_26A_trit1 = HelmetA_26A_trix(1);
HelmetA_26A_tritf = HelmetA_26A_trix(end);
HelmetA_26A_tridif = HelmetA_26A_tritf - HelmetA_26A_trit1;

HelmetA_26B_trit1 = HelmetA_26B_trix(1);
HelmetA_26B_tritf = HelmetA_26B_trix(end);
HelmetA_26B_tridif = HelmetA_26B_tritf - HelmetA_26B_trit1;

HelmetA_26C_trit1 = HelmetA_26C_trix(1);
HelmetA_26C_tritf = HelmetA_26C_trix(end);
HelmetA_26C_tridif = HelmetA_26C_tritf - HelmetA_26C_trit1;

HelmetA_26D_trit1 = HelmetA_26D_trix(1);
HelmetA_26D_tritf = HelmetA_26D_trix(end);
HelmetA_26D_tridif = HelmetA_26D_tritf - HelmetA_26D_trit1;

HelmetA_26E_trit1 = HelmetA_26E_trix(1);
HelmetA_26E_tritf = HelmetA_26E_trix(end);
HelmetA_26E_tridif = HelmetA_26E_tritf - HelmetA_26E_trit1;

HelmetA_26avg_trit1 = HelmetA_26avg_trix(1);
HelmetA_26avg_tritf = HelmetA_26avg_trix(end);
HelmetA_26avg_tridif = HelmetA_26avg_tritf - HelmetA_26avg_trit1;
```

107

```matlab
%% **************************** Non - Weighted
*********************************************************
 %% 12 Y-Tri-------------------------------------------------------------------------------

HelmetA_12A_trit1NW = HelmetA_12A_trixNW(1);
HelmetA_12A_tritfNW = HelmetA_12A_trixNW(end);
HelmetA_12A_tridifNW = HelmetA_12A_tritfNW - HelmetA_12A_trit1NW;

HelmetA_12B_trit1NW = HelmetA_12B_trixNW(1);
HelmetA_12B_tritfNW = HelmetA_12B_trixNW(end);
HelmetA_12B_tridifNW = HelmetA_12B_tritfNW - HelmetA_12B_trit1NW;

HelmetA_12C_trit1NW = HelmetA_12C_trixNW(1);
HelmetA_12C_tritfNW = HelmetA_12C_trixNW(end);
HelmetA_12C_tridifNW = HelmetA_12C_tritfNW - HelmetA_12C_trit1NW;

HelmetA_12D_trit1NW = HelmetA_12D_trixNW(1);
HelmetA_12D_tritfNW = HelmetA_12D_trixNW(end);
HelmetA_12D_tridifNW = HelmetA_12D_tritfNW - HelmetA_12D_trit1NW;
 HelmetA_12E_trit1NW = HelmetA_12E_trixNW(1);
HelmetA_12E_tritfNW = HelmetA_12E_trixNW(end);
HelmetA_12E_tridifNW = HelmetA_12E_tritfNW - HelmetA_12E_trit1NW;

HelmetA_12avg_trit1NW = HelmetA_12avg_trixNW(1);
HelmetA_12avg_tritfNW = HelmetA_12avg_trixNW(end);
HelmetA_12avg_tridifNW = HelmetA_12avg_tritfNW - HelmetA_12avg_trit1NW;
 %% 26 Y-Tri-------------------------------------------------------------------------------

HelmetA_26A_trit1NW = HelmetA_26A_trixNW(1);
HelmetA_26A_tritfNW = HelmetA_26A_trixNW(end);
HelmetA_26A_tridifNW = HelmetA_26A_tritfNW - HelmetA_26A_trit1NW;

HelmetA_26B_trit1NW = HelmetA_26B_trixNW(1);
HelmetA_26B_tritfNW = HelmetA_26B_trixNW(end);
HelmetA_26B_tridifNW = HelmetA_26B_tritfNW - HelmetA_26B_trit1NW;

HelmetA_26C_trit1NW = HelmetA_26C_trixNW(1);
HelmetA_26C_tritfNW = HelmetA_26C_trixNW(end);
HelmetA_26C_tridifNW = HelmetA_26C_tritfNW - HelmetA_26C_trit1NW;

HelmetA_26D_trit1NW = HelmetA_26D_trixNW(1);
HelmetA_26D_tritfNW = HelmetA_26D_trixNW(end);
HelmetA_26D_tridifNW = HelmetA_26D_tritfNW - HelmetA_26D_trit1NW;

HelmetA_26E_trit1NW = HelmetA_26E_trixNW(1);
HelmetA_26E_tritfNW = HelmetA_26E_trixNW(end);
HelmetA_26E_tridifNW = HelmetA_26E_tritfNW - HelmetA_26E_trit1NW;

HelmetA_26avg_trit1NW = HelmetA_26avg_trixNW(1);
HelmetA_26avg_tritfNW = HelmetA_26avg_trixNW(end);
HelmetA_26avg_tridifNW = HelmetA_26avg_tritfNW - HelmetA_26avg_trit1NW;
%% LBT Helmet
B***********************************************************************************************
 %% ********************  Weighted
*********************************************************************
 %% 12 -----------------------------------------------------------------------------------
HelmetB_12A_trit1 = HelmetB_12A_trix(1);
HelmetB_12A_tritf = HelmetB_12A_trix(end);
HelmetB_12A_tridif = HelmetB_12A_tritf - HelmetB_12A_trit1;

HelmetB_12B_trit1 = HelmetB_12B_trix(1);
HelmetB_12B_tritf = HelmetB_12B_trix(end);
HelmetB_12B_tridif = HelmetB_12B_tritf - HelmetB_12B_trit1;

HelmetB_12C_trit1 = HelmetB_12C_trix(1);
HelmetB_12C_tritf = HelmetB_12C_trix(end);
HelmetB_12C_tridif = HelmetB_12C_tritf - HelmetB_12C_trit1;

HelmetB_12D_trit1 = HelmetB_12D_trix(1);
HelmetB_12D_tritf = HelmetB_12D_trix(end);
HelmetB_12D_tridif = HelmetB_12D_tritf - HelmetB_12D_trit1;

HelmetB_12E_trit1 = HelmetB_12E_trix(1);
HelmetB_12E_tritf = HelmetB_12E_trix(end);
HelmetB_12E_tridif = HelmetB_12E_tritf - HelmetB_12E_trit1;
```

```
HelmetB_12avg_trit1 = HelmetB_12avg_trix(1);
HelmetB_12avg_tritf = HelmetB_12avg_trix(end);
HelmetB_12avg_tridif = HelmetB_12avg_tritf - HelmetB_12avg_trit1;
%% 26 -----------------------------------------------------------------------------------
HelmetB_26A_trit1 = HelmetB_26A_trix(1);
HelmetB_26A_tritf = HelmetB_26A_trix(end);
HelmetB_26A_tridif = HelmetB_26A_tritf - HelmetB_26A_trit1;

HelmetB_26B_trit1 = HelmetB_26B_trix(1);
HelmetB_26B_tritf = HelmetB_26B_trix(end);
HelmetB_26B_tridif = HelmetB_26B_tritf - HelmetB_26B_trit1;

HelmetB_26C_trit1 = HelmetB_26C_trix(1);
HelmetB_26C_tritf = HelmetB_26C_trix(end);
HelmetB_26C_tridif = HelmetB_26C_tritf - HelmetB_26C_trit1;

HelmetB_26D_trit1 = HelmetB_26D_trix(1);
HelmetB_26D_tritf = HelmetB_26D_trix(end);
HelmetB_26D_tridif = HelmetB_26D_tritf - HelmetB_26D_trit1;

HelmetB_26E_trit1 = HelmetB_26E_trix(1);
HelmetB_26E_tritf = HelmetB_26E_trix(end);
HelmetB_26E_tridif = HelmetB_26E_tritf - HelmetB_26E_trit1;
 HelmetB_26avg_trit1 = HelmetB_26avg_trix(1);
HelmetB_26avg_tritf = HelmetB_26avg_trix(end);
HelmetB_26avg_tridif = HelmetB_26avg_tritf - HelmetB_26avg_trit1;
 %% *************************** Non - Weighted
************************************************************
%% 12 Y-Tri-----------------------------------------------------------------------------------------------
HelmetB_12A_trit1NW = HelmetB_12A_trixNW(1);
HelmetB_12A_tritfNW = HelmetB_12A_trixNW(end);
HelmetB_12A_tridifNW = HelmetB_12A_tritfNW - HelmetB_12A_trit1NW;

HelmetB_12B_trit1NW = HelmetB_12B_trixNW(1);
HelmetB_12B_tritfNW = HelmetB_12B_trixNW(end);
HelmetB_12B_tridifNW = HelmetB_12B_tritfNW - HelmetB_12B_trit1NW;

HelmetB_12C_trit1NW = HelmetB_12C_trixNW(1);
HelmetB_12C_tritfNW = HelmetB_12C_trixNW(end);
HelmetB_12C_tridifNW = HelmetB_12C_tritfNW - HelmetB_12C_trit1NW;

HelmetB_12D_trit1NW = HelmetB_12D_trixNW(1);
HelmetB_12D_tritfNW = HelmetB_12D_trixNW(end);
HelmetB_12D_tridifNW = HelmetB_12D_tritfNW - HelmetB_12D_trit1NW;

HelmetB_12E_trit1NW = HelmetB_12E_trixNW(1);
HelmetB_12E_tritfNW = HelmetB_12E_trixNW(end);
HelmetB_12E_tridifNW = HelmetB_12E_tritfNW - HelmetB_12E_trit1NW;

HelmetB_12avg_trit1NW = HelmetB_12avg_trixNW(1);
HelmetB_12avg_tritfNW = HelmetB_12avg_trixNW(end);
HelmetB_12avg_tridifNW = HelmetB_12avg_tritfNW - HelmetB_12avg_trit1NW;
 %% 26 Y-Tri-----------------------------------------------------------------------------------------------

HelmetB_26A_trit1NW = HelmetB_26A_trixNW(1);
HelmetB_26A_tritfNW = HelmetB_26A_trixNW(end);
HelmetB_26A_tridifNW = HelmetB_26A_tritfNW - HelmetB_26A_trit1NW;

HelmetB_26B_trit1NW = HelmetB_26B_trixNW(1);
HelmetB_26B_tritfNW = HelmetB_26B_trixNW(end);
HelmetB_26B_tridifNW = HelmetB_26B_tritfNW - HelmetB_26B_trit1NW;

HelmetB_26C_trit1NW = HelmetB_26C_trixNW(1);
HelmetB_26C_tritfNW = HelmetB_26C_trixNW(end);
HelmetB_26C_tridifNW = HelmetB_26C_tritfNW - HelmetB_26C_trit1NW;

HelmetB_26D_trit1NW = HelmetB_26D_trixNW(1);
HelmetB_26D_tritfNW = HelmetB_26D_trixNW(end);
HelmetB_26D_tridifNW = HelmetB_26D_tritfNW - HelmetB_26D_trit1NW;

HelmetB_26E_trit1NW = HelmetB_26E_trixNW(1);
HelmetB_26E_tritfNW = HelmetB_26E_trixNW(end);
HelmetB_26E_tridifNW = HelmetB_26E_tritfNW - HelmetB_26E_trit1NW;

HelmetB_26avg_trit1NW = HelmetB_26avg_trixNW(1);
HelmetB_26avg_tritfNW = HelmetB_26avg_trixNW(end);
```

```
HelmetB_26avg_tridifNW = HelmetB_26avg_tritfNW - HelmetB_26avg_trit1NW;
%% LBT Pitcher-------------------------------------------------------------------------------

%% ********************  Weighted
********************************************************************
%% 12 -----------------------------------------------------------------------------------------
Pitcher_12A_trit1 = Pitcher_12A_trix(1);
Pitcher_12A_tritf = Pitcher_12A_trix(end);
Pitcher_12A_tridif = Pitcher_12A_tritf - Pitcher_12A_trit1;

Pitcher_12B_trit1 = Pitcher_12B_trix(1);
Pitcher_12B_tritf = Pitcher_12B_trix(end);
Pitcher_12B_tridif = Pitcher_12B_tritf - Pitcher_12B_trit1;

Pitcher_12C_trit1 = Pitcher_12C_trix(1);
Pitcher_12C_tritf = Pitcher_12C_trix(end);
Pitcher_12C_tridif = Pitcher_12C_tritf - Pitcher_12C_trit1;

Pitcher_12D_trit1 = Pitcher_12D_trix(1);
Pitcher_12D_tritf = Pitcher_12D_trix(end);
Pitcher_12D_tridif = Pitcher_12D_tritf - Pitcher_12D_trit1;

Pitcher_12E_trit1 = Pitcher_12E_trix(1);
Pitcher_12E_tritf = Pitcher_12E_trix(end);
Pitcher_12E_tridif = Pitcher_12E_tritf - Pitcher_12E_trit1;

Pitcher_12avg_trit1 = Pitcher_12avg_trix(1);
Pitcher_12avg_tritf = Pitcher_12avg_trix(end);
Pitcher_12avg_tridif = Pitcher_12avg_tritf - Pitcher_12avg_trit1;

%% 26 -----------------------------------------------------------------------------------------
Pitcher_26A_trit1 = Pitcher_26A_trix(1);
Pitcher_26A_tritf = Pitcher_26A_trix(end);
Pitcher_26A_tridif = Pitcher_26A_tritf - Pitcher_26A_trit1;

Pitcher_26B_trit1 = Pitcher_26B_trix(1);
Pitcher_26B_tritf = Pitcher_26B_trix(end);
Pitcher_26B_tridif = Pitcher_26B_tritf - Pitcher_26B_trit1;

Pitcher_26C_trit1 = Pitcher_26C_trix(1);
Pitcher_26C_tritf = Pitcher_26C_trix(end);
Pitcher_26C_tridif = Pitcher_26C_tritf - Pitcher_26C_trit1;

Pitcher_26D_trit1 = Pitcher_26D_trix(1);
Pitcher_26D_tritf = Pitcher_26D_trix(end);
Pitcher_26D_tridif = Pitcher_26D_tritf - Pitcher_26D_trit1;

Pitcher_26E_trit1 = Pitcher_26E_trix(1);
Pitcher_26E_tritf = Pitcher_26E_trix(end);
Pitcher_26E_tridif = Pitcher_26E_tritf - Pitcher_26E_trit1;

Pitcher_26avg_trit1 = Pitcher_26avg_trix(1);
Pitcher_26avg_tritf = Pitcher_26avg_trix(end);
Pitcher_26avg_tridif = Pitcher_26avg_tritf - Pitcher_26avg_trit1;

%% *************************** Non - Weighted
********************************************************
 %% 12 Y-Tri------------------------------------------------------------------------------------

Pitcher_12A_trit1NW = Pitcher_12A_trixNW(1);
Pitcher_12A_tritfNW = Pitcher_12A_trixNW(end);
Pitcher_12A_tridifNW = Pitcher_12A_tritfNW - Pitcher_12A_trit1NW;

Pitcher_12B_trit1NW = Pitcher_12B_trixNW(1);
Pitcher_12B_tritfNW = Pitcher_12B_trixNW(end);
Pitcher_12B_tridifNW = Pitcher_12B_tritfNW - Pitcher_12B_trit1NW;

Pitcher_12C_trit1NW = Pitcher_12C_trixNW(1);
Pitcher_12C_tritfNW = Pitcher_12C_trixNW(end);
Pitcher_12C_tridifNW = Pitcher_12C_tritfNW - Pitcher_12C_trit1NW;

Pitcher_12D_trit1NW = Pitcher_12D_trixNW(1);
Pitcher_12D_tritfNW = Pitcher_12D_trixNW(end);
Pitcher_12D_tridifNW = Pitcher_12D_tritfNW - Pitcher_12D_trit1NW;

Pitcher_12E_trit1NW = Pitcher_12E_trixNW(1);
```

```
Pitcher_12E_tritfNW = Pitcher_12E_trixNW(end);
Pitcher_12E_tridifNW = Pitcher_12E_tritfNW - Pitcher_12E_trit1NW;

Pitcher_12avg_trit1NW = Pitcher_12avg_trixNW(1);
Pitcher_12avg_tritfNW = Pitcher_12avg_trixNW(end);
Pitcher_12avg_tridifNW = Pitcher_12avg_tritfNW - Pitcher_12avg_trit1NW;
 %% 26 Y-Tri--------------------------------------------------------------------------------

Pitcher_26A_trit1NW = Pitcher_26A_trixNW(1);
Pitcher_26A_tritfNW = Pitcher_26A_trixNW(end);
Pitcher_26A_tridifNW = Pitcher_26A_tritfNW - Pitcher_26A_trit1NW;

Pitcher_26B_trit1NW = Pitcher_26B_trixNW(1);
Pitcher_26B_tritfNW = Pitcher_26B_trixNW(end);
Pitcher_26B_tridifNW = Pitcher_26B_tritfNW - Pitcher_26B_trit1NW;

Pitcher_26C_trit1NW = Pitcher_26C_trixNW(1);
Pitcher_26C_tritfNW = Pitcher_26C_trixNW(end);
Pitcher_26C_tridifNW = Pitcher_26C_tritfNW - Pitcher_26C_trit1NW;

Pitcher_26D_trit1NW = Pitcher_26D_trixNW(1);
Pitcher_26D_tritfNW = Pitcher_26D_trixNW(end);
Pitcher_26D_tridifNW = Pitcher_26D_tritfNW - Pitcher_26D_trit1NW;

Pitcher_26E_trit1NW = Pitcher_26E_trixNW(1);
Pitcher_26E_tritfNW = Pitcher_26E_trixNW(end);
Pitcher_26E_tridifNW = Pitcher_26E_tritfNW - Pitcher_26E_trit1NW;

Pitcher_26avg_trit1NW = Pitcher_26avg_trixNW(1);
Pitcher_26avg_tritfNW = Pitcher_26avg_trixNW(end);
Pitcher_26avg_tridifNW = Pitcher_26avg_tritfNW - Pitcher_26avg_trit1NW;

%% LBT Headform*********************************************************************
%% ******************** Weighted
******************************************************************
%% 12 ---------------------------------------------------------------------------------------
---
Headform_12A_trit1 = Headform_12A_trix(1);
Headform_12A_tritf = Headform_12A_trix(end);
Headform_12A_tridif = Headform_12A_tritf - Headform_12A_trit1;

Headform_12B_trit1 = Headform_12B_trix(1);
Headform_12B_tritf = Headform_12B_trix(end);
Headform_12B_tridif = Headform_12B_tritf - Headform_12B_trit1;

Headform_12C_trit1 = Headform_12C_trix(1);
Headform_12C_tritf = Headform_12C_trix(end);
Headform_12C_tridif = Headform_12C_tritf - Headform_12C_trit1;

Headform_12D_trit1 = Headform_12D_trix(1);
Headform_12D_tritf = Headform_12D_trix(end);
Headform_12D_tridif = Headform_12D_tritf - Headform_12D_trit1;

Headform_12E_trit1 = Headform_12E_trix(1);
Headform_12E_tritf = Headform_12E_trix(end);
Headform_12E_tridif = Headform_12E_tritf - Headform_12E_trit1;

Headform_12avg_trit1 = Headform_12avg_trix(1);
Headform_12avg_tritf = Headform_12avg_trix(end);
Headform_12avg_tridif = Headform_12avg_tritf - Headform_12avg_trit1;

%% 26 ---------------------------------------------------------------------------------------
---
Headform_26A_trit1 = Headform_26A_trix(1);
Headform_26A_tritf = Headform_26A_trix(end);
Headform_26A_tridif = Headform_26A_tritf - Headform_26A_trit1;

Headform_26B_trit1 = Headform_26B_trix(1);
Headform_26B_tritf = Headform_26B_trix(end);
Headform_26B_tridif = Headform_26B_tritf - Headform_26B_trit1;

Headform_26C_trit1 = Headform_26C_trix(1);
Headform_26C_tritf = Headform_26C_trix(end);
Headform_26C_tridif = Headform_26C_tritf - Headform_26C_trit1;

Headform_26D_trit1 = Headform_26D_trix(1);
```

```
Headform_26D_tritf = Headform_26D_trix(end);
Headform_26D_tridif = Headform_26D_tritf - Headform_26D_trit1;


Headform_26E_trit1 = Headform_26E_trix(1);
Headform_26E_tritf = Headform_26E_trix(end);
Headform_26E_tridif = Headform_26E_tritf - Headform_26E_trit1;


Headform_26avg_trit1 = Headform_26avg_trix(1);
Headform_26avg_tritf = Headform_26avg_trix(end);
Headform_26avg_tridif = Headform_26avg_tritf - Headform_26avg_trit1;
 %% *************************** Non - Weighted
 *********************************************************
 %% 12 Y-Tri-------------------------------------------------------------------------------------
 ---------
Headform_12A_trit1NW = Headform_12A_trixNW(1);
Headform_12A_tritfNW = Headform_12A_trixNW(end);
Headform_12A_tridifNW = Headform_12A_tritfNW - Headform_12A_trit1NW;

Headform_12B_trit1NW = Headform_12B_trixNW(1);
Headform_12B_tritfNW = Headform_12B_trixNW(end);
Headform_12B_tridifNW = Headform_12B_tritfNW - Headform_12B_trit1NW;

Headform_12C_trit1NW = Headform_12C_trixNW(1);
Headform_12C_tritfNW = Headform_12C_trixNW(end);
Headform_12C_tridifNW = Headform_12C_tritfNW - Headform_12C_trit1NW;

Headform_12D_trit1NW = Headform_12D_trixNW(1);
Headform_12D_tritfNW = Headform_12D_trixNW(end);
Headform_12D_tridifNW = Headform_12D_tritfNW - Headform_12D_trit1NW;

Headform_12E_trit1NW = Headform_12E_trixNW(1);
Headform_12E_tritfNW = Headform_12E_trixNW(end);
Headform_12E_tridifNW = Headform_12E_tritfNW - Headform_12E_trit1NW;

Headform_12avg_trit1NW = Headform_12avg_trixNW(1);
Headform_12avg_tritfNW = Headform_12avg_trixNW(end);
Headform_12avg_tridifNW = Headform_12avg_tritfNW - Headform_12avg_trit1NW;
 %% 26 Y-Tri-------------------------------------------------------------------------------------
 ---------
Headform_26A_trit1NW = Headform_26A_trixNW(1);
Headform_26A_tritfNW = Headform_26A_trixNW(end);
Headform_26A_tridifNW = Headform_26A_tritfNW - Headform_26A_trit1NW;

Headform_26B_trit1NW = Headform_26B_trixNW(1);
Headform_26B_tritfNW = Headform_26B_trixNW(end);
Headform_26B_tridifNW = Headform_26B_tritfNW - Headform_26B_trit1NW;

Headform_26C_trit1NW = Headform_26C_trixNW(1);
Headform_26C_tritfNW = Headform_26C_trixNW(end);
Headform_26C_tridifNW = Headform_26C_tritfNW - Headform_26C_trit1NW;

Headform_26D_trit1NW = Headform_26D_trixNW(1);
Headform_26D_tritfNW = Headform_26D_trixNW(end);
Headform_26D_tridifNW = Headform_26D_tritfNW - Headform_26D_trit1NW;

Headform_26E_trit1NW = Headform_26E_trixNW(1);
Headform_26E_tritfNW = Headform_26E_trixNW(end);
Headform_26E_tridifNW = Headform_26E_tritfNW - Headform_26E_trit1NW;

Headform_26avg_trit1NW = Headform_26avg_trixNW(1);
Headform_26avg_tritfNW = Headform_26avg_trixNW(end);
Headform_26avg_tridifNW = Headform_26avg_tritfNW - Headform_26avg_trit1NW;
 %% Integration
g = 9.8067;
p = 5/2;

%% Helmet
A*********************************************************************************************************
*************************
%% Helmet A Velocities **--**--**--**--**--**--**--**--**--**--**--**--**--**--**--**--**--**--**--**-
-*--**--**--**--**
%% Helmet A Velocity---------------------------------------------------------------------------------
%% ****************************** WEIGHTED
%% 12-----------------------------------------------------------------------------------------------
-----------------
HelmetA_12A_tri_vel = trapz(HelmetA_12A_trix,(HelmetA_12A_triy))
```
112

```matlab
 HelmetA_12B_tri_vel = trapz(HelmetA_12B_trix,(HelmetA_12B_triy))

HelmetA_12C_tri_vel = trapz(HelmetA_12C_trix,(HelmetA_12C_triy))

HelmetA_12D_tri_vel = trapz(HelmetA_12D_trix,(HelmetA_12D_triy))

HelmetA_12E_tri_vel = trapz(HelmetA_12E_trix,(HelmetA_12E_triy))

HelmetA_12avg_tri_vel = trapz(HelmetA_12avg_trix,(HelmetA_12avg_triy))

%% 26 -----------------------------------------------------------------------------------------------
HelmetA_26A_tri_vel = trapz(HelmetA_26A_trix,(HelmetA_26A_triy))

HelmetA_26B_tri_vel = trapz(HelmetA_26B_trix,(HelmetA_26B_triy))

HelmetA_26C_tri_vel = trapz(HelmetA_26C_trix,(HelmetA_26C_triy))

HelmetA_26D_tri_vel = trapz(HelmetA_26D_trix,(HelmetA_26D_triy))

HelmetA_26E_tri_vel = trapz(HelmetA_26E_trix,(HelmetA_26E_triy))

HelmetA_26avg_tri_vel = trapz(HelmetA_26avg_trix,(HelmetA_26avg_triy))

%% **************************  Non - Weighted
*****************************************************************
 %% Helmet A Y-Tri-Axial Velocity ----------------------------------------------------------------------
------
HelmetA_12A_tri_velNW = trapz(HelmetA_12A_trixNW,(HelmetA_12A_triyNW))

HelmetA_12B_tri_velNW = trapz(HelmetA_12B_trixNW,(HelmetA_12B_triyNW))

HelmetA_12C_tri_velNW = trapz(HelmetA_12C_trixNW,(HelmetA_12C_triyNW))

HelmetA_12D_tri_velNW = trapz(HelmetA_12D_trixNW,(HelmetA_12D_triyNW))

HelmetA_12E_tri_velNW = trapz(HelmetA_12E_trixNW,(HelmetA_12E_triyNW))

HelmetA_12avg_tri_velNW = trapz(HelmetA_12avg_trixNW,(HelmetA_12avg_triyNW))

HelmetA_26A_tri_velNW = trapz(HelmetA_26A_trixNW,(HelmetA_26A_triyNW))

HelmetA_26B_tri_velNW = trapz(HelmetA_26B_trixNW,(HelmetA_26B_triyNW))

HelmetA_26C_tri_velNW = trapz(HelmetA_26C_trixNW,(HelmetA_26C_triyNW))

HelmetA_26D_tri_velNW = trapz(HelmetA_26D_trixNW,(HelmetA_26D_triyNW))

HelmetA_26E_tri_velNW = trapz(HelmetA_26E_trixNW,(HelmetA_26E_triyNW))

HelmetA_26avg_tri_velNW = trapz(HelmetA_26avg_trixNW,(HelmetA_26avg_triyNW))
%% Helmet A SI Values **--**--**--**--**--**--**--**--**--**--**--**--**--**--**--**--**--**--**--
**--**--**--**--**--**
%% Helmet A Y-Tri-Axial SI-------------------------------------------------------------------------------
%% ***************************  Weighted
*****************************************************************
%% 12-------------------------------------------------------------------------------------------------
-----------------------
HelmetA_12A_tri_SI = trapz(HelmetA_12A_trix,(abs((HelmetA_12A_triy))./g).^p)

HelmetA_12B_tri_SI = trapz(HelmetA_12B_trix,(abs((HelmetA_12B_triy))./g).^p)

HelmetA_12C_tri_SI = trapz(HelmetA_12C_trix,(abs((HelmetA_12C_triy))./g).^p)

HelmetA_12D_tri_SI = trapz(HelmetA_12D_trix,(abs((HelmetA_12D_triy))./g).^p)

HelmetA_12E_tri_SI = trapz(HelmetA_12E_trix,(abs((HelmetA_12E_triy))./g).^p)

HelmetA_12avg_tri_SI = trapz(HelmetA_12avg_trix,(abs((HelmetA_12avg_triy))./g).^p)
 %% 26 -------------------------------------------------------------------------------------------------
-------------------------
HelmetA_26A_tri_SI = trapz(HelmetA_26A_trix,(abs((HelmetA_26A_triy))./g).^p)

HelmetA_26B_tri_SI = trapz(HelmetA_26B_trix,(abs((HelmetA_26B_triy))./g).^p)

HelmetA_26C_tri_SI = trapz(HelmetA_26C_trix,(abs((HelmetA_26C_triy))./g).^p)
```

```
HelmetA_26D_tri_SI = trapz(HelmetA_26D_trix,(abs((HelmetA_26D_triy))./g).^p)

HelmetA_26E_tri_SI = trapz(HelmetA_26E_trix,(abs((HelmetA_26E_triy))./g).^p)

HelmetA_26avg_tri_SI = trapz(HelmetA_26avg_trix,(abs((HelmetA_26avg_triy))./g).^p)
 %% ****************************** Non - Weighted
 ****************************************************
%% Helmet A Y-Tri-Axial SI----------------------------------------------

HelmetA_12A_tri_SINW = trapz(HelmetA_12A_trixNW,(abs((HelmetA_12A_triyNW))./g).^p)

HelmetA_12B_tri_SINW = trapz(HelmetA_12B_trixNW,(abs((HelmetA_12B_triyNW))./g).^p)

HelmetA_12C_tri_SINW = trapz(HelmetA_12C_trixNW,(abs((HelmetA_12C_triyNW))./g).^p)

HelmetA_12D_tri_SINW = trapz(HelmetA_12D_trixNW,(abs((HelmetA_12D_triyNW))./g).^p)

HelmetA_12E_tri_SINW = trapz(HelmetA_12E_trixNW,(abs((HelmetA_12E_triyNW))./g).^p)

HelmetA_12avg_tri_SINW = trapz(HelmetA_12avg_trixNW,(abs((HelmetA_12avg_triyNW))./g).^p)

HelmetA_26A_tri_SINW = trapz(HelmetA_26A_trixNW,(abs((HelmetA_26A_triyNW))./g).^p)

HelmetA_26B_tri_SINW = trapz(HelmetA_26B_trixNW,(abs((HelmetA_26B_triyNW))./g).^p)

HelmetA_26C_tri_SINW = trapz(HelmetA_26C_trixNW,(abs((HelmetA_26C_triyNW))./g).^p)

HelmetA_26D_tri_SINW = trapz(HelmetA_26D_trixNW,(abs((HelmetA_26D_triyNW))./g).^p)

HelmetA_26E_tri_SINW = trapz(HelmetA_26E_trixNW,(abs((HelmetA_26E_triyNW))./g).^p)

HelmetA_26avg_tri_SINW = trapz(HelmetA_26avg_trixNW,(abs((HelmetA_26avg_triyNW))./g).^p)

%% Helmet A HIC Values **--**--**--**--**--**--**--**--**--**--**--**--**--**--**--**--**--**--
-**--**--**--**--**--**
 %% Helmet A HIC --------------------------------------------------------------------------
--------------------
 %% ********************************* Weighted
 *******************************************************************************

%% 12 ------------------------------------------------------------------------------------
--------------------
HelmetA_12A_tri_HIC =
HelmetA_12A_tridif*(((1/HelmetA_12A_tridif)*(trapz(HelmetA_12A_trix,((HelmetA_12A_triy)./g))))^p)

HelmetA_12B_tri_HIC =
HelmetA_12B_tridif*(((1/HelmetA_12B_tridif)*(trapz(HelmetA_12B_trix,((HelmetA_12B_triy)./g))))^p)

HelmetA_12C_tri_HIC =
HelmetA_12C_tridif*(((1/HelmetA_12C_tridif)*(trapz(HelmetA_12C_trix,((HelmetA_12C_triy)./g))))^p)

HelmetA_12D_tri_HIC =
HelmetA_12D_tridif*(((1/HelmetA_12D_tridif)*(trapz(HelmetA_12D_trix,((HelmetA_12D_triy)./g))))^p)

HelmetA_12E_tri_HIC =
HelmetA_12E_tridif*(((1/HelmetA_12E_tridif)*(trapz(HelmetA_12E_trix,((HelmetA_12E_triy)./g))))^p)

HelmetA_12avg_tri_HIC =
HelmetA_12avg_tridif*(((1/HelmetA_12avg_tridif)*(trapz(HelmetA_12avg_trix,((HelmetA_12avg_triy)./g))))
^p)
 %% 26 ------------------------------------------------------------------------------------
--------------------
HelmetA_26A_tri_HIC =
HelmetA_26A_tridif*(((1/HelmetA_26A_tridif)*(trapz(HelmetA_26A_trix,((HelmetA_26A_triy)./g))))^p)

HelmetA_26B_tri_HIC =
HelmetA_26B_tridif*(((1/HelmetA_26B_tridif)*(trapz(HelmetA_26B_trix,((HelmetA_26B_triy)./g))))^p)

HelmetA_26C_tri_HIC =
HelmetA_26C_tridif*(((1/HelmetA_26C_tridif)*(trapz(HelmetA_26C_trix,((HelmetA_26C_triy)./g))))^p)

HelmetA_26D_tri_HIC =
HelmetA_26D_tridif*(((1/HelmetA_26D_tridif)*(trapz(HelmetA_26D_trix,((HelmetA_26D_triy)./g))))^p)

HelmetA_26E_tri_HIC =
HelmetA_26E_tridif*(((1/HelmetA_26E_tridif)*(trapz(HelmetA_26E_trix,((HelmetA_26E_triy)./g))))^p)
```

```matlab
 HelmetA_26avg_tri_HIC =
HelmetA_26avg_tridif*(((1/HelmetA_26avg_tridif)*(trapz(HelmetA_26avg_trix,((HelmetA_26avg_triy)./g))))
^p)
 %% ********************************** Non - Weighted
****************************************************************************
%% Helmet A Y-Tri-Axial HIC ---------------------------------------------------------

HelmetA_12A_tri_HICNW =
HelmetA_12A_tridifNW*(((1/HelmetA_12A_tridifNW)*(trapz(HelmetA_12A_trixNW,((HelmetA_12A_triyNW)./g))))
^p)

HelmetA_12B_tri_HICNW =
HelmetA_12B_tridifNW*(((1/HelmetA_12B_tridifNW)*(trapz(HelmetA_12B_trixNW,((HelmetA_12B_triyNW)./g))))
^p)

HelmetA_12C_tri_HICNW =
HelmetA_12C_tridifNW*(((1/HelmetA_12C_tridifNW)*(trapz(HelmetA_12C_trixNW,((HelmetA_12C_triyNW)./g))))
^p)

HelmetA_12D_tri_HICNW =
HelmetA_12D_tridifNW*(((1/HelmetA_12D_tridifNW)*(trapz(HelmetA_12D_trixNW,((HelmetA_12D_triyNW)./g))))
^p)

HelmetA_12E_tri_HICNW =
HelmetA_12E_tridifNW*(((1/HelmetA_12E_tridifNW)*(trapz(HelmetA_12E_trixNW,((HelmetA_12E_triyNW)./g))))
^p)

HelmetA_12avg_tri_HICNW =
HelmetA_12avg_tridifNW*(((1/HelmetA_12avg_tridifNW)*(trapz(HelmetA_12avg_trixNW,((HelmetA_12avg_triyNW
)./g))))^p)


HelmetA_26A_tri_HICNW =
HelmetA_26A_tridifNW*(((1/HelmetA_26A_tridifNW)*(trapz(HelmetA_26A_trixNW,((HelmetA_26A_triyNW)./g))))
^p)

HelmetA_26B_tri_HICNW =
HelmetA_26B_tridifNW*(((1/HelmetA_26B_tridifNW)*(trapz(HelmetA_26B_trixNW,((HelmetA_26B_triyNW)./g))))
^p)

HelmetA_26C_tri_HICNW =
HelmetA_26C_tridifNW*(((1/HelmetA_26C_tridifNW)*(trapz(HelmetA_26C_trixNW,((HelmetA_26C_triyNW)./g))))
^p)
HelmetA_26D_tri_HICNW =
HelmetA_26D_tridifNW*(((1/HelmetA_26D_tridifNW)*(trapz(HelmetA_26D_trixNW,((HelmetA_26D_triyNW)./g))))
^p)

HelmetA_26E_tri_HICNW =
HelmetA_26E_tridifNW*(((1/HelmetA_26E_tridifNW)*(trapz(HelmetA_26E_trixNW,((HelmetA_26E_triyNW)./g))))
^p)

HelmetA_26avg_tri_HICNW =
HelmetA_26avg_tridifNW*(((1/HelmetA_26avg_tridifNW)*(trapz(HelmetA_26avg_trixNW,((HelmetA_26avg_triyNW
)./g))))^p)

%% Helmet B
*************************************************************************************************
%% Helmet B Velocities **--**--**--**--**--**--**--**--**--**--**--**--**--**--**--**--**--**--**--
-**--**--**--**--**

 %% Helmet B Velocity ----------------------------------------------------------------------------
-------------------
 %% ********************************** Weighted
****************************************************************************
 %% 12 ------------------------------------------------------------------------------------------
-
HelmetB_12A_tri_vel = trapz(HelmetB_12A_trix,(HelmetB_12A_triy))

HelmetB_12B_tri_vel = trapz(HelmetB_12B_trix,(HelmetB_12B_triy))

HelmetB_12C_tri_vel = trapz(HelmetB_12C_trix,(HelmetB_12C_triy))

HelmetB_12D_tri_vel = trapz(HelmetB_12D_trix,(HelmetB_12D_triy))

HelmetB_12E_tri_vel = trapz(HelmetB_12E_trix,(HelmetB_12E_triy))

HelmetB_12avg_tri_vel = trapz(HelmetB_12avg_trix,(HelmetB_12avg_triy))
```

```matlab
%% 26 ----------------------------------------------------------------------------------------------
-
HelmetB_26A_tri_vel = trapz(HelmetB_26A_trix,(HelmetB_26A_triy))

HelmetB_26B_tri_vel = trapz(HelmetB_26B_trix,(HelmetB_26B_triy))

HelmetB_26C_tri_vel = trapz(HelmetB_26C_trix,(HelmetB_26C_triy))

HelmetB_26D_tri_vel = trapz(HelmetB_26D_trix,(HelmetB_26D_triy))

HelmetB_26E_tri_vel = trapz(HelmetB_26E_trix,(HelmetB_26E_triy))

HelmetB_26avg_tri_vel = trapz(HelmetB_26avg_trix,(HelmetB_26avg_triy))

%% *************************************** Non - Weighted
%% Helmet B Y-Tri-Axial Velocity ----------------------------------------------------------------------
%% 12 Y-Tri----------------------------------------------------------------------------------------
-----
HelmetB_12A_tri_velNW = trapz(HelmetB_12A_trixNW,(HelmetB_12A_triyNW))

HelmetB_12B_tri_velNW = trapz(HelmetB_12B_trixNW,(HelmetB_12B_triyNW))

HelmetB_12C_tri_velNW = trapz(HelmetB_12C_trixNW,(HelmetB_12C_triyNW))

HelmetB_12D_tri_velNW = trapz(HelmetB_12D_trixNW,(HelmetB_12D_triyNW))

HelmetB_12E_tri_velNW = trapz(HelmetB_12E_trixNW,(HelmetB_12E_triyNW))

HelmetB_12avg_tri_velNW = trapz(HelmetB_12avg_trixNW,(HelmetB_12avg_triyNW))

%% 26 Y-Tri----------------------------------------------------------------------------------------
-----
HelmetB_26A_tri_velNW = trapz(HelmetB_26A_trixNW,(HelmetB_26A_triyNW))

HelmetB_26B_tri_velNW = trapz(HelmetB_26B_trixNW,(HelmetB_26B_triyNW))

HelmetB_26C_tri_velNW = trapz(HelmetB_26C_trixNW,(HelmetB_26C_triyNW))

HelmetB_26D_tri_velNW = trapz(HelmetB_26D_trixNW,(HelmetB_26D_triyNW))

HelmetB_26E_tri_velNW = trapz(HelmetB_26E_trixNW,(HelmetB_26E_triyNW))

HelmetB_26avg_tri_velNW = trapz(HelmetB_26avg_trixNW,(HelmetB_26avg_triyNW))
%% Helmet B SI Values **--**--**--**--**--**--**--**--**--**--**--**--**--**--**--**--**--**--**--
**--**--**--**--**--**
%% Helmet B SI------------------------------------------------------------------------------------

%% *************************** WEIGHTED
%% 12----------------------------------------------------------------------------------------------
-
HelmetB_12A_tri_SI = trapz(HelmetB_12A_trix,(abs((HelmetB_12A_triy))./g).^p)

HelmetB_12B_tri_SI = trapz(HelmetB_12B_trix,(abs((HelmetB_12B_triy))./g).^p)

HelmetB_12C_tri_SI = trapz(HelmetB_12C_trix,(abs((HelmetB_12C_triy))./g).^p)

HelmetB_12D_tri_SI = trapz(HelmetB_12D_trix,(abs((HelmetB_12D_triy))./g).^p)

HelmetB_12E_tri_SI = trapz(HelmetB_12E_trix,(abs((HelmetB_12E_triy))./g).^p)

HelmetB_12avg_tri_SI = trapz(HelmetB_12avg_trix,(abs((HelmetB_12avg_triy))./g).^p)

%% 26----------------------------------------------------------------------------------------------
-
HelmetB_26A_tri_SI = trapz(HelmetB_26A_trix,(abs((HelmetB_26A_triy))./g).^p)

HelmetB_26B_tri_SI = trapz(HelmetB_26B_trix,(abs((HelmetB_26B_triy))./g).^p)

HelmetB_26C_tri_SI = trapz(HelmetB_26C_trix,(abs((HelmetB_26C_triy))./g).^p)

HelmetB_26D_tri_SI = trapz(HelmetB_26D_trix,(abs((HelmetB_26D_triy))./g).^p)

HelmetB_26E_tri_SI = trapz(HelmetB_26E_trix,(abs((HelmetB_26E_triy))./g).^p)

HelmetB_26avg_tri_SI = trapz(HelmetB_26avg_trix,(abs((HelmetB_26avg_triy))./g).^p)
```

```
%% ****************************** NON - WEIGHTED
%% Helmet B Y-Tri-Axial SI------------------------------------------------------------------------------
-
%% 12------------------------------------------------------------------------------------------------
-
HelmetB_12A_tri_SINW = trapz(HelmetB_12A_trixNW,(abs((HelmetB_12A_triyNW))./g).^p)

HelmetB_12B_tri_SINW = trapz(HelmetB_12B_trixNW,(abs((HelmetB_12B_triyNW))./g).^p)

HelmetB_12C_tri_SINW = trapz(HelmetB_12C_trixNW,(abs((HelmetB_12C_triyNW))./g).^p)

HelmetB_12D_tri_SINW = trapz(HelmetB_12D_trixNW,(abs((HelmetB_12D_triyNW))./g).^p)

HelmetB_12E_tri_SINW = trapz(HelmetB_12E_trixNW,(abs((HelmetB_12E_triyNW))./g).^p)

HelmetB_12avg_tri_SINW = trapz(HelmetB_12avg_trixNW,(abs((HelmetB_12avg_triyNW))./g).^p)

%% 26------------------------------------------------------------------------------------------------
-
HelmetB_26A_tri_SINW = trapz(HelmetB_26A_trixNW,(abs((HelmetB_26A_triyNW))./g).^p)

HelmetB_26B_tri_SINW = trapz(HelmetB_26B_trixNW,(abs((HelmetB_26B_triyNW))./g).^p)

HelmetB_26C_tri_SINW = trapz(HelmetB_26C_trixNW,(abs((HelmetB_26C_triyNW))./g).^p)

HelmetB_26D_tri_SINW = trapz(HelmetB_26D_trixNW,(abs((HelmetB_26D_triyNW))./g).^p)

HelmetB_26E_tri_SINW = trapz(HelmetB_26E_trixNW,(abs((HelmetB_26E_triyNW))./g).^p)

HelmetB_26avg_tri_SINW = trapz(HelmetB_26avg_trixNW,(abs((HelmetB_26avg_triyNW))./g).^p)

%% Helmet B HIC ---------------------------------------------------------------------------------
%% ************************************* WEIGHTED
%% 12 Y-Tri------------------------------------------------------------------------------------------
------------------------------
HelmetB_12A_tri_HIC =
HelmetB_12A_tridif*(((1/HelmetB_12A_tridif)*(trapz(HelmetB_12A_trix,((HelmetB_12A_triy)./g))))^p)

HelmetB_12B_tri_HIC =
HelmetB_12B_tridif*(((1/HelmetB_12B_tridif)*(trapz(HelmetB_12B_trix,((HelmetB_12B_triy)./g))))^p)

HelmetB_12C_tri_HIC =
HelmetB_12C_tridif*(((1/HelmetB_12C_tridif)*(trapz(HelmetB_12C_trix,((HelmetB_12C_triy)./g))))^p)

HelmetB_12D_tri_HIC =
HelmetB_12D_tridif*(((1/HelmetB_12D_tridif)*(trapz(HelmetB_12D_trix,((HelmetB_12D_triy)./g))))^p)

HelmetB_12E_tri_HIC =
HelmetB_12E_tridif*(((1/HelmetB_12E_tridif)*(trapz(HelmetB_12E_trix,((HelmetB_12E_triy)./g))))^p)

HelmetB_12avg_tri_HIC =
HelmetB_12avg_tridif*(((1/HelmetB_12avg_tridif)*(trapz(HelmetB_12avg_trix,((HelmetB_12avg_triy)./g))))
^p)
% 26 Y-Tri------------------------------------------------------------------------------------------
------------------------------
HelmetB_26A_tri_HIC =
HelmetB_26A_tridif*(((1/HelmetB_26A_tridif)*(trapz(HelmetB_26A_trix,((HelmetB_26A_triy)./g))))^p)

HelmetB_26B_tri_HIC =
HelmetB_26B_tridif*(((1/HelmetB_26B_tridif)*(trapz(HelmetB_26B_trix,((HelmetB_26B_triy)./g))))^p)

HelmetB_26C_tri_HIC =
HelmetB_26C_tridif*(((1/HelmetB_26C_tridif)*(trapz(HelmetB_26C_trix,((HelmetB_26C_triy)./g))))^p)

HelmetB_26D_tri_HIC =
HelmetB_26D_tridif*(((1/HelmetB_26D_tridif)*(trapz(HelmetB_26D_trix,((HelmetB_26D_triy)./g))))^p)

HelmetB_26E_tri_HIC =
HelmetB_26E_tridif*(((1/HelmetB_26E_tridif)*(trapz(HelmetB_26E_trix,((HelmetB_26E_triy)./g))))^p)

HelmetB_26avg_tri_HIC =
HelmetB_26avg_tridif*(((1/HelmetB_26avg_tridif)*(trapz(HelmetB_26avg_trix,((HelmetB_26avg_triy)./g))))
^p)

%% ************************************* NON - WEIGHTED
```

```
%% Helmet B Y-Tri-Axial HIC ----------------------------------------------------------------------------
----------------------------
%% 12 Y-Tri----------------------------------------------------------------------------------------------
--------------------------------
HelmetB_12A_tri_HICNW =
HelmetB_12A_tridifNW*(((1/HelmetB_12A_tridifNW)*(trapz(HelmetB_12A_trixNW,((HelmetB_12A_triyNW)./g))))
^p)

HelmetB_12B_tri_HICNW =
HelmetB_12B_tridifNW*(((1/HelmetB_12B_tridifNW)*(trapz(HelmetB_12B_trixNW,((HelmetB_12B_triyNW)./g))))
^p)

HelmetB_12C_tri_HICNW =
HelmetB_12C_tridifNW*(((1/HelmetB_12C_tridifNW)*(trapz(HelmetB_12C_trixNW,((HelmetB_12C_triyNW)./g))))
^p)

HelmetB_12D_tri_HICNW =
HelmetB_12D_tridifNW*(((1/HelmetB_12D_tridifNW)*(trapz(HelmetB_12D_trixNW,((HelmetB_12D_triyNW)./g))))
^p)

HelmetB_12E_tri_HICNW =
HelmetB_12E_tridifNW*(((1/HelmetB_12E_tridifNW)*(trapz(HelmetB_12E_trixNW,((HelmetB_12E_triyNW)./g))))
^p)

HelmetB_12avg_tri_HICNW =
HelmetB_12avg_tridifNW*(((1/HelmetB_12avg_tridifNW)*(trapz(HelmetB_12avg_trixNW,((HelmetB_12avg_triyNW
)./g))))^p)

%% 26 Y-Tri----------------------------------------------------------------------------------------------
--------------------------------
HelmetB_26A_tri_HICNW =
HelmetB_26A_tridifNW*(((1/HelmetB_26A_tridifNW)*(trapz(HelmetB_26A_trixNW,((HelmetB_26A_triyNW)./g))))
^p)

HelmetB_26B_tri_HICNW =
HelmetB_26B_tridifNW*(((1/HelmetB_26B_tridifNW)*(trapz(HelmetB_26B_trixNW,((HelmetB_26B_triyNW)./g))))
^p)

HelmetB_26C_tri_HICNW =
HelmetB_26C_tridifNW*(((1/HelmetB_26C_tridifNW)*(trapz(HelmetB_26C_trixNW,((HelmetB_26C_triyNW)./g))))
^p)

HelmetB_26D_tri_HICNW =
HelmetB_26D_tridifNW*(((1/HelmetB_26D_tridifNW)*(trapz(HelmetB_26D_trixNW,((HelmetB_26D_triyNW)./g))))
^p)

HelmetB_26E_tri_HICNW =
HelmetB_26E_tridifNW*(((1/HelmetB_26E_tridifNW)*(trapz(HelmetB_26E_trixNW,((HelmetB_26E_triyNW)./g))))
^p)

HelmetB_26avg_tri_HICNW =
HelmetB_26avg_tridifNW*(((1/HelmetB_26avg_tridifNW)*(trapz(HelmetB_26avg_trixNW,((HelmetB_26avg_triyNW
)./g))))^p)

%% Headform

%% Headform Velocities **--**--**--**--**--**--**--**--**--**--**--**--**--**--**--**--**--**--**--**--
-**--**--**--**--**
 %% Headform Velocity --------------------------------------------------------------------------------
--------------------
 %% **************************************** WEIGHTED
*****************************************************************
%% 12 ---------------------------------------------------------------------------------------------------
---
Headform_12A_tri_vel = trapz(Headform_12A_trix,(Headform_12A_triy))

Headform_12B_tri_vel = trapz(Headform_12B_trix,(Headform_12B_triy))

Headform_12C_tri_vel = trapz(Headform_12C_trix,(Headform_12C_triy))

Headform_12D_tri_vel = trapz(Headform_12D_trix,(Headform_12D_triy))

Headform_12E_tri_vel = trapz(Headform_12E_trix,(Headform_12E_triy))

Headform_12avg_tri_vel = trapz(Headform_12avg_trix,(Headform_12avg_triy))
```

```
%% 26 ----------------------------------------------------------------------------------------------------
----
Headform_26A_tri_vel = trapz(Headform_26A_trix,(Headform_26A_triy))

Headform_26B_tri_vel = trapz(Headform_26B_trix,(Headform_26B_triy))

Headform_26C_tri_vel = trapz(Headform_26C_trix,(Headform_26C_triy))

Headform_26D_tri_vel = trapz(Headform_26D_trix,(Headform_26D_triy))

Headform_26E_tri_vel = trapz(Headform_26E_trix,(Headform_26E_triy))

Headform_26avg_tri_vel = trapz(Headform_26avg_trix,(Headform_26avg_triy))

%% ********************* NON - WEIGHTED
*****************************************************************************
%% Headform Y-Tri-Axial Velocity -------------------------------------------------------------------------
--------
%% 12 Y-tri-----------------------------------------------------------------------------------------------
--------
Headform_12A_tri_velNW = trapz(Headform_12A_trixNW,(Headform_12A_triyNW))

Headform_12B_tri_velNW = trapz(Headform_12B_trixNW,(Headform_12B_triyNW))

Headform_12C_tri_velNW = trapz(Headform_12C_trixNW,(Headform_12C_triyNW))

Headform_12D_tri_velNW = trapz(Headform_12D_trixNW,(Headform_12D_triyNW))

Headform_12E_tri_velNW = trapz(Headform_12E_trixNW,(Headform_12E_triyNW))

Headform_12avg_tri_velNW = trapz(Headform_12avg_trixNW,(Headform_12avg_triyNW))

%% 26 Y-tri-----------------------------------------------------------------------------------------------
---------
Headform_26A_tri_velNW = trapz(Headform_26A_trixNW,(Headform_26A_triyNW))

Headform_26B_tri_velNW = trapz(Headform_26B_trixNW,(Headform_26B_triyNW))

Headform_26C_tri_velNW = trapz(Headform_26C_trixNW,(Headform_26C_triyNW))

Headform_26D_tri_velNW = trapz(Headform_26D_trixNW,(Headform_26D_triyNW))

Headform_26E_tri_velNW = trapz(Headform_26E_trixNW,(Headform_26E_triyNW))

Headform_26avg_tri_velNW = trapz(Headform_26avg_trixNW,(Headform_26avg_triyNW))

%% Headform SI Values **--**--**--**--**--**--**--**--**--**--**--**--**--**--**--**--**--**--**--**--**--
**--**--**--**--**--**
%% Headform Y SI----------------------------------------------------------------------------------------
---------------
%% ***************************** WEIGHTED
***********************************************************************
%% 12 --------------------------------------------------------------------------------------------------
-
Headform_12A_tri_SI = trapz(Headform_12A_trix,(abs((Headform_12A_triy))./g).^p)

Headform_12B_tri_SI = trapz(Headform_12B_trix,(abs((Headform_12B_triy))./g).^p)

Headform_12C_tri_SI = trapz(Headform_12C_trix,(abs((Headform_12C_triy))./g).^p)

Headform_12D_tri_SI = trapz(Headform_12D_trix,(abs((Headform_12D_triy))./g).^p)

Headform_12E_tri_SI = trapz(Headform_12E_trix,(abs((Headform_12E_triy))./g).^p)

Headform_12avg_tri_SI = trapz(Headform_12avg_trix,(abs((Headform_12avg_triy))./g).^p)

%% 26 --------------------------------------------------------------------------------------------------
Headform_26A_tri_SI = trapz(Headform_26A_trix,(abs((Headform_26A_triy))./g).^p)

Headform_26B_tri_SI = trapz(Headform_26B_trix,(abs((Headform_26B_triy))./g).^p)

Headform_26C_tri_SI = trapz(Headform_26C_trix,(abs((Headform_26C_triy))./g).^p)

Headform_26D_tri_SI = trapz(Headform_26D_trix,(abs((Headform_26D_triy))./g).^p)

Headform_26E_tri_SI = trapz(Headform_26E_trix,(abs((Headform_26E_triy))./g).^p)
```

```matlab
  Headform_26avg_tri_SI = trapz(Headform_26avg_trix,(abs((Headform_26avg_triy))./g).^p)

%% ******************************* NON - WEIGHTED
%% Headform Y-Tri-Axial SI-----------------------------------------------------------------------------
-----
%% 12 Y-tri----------------------------------------------------------------------------------------------
-----
Headform_12A_tri_SINW = trapz(Headform_12A_trixNW,(abs((Headform_12A_triyNW))./g).^p)

Headform_12B_tri_SINW = trapz(Headform_12B_trixNW,(abs((Headform_12B_triyNW))./g).^p)

Headform_12C_tri_SINW = trapz(Headform_12C_trixNW,(abs((Headform_12C_triyNW))./g).^p)

Headform_12D_tri_SINW = trapz(Headform_12D_trixNW,(abs((Headform_12D_triyNW))./g).^p)

Headform_12E_tri_SINW = trapz(Headform_12E_trixNW,(abs((Headform_12E_triyNW))./g).^p)

Headform_12avg_tri_SINW = trapz(Headform_12avg_trixNW,(abs((Headform_12avg_triyNW))./g).^p)

%% 26 Y-tri----------------------------------------------------------------------------------------------
-----
Headform_26A_tri_SINW = trapz(Headform_26A_trixNW,(abs((Headform_26A_triyNW))./g).^p)

Headform_26B_tri_SINW = trapz(Headform_26B_trixNW,(abs((Headform_26B_triyNW))./g).^p)

Headform_26C_tri_SINW = trapz(Headform_26C_trixNW,(abs((Headform_26C_triyNW))./g).^p)

Headform_26D_tri_SINW = trapz(Headform_26D_trixNW,(abs((Headform_26D_triyNW))./g).^p)

Headform_26E_tri_SINW = trapz(Headform_26E_trixNW,(abs((Headform_26E_triyNW))./g).^p)

Headform_26avg_tri_SINW = trapz(Headform_26avg_trixNW,(abs((Headform_26avg_triyNW))./g).^p)

%% Headform HIC Values **--**--**--**--**--**--**--**--**--**--**--**--**--**--**--**--**--**--
-**--**--**--**--**--**
 %% Headform Y-Tri-Axial HIC ----------------------------------------------------------------------
%% *************************** WEIGHTED
%% 12 Y-tri----------------------------------------------------------------------------------------------
Headform_12A_tri_HIC =
Headform_12A_tridif*(((1/Headform_12A_tridif)*(trapz(Headform_12A_trix,((Headform_12A_triy)./g))))^p)

Headform_12B_tri_HIC =
Headform_12B_tridif*(((1/Headform_12B_tridif)*(trapz(Headform_12B_trix,((Headform_12B_triy)./g))))^p)

Headform_12C_tri_HIC =
Headform_12C_tridif*(((1/Headform_12C_tridif)*(trapz(Headform_12C_trix,((Headform_12C_triy)./g))))^p)

Headform_12D_tri_HIC =
Headform_12D_tridif*(((1/Headform_12D_tridif)*(trapz(Headform_12D_trix,((Headform_12D_triy)./g))))^p)

Headform_12E_tri_HIC =
Headform_12E_tridif*(((1/Headform_12E_tridif)*(trapz(Headform_12E_trix,((Headform_12E_triy)./g))))^p)

Headform_12avg_tri_HIC =
Headform_12avg_tridif*(((1/Headform_12avg_tridif)*(trapz(Headform_12avg_trix,((Headform_12avg_triy)./g
))))^p)

%% 26 Y-tri----------------------------------------------------------------------------------------------
Headform_26A_tri_HIC =
Headform_26A_tridif*(((1/Headform_26A_tridif)*(trapz(Headform_26A_trix,((Headform_26A_triy)./g))))^p)

Headform_26B_tri_HIC =
Headform_26B_tridif*(((1/Headform_26B_tridif)*(trapz(Headform_26B_trix,((Headform_26B_triy)./g))))^p)

Headform_26C_tri_HIC =
Headform_26C_tridif*(((1/Headform_26C_tridif)*(trapz(Headform_26C_trix,((Headform_26C_triy)./g))))^p)

Headform_26D_tri_HIC =
Headform_26D_tridif*(((1/Headform_26D_tridif)*(trapz(Headform_26D_trix,((Headform_26D_triy)./g))))^p)

Headform_26E_tri_HIC =
Headform_26E_tridif*(((1/Headform_26E_tridif)*(trapz(Headform_26E_trix,((Headform_26E_triy)./g))))^p)

Headform_26avg_tri_HIC =
Headform_26avg_tridif*(((1/Headform_26avg_tridif)*(trapz(Headform_26avg_trix,((Headform_26avg_triy)./g
))))^p)
```

120

```
%% ********************************* NON - WEIGHTED ************************
 %% Headform Y-Tri-Axial HIC -----------------------------------------------------------------------
-----------------------------------
%% 12 Y-tri------------------------------------------------------------------------------------------
--------------------------------
Headform_12A_tri_HICNW =
Headform_12A_tridifNW*(((1/Headform_12A_tridifNW)*(trapz(Headform_12A_trixNW,((Headform_12A_triyNW)./g
))))^p)

Headform_12B_tri_HICNW =
Headform_12B_tridifNW*(((1/Headform_12B_tridifNW)*(trapz(Headform_12B_trixNW,((Headform_12B_triyNW)./g
))))^p)

Headform_12C_tri_HICNW =
Headform_12C_tridifNW*(((1/Headform_12C_tridifNW)*(trapz(Headform_12C_trixNW,((Headform_12C_triyNW)./g
))))^p)

Headform_12D_tri_HICNW =
Headform_12D_tridifNW*(((1/Headform_12D_tridifNW)*(trapz(Headform_12D_trixNW,((Headform_12D_triyNW)./g
))))^p)

Headform_12E_tri_HICNW =
Headform_12E_tridifNW*(((1/Headform_12E_tridifNW)*(trapz(Headform_12E_trixNW,((Headform_12E_triyNW)./g
))))^p)

Headform_12avg_tri_HICNW =
Headform_12avg_tridifNW*(((1/Headform_12avg_tridifNW)*(trapz(Headform_12avg_trixNW,((Headform_12avg_tr
iyNW)./g))))^p)

 %% 26 Y-tri-----------------------------------------------------------------------------------------
----------------------------------
Headform_26A_tri_HICNW =
Headform_26A_tridifNW*(((1/Headform_26A_tridifNW)*(trapz(Headform_26A_trixNW,((Headform_26A_triyNW)./g
))))^p)

Headform_26B_tri_HICNW =
Headform_26B_tridifNW*(((1/Headform_26B_tridifNW)*(trapz(Headform_26B_trixNW,((Headform_26B_triyNW)./g
))))^p)

Headform_26C_tri_HICNW =
Headform_26C_tridifNW*(((1/Headform_26C_tridifNW)*(trapz(Headform_26C_trixNW,((Headform_26C_triyNW)./g
))))^p)

Headform_26D_tri_HICNW =
Headform_26D_tridifNW*(((1/Headform_26D_tridifNW)*(trapz(Headform_26D_trixNW,((Headform_26D_triyNW)./g
))))^p)

Headform_26E_tri_HICNW =
Headform_26E_tridifNW*(((1/Headform_26E_tridifNW)*(trapz(Headform_26E_trixNW,((Headform_26E_triyNW)./g
))))^p)

Headform_26avg_tri_HICNW =
Headform_26avg_tridifNW*(((1/Headform_26avg_tridifNW)*(trapz(Headform_26avg_trixNW,((Headform_26avg_tr
iyNW)./g))))^p)
 %% Pitcher
%% Pitcher Velocities **--**--**--**--**--**--**--**--**--**--**--**--**--**--**--**--**--**--**--**--
**--**--**--**--**

 %% Pitcher Y-Tri-Axial Velocity -------------------------------------------------------------------
------

%% ******************************** WEIGHTED
%% 12 Y-Tri------------------------------------------------------------------------------------------
-----
Pitcher_12A_tri_vel = trapz(Pitcher_12A_trix,(Pitcher_12A_triy))

Pitcher_12B_tri_vel = trapz(Pitcher_12B_trix,(Pitcher_12B_triy))

Pitcher_12C_tri_vel = trapz(Pitcher_12C_trix,(Pitcher_12C_triy))

Pitcher_12D_tri_vel = trapz(Pitcher_12D_trix,(Pitcher_12D_triy))

Pitcher_12E_tri_vel = trapz(Pitcher_12E_trix,(Pitcher_12E_triy))

Pitcher_12avg_tri_vel = trapz(Pitcher_12avg_trix,(Pitcher_12avg_triy))
```

```matlab
%% 26 Y-Tri---------------------------------------------------------------------------------------------
-----
Pitcher_26A_tri_vel = trapz(Pitcher_26A_trix,(Pitcher_26A_triy))

Pitcher_26B_tri_vel = trapz(Pitcher_26B_trix,(Pitcher_26B_triy))

Pitcher_26C_tri_vel = trapz(Pitcher_26C_trix,(Pitcher_26C_triy))

Pitcher_26D_tri_vel = trapz(Pitcher_26D_trix,(Pitcher_26D_triy))

Pitcher_26E_tri_vel = trapz(Pitcher_26E_trix,(Pitcher_26E_triy))

Pitcher_26avg_tri_vel = trapz(Pitcher_26avg_trix,(Pitcher_26avg_triy))

%% ***************************** NON - WEIGHTED
*********************************************************************
 %% Pitcher Y-Tri-Axial Velocity -----------------------------------------------------------------------
------
%% 12 Y-Tri---------------------------------------------------------------------------------------------
-----
Pitcher_12A_tri_velNW = trapz(Pitcher_12A_trixNW,(Pitcher_12A_triyNW))

Pitcher_12B_tri_velNW = trapz(Pitcher_12B_trixNW,(Pitcher_12B_triyNW))

Pitcher_12C_tri_velNW = trapz(Pitcher_12C_trixNW,(Pitcher_12C_triyNW))

Pitcher_12D_tri_velNW = trapz(Pitcher_12D_trixNW,(Pitcher_12D_triyNW))

Pitcher_12E_tri_velNW = trapz(Pitcher_12E_trixNW,(Pitcher_12E_triyNW))

Pitcher_12avg_tri_velNW = trapz(Pitcher_12avg_trixNW,(Pitcher_12avg_triyNW))

%% 26 Y-Tri---------------------------------------------------------------------------------------------
-----
Pitcher_26A_tri_velNW = trapz(Pitcher_26A_trixNW,(Pitcher_26A_triyNW))

Pitcher_26B_tri_velNW = trapz(Pitcher_26B_trixNW,(Pitcher_26B_triyNW))

Pitcher_26C_tri_velNW = trapz(Pitcher_26C_trixNW,(Pitcher_26C_triyNW))

Pitcher_26D_tri_velNW = trapz(Pitcher_26D_trixNW,(Pitcher_26D_triyNW))

Pitcher_26E_tri_velNW = trapz(Pitcher_26E_trixNW,(Pitcher_26E_triyNW))

Pitcher_26avg_tri_velNW = trapz(Pitcher_26avg_trixNW,(Pitcher_26avg_triyNW))

%% Pitcher SI Values **--**--**--**--**--**--**--**--**--**--**--**--**--**--**--**--**--**--**--**--
**--**--**--**--**--**
 %% Pitcher Y-Tri-Axial SI------------------------------------------------------------------------------
%% ************************* WEIGHTED
*********************************************************************
 %% 12------------------------------------------------------------------------------------------------
--
Pitcher_12A_tri_SI = trapz(Pitcher_12A_trix,(abs((Pitcher_12A_triy))./g).^p)

Pitcher_12B_tri_SI = trapz(Pitcher_12B_trix,(abs((Pitcher_12B_triy))./g).^p)

Pitcher_12C_tri_SI = trapz(Pitcher_12C_trix,(abs((Pitcher_12C_triy))./g).^p)

Pitcher_12D_tri_SI = trapz(Pitcher_12D_trix,(abs((Pitcher_12D_triy))./g).^p)

Pitcher_12E_tri_SI = trapz(Pitcher_12E_trix,(abs((Pitcher_12E_triy))./g).^p)

Pitcher_12avg_tri_SI = trapz(Pitcher_12avg_trix,(abs((Pitcher_12avg_triy))./g).^p)

%% 26------------------------------------------------------------------------------------------------
-
Pitcher_26A_tri_SI = trapz(Pitcher_26A_trix,(abs((Pitcher_26A_triy))./g).^p)

Pitcher_26B_tri_SI = trapz(Pitcher_26B_trix,(abs((Pitcher_26B_triy))./g).^p)

Pitcher_26C_tri_SI = trapz(Pitcher_26C_trix,(abs((Pitcher_26C_triy))./g).^p)

Pitcher_26D_tri_SI = trapz(Pitcher_26D_trix,(abs((Pitcher_26D_triy))./g).^p)
```

```
Pitcher_26E_tri_SI = trapz(Pitcher_26E_trix,(abs((Pitcher_26E_triy))./g).^p)

Pitcher_26avg_tri_SI = trapz(Pitcher_26avg_trix,(abs((Pitcher_26avg_triy))./g).^p)

%% *************************** NON - WEIGHTED
********************************************************************************
 %% Pitcher Y-Tri-Axial SI----------------------------------------------------------------------------
%% 12------------------------------------------------------------------------------------------------
-
Pitcher_12A_tri_SINW = trapz(Pitcher_12A_trixNW,(abs((Pitcher_12A_triyNW))./g).^p)

Pitcher_12B_tri_SINW = trapz(Pitcher_12B_trixNW,(abs((Pitcher_12B_triyNW))./g).^p)

Pitcher_12C_tri_SINW = trapz(Pitcher_12C_trixNW,(abs((Pitcher_12C_triyNW))./g).^p)

Pitcher_12D_tri_SINW = trapz(Pitcher_12D_trixNW,(abs((Pitcher_12D_triyNW))./g).^p)

Pitcher_12E_tri_SINW = trapz(Pitcher_12E_trixNW,(abs((Pitcher_12E_triyNW))./g).^p)

Pitcher_12avg_tri_SINW = trapz(Pitcher_12avg_trixNW,(abs((Pitcher_12avg_triyNW))./g).^p)

%% 26------------------------------------------------------------------------------------------------
Pitcher_26A_tri_SINW = trapz(Pitcher_26A_trixNW,(abs((Pitcher_26A_triyNW))./g).^p)

Pitcher_26B_tri_SINW = trapz(Pitcher_26B_trixNW,(abs((Pitcher_26B_triyNW))./g).^p)

Pitcher_26C_tri_SINW = trapz(Pitcher_26C_trixNW,(abs((Pitcher_26C_triyNW))./g).^p)

Pitcher_26D_tri_SINW = trapz(Pitcher_26D_trixNW,(abs((Pitcher_26D_triyNW))./g).^p)

Pitcher_26E_tri_SINW = trapz(Pitcher_26E_trixNW,(abs((Pitcher_26E_triyNW))./g).^p)

Pitcher_26avg_tri_SINW = trapz(Pitcher_26avg_trixNW,(abs((Pitcher_26avg_triyNW))./g).^p)
```

A-5. NOTES

[1] The total of the annual averages for the years spanning 2001-2005.

[2] The total of the annual average percentages of ED visits for all recreational and SR TBIs for the years spanning 2001-2005; not just the three sports presented in the table.

[3] Percentage of all ED visits attributed to TBIs for activity for the years spanning 2001-2005.

[4] Percentage of all hospitalizations attributed to SR TBIs for activity for the years spanning 2001-2005.

[5] Not conducted for LBT tests.

[1b] 1/8" MEP Faceguard Testing or 3" MEP Calibration Pads can also be used.

[2b] Small or large headforms can also be used.

10. WORKS CITED

[1] 'Sports Related Head Injury': American Association of Neurological Surgeons (AANS) <http://www.aans.org/patient%20information/conditions%20and%20treatments/sports-related%20head%20injury.aspx?p=1>; 2014

[2] <http://www.astm.org/Standards/sports-and-recreation-standards.html> American Society for Testing and Materials (ASTM)

[3] 'Injury Prevention & Control: Traumatic Brain Injury': Center for Disease Control and Prevention; <http://www.cdc.gov/traumaticbraininjury/>

[4] 'National Electronic Injury Surveillance System (NEISS)': Consumer Product Safety Commission, <http://www.cpsc.gov/en/research--statistics/neiss-injury-data/>

[5] 'Engineering Principles of Mechanical Vibration': Reynolds, D. 2nd Edition, Trafford Publishing, 2011

[6] 'Concussion in professional football: reconstruction of game impacts and injuries': Pellman et al.; 2003, <http://www.ncbi.nlm.nih.gov/pubmed/14519212>

[7] 'Head Impact Severity Measures for Evaluating Mild Traumatic Brain Injury Risk Exposure'; Greenwald et al.; 2009, <http://www.ncbi.nlm.nih.gov/pmc/articles/PMC2790598/>

[8] <http://nocsae.org/>

[9] <http://www.seinet.org/seitestingstandards.htm>

[10] <http://www.soimpact.com/services.html>

[11] http://www.vt.edu/spotlight/achievement/2013-02-04-duma/helmets.html

[12] 'Method and apparatus for testing football helmets': United States Patent 6,871,525; Withnall and Bayne; 29 Mar 2005; <http://patft.uspto.gov/netacgi/nph-Parser?Sect1=PTO2&Sect2=HITOFF&u=%2Fnetahtml%2FPTO%2Fsearch-

adv.htm&r=6&p=1&f=G&l=50&d=PTXT&S1=(withnall+AND+bayne)&OS=withnall+and+bayne&RS=(withnall+AND+bayne)>

[13] 'PULSE®': Brüel & Kjær http://www.bksv.com/Products/pulse-analyzer/pulse-platform

[14] 'Matlab & Simulink': Mathworks; Sudent Version R2011a; <http://www.mathworks.com/>

[15] 'Modeling and Analysis of Dynamic Systems': Close et al., Third Edition, Wiley Publishing 2002, pg. 97, pg.115-116

[16] 'Development of Improved injury Criteria for the Assessment of Advanced Automotive Restraint Systems – II', Eppinger, Sun et al., 1999 –National Highway Traffic Safety Administration, Vehicle Research & Test Center.

11. CIRRICULUM VITAE

EDUCATION

University of Nevada, Las Vegas   Las Vegas, Nevada

Master of Science in Mechanical Engineering   May 2015

Fluids/Thermal Sciences Concentration   GPA: 3.67

University of Nevada, Las Vegas   Las Vegas, Nevada

Bachelor of Science in Mechanical Engineering   May 2012

Minor: Mathematics   GPA: 3.39

College of Southern Nevada   Henderson, Nevada

Associate of Science with Honors   Dec. 2007

ACADEMIC ENGINEERING PROJECTS

EmeraChem Muffler Model EC-2150-C-XX   Dec 2013

University of Nevada, Las Vegas

- Determined the sound attenuation of Catalytic Reactor Housing and Silencer using Brüel & Kjær Acoustic Analyzer.

Comparison of aerodynamic characteristics of HSNLF and Supersonic airfoils   Nov 2013

University of Nevada, Las Vegas

- Compared the aerodynamic characteristics of subsonic & sonic airfoils in subsonic & supersonic flow regimes using Comsol® Multiphysics.

Phase Change Material (PCM) Enhanced Turn-Out Coat   May 2012

University of Nevada, Las Vegas

- Worked as part of a team to develop a model which incorporated a phase change material layer in fireman's turn-out coat.

INTERNSHIPS

National Aeronautics and Space Administration (NASA)   Jun 2011 – Aug 2011

Glenn Research Center: Undergraduate Student Research Program (USRP).

- Establish Damping Factors and Application Strategy for use in designing Typical GRC Spaceflight Payloads and Experiments.

SOFTWARE

- MATLAB®
- Microsoft Office® Suite

- SolidWorks®
- Brüel & Kjær's PULSE®

Mechanical Engineer Intern   Mar 2015 – Present

United States Air Force   Las Vegas, NV

- Practical application of mechanical engineering principles, concepts and techniques to solve mechanical engineering problems.
- Uses governing codes, standards & best practices for design, construction, operations, and maintenance of mechanical systems.
- Implement elements of programming and funding in the Air Force to build work requirements.

Knowledge Operations Specialist   Jan 2013 – Present

United States Air Force Reserves   Las Vegas, NV

- Perform, supervise and manage data, information and knowledge-sharing services in a fixed and expeditionary environment.
- Plan, coordinate, share and control an organization's data and information assets.
- Manage technologies to capture, organize and store tacit and explicit knowledge.

University Police Officer   Jul 2005 – Oct 2005

University of Nevada Las Vegas   Las Vegas, NV

Worked as part of a proactive patrol team to be a visible presence, deter crime, and reassure the school community.

- Issued citations for moving and non-moving traffic violations.

Police Officer   Jul 2002 – May 2005

New York City Police Department   New York City, NY

- As a member of a regimented team, intervened in situations involving crimes; conducted arrests with due regard for the human rights, security, and safety of detained individuals and safety of colleagues.
- Issued citations for moving and non-moving traffic violations.

Air Traffic Controller   May 1995 – May 2000

United States Army   Various Locations

- Within a systematic and coordinated team environment, sequenced arrival aircraft for landing and issued departure clearances; controlled the movement of aircraft on taxiways and prioritized flight data; issued weather advisories; assisted in the installation and

operation of tactical air traffic control facilities.

ACADEMIC ACHIEVEMENTS

Successfully Passed Fundamentals of Engineering Exam: EIT #OT6623, 2011.

Successfully completed NASA USRP Internship at John H. Glenn Research Center, Cleveland OH summer 2011.

Alliance of Professionals of African Heritage: Certificate for Outstanding Academic Achievement, 2010.

College of Southern Nevada: Outstanding Student of the Year, Physical Sciences, 2006 – 2007.

CERTIFICATIONS

- CompTIA® Network+ Certified 2006.

PROFESSIONAL AFFILIATIONS

Member, Tau Beta Pi Engineering Honor Society, 2011 – Present.

Member, National Society of Black Engineers, NSBE, 2010 – Present.

Member, American Society of Mechanical Engineers, ASME, 2010 – Present.

Member, American Institute of Aeronautics and Astronautics, AIAA, 2010 – Present.

PROFESSIONAL AWARDS

United States Air Force Civil Service Pin, 2015

NYPD Certificate of Achievement for Perfect Attendance, 2004.

U.S. Army Commendation Medal, 03/2000.

U.S. Army Achievement Medal (2), 07/1998 & 01/1999.

U.S. Army Good Conduct Medal, 05/1998.